



AFIT/GST/OS/84M-3

AD-A141 034

AN INVESTIGATION OF OPTIMAL AIMPOINTS  
FOR MULTIPLE NUCLEAR WEAPONS AGAINST  
INSTALLATIONS IN A TARGET COMPLEX

THESIS

Edmund G. Boy  
Captain, USAF

AFIT/GST/OS/84M-3

DTIC FILE COPY

DTIC  
ELECTE  
MAY 15 1984  
S E D

Approved for public release; distribution unlimited

84 05 15 052

AN INVESTIGATION OF OPTIMAL AIMPOINTS  
FOR MULTIPLE NUCLEAR WEAPONS AGAINST  
INSTALLATIONS IN A TARGET COMPLEX

THESIS

Presented to the Faculty of the School of Engineering  
of the Air Force Institute of Technology  
Air University  
In Partial Fulfillment of the  
Requirements for the Degree of  
Master of Science in Operations Research

Edmund G. Boy, B. S.  
Captain, USAF



March 1984

Accession For	
NTIS GRA&I	<input checked="" type="checkbox"/>
DTIC TAB	<input type="checkbox"/>
Unannounced	<input type="checkbox"/>
Justification	
By _____	
Distribution/	
Availability Codes	
Dist	Avail and/or Special
A-1	

Approved for public release; distribution unlimited

## REPORT DOCUMENTATION PAGE

1a. REPORT SECURITY CLASSIFICATION <b>UNCLASSIFIED</b>			1b. RESTRICTIVE MARKINGS			
2a. SECURITY CLASSIFICATION AUTHORITY			3. DISTRIBUTION/AVAILABILITY OF REPORT  Approved for public release; distribution unlimited.			
2b. DECLASSIFICATION/DOWNGRADING SCHEDULE			4. PERFORMING ORGANIZATION REPORT NUMBER(S)  AFIT/GST/OS/84M-3			
4. PERFORMING ORGANIZATION REPORT NUMBER(S)			5. MONITORING ORGANIZATION REPORT NUMBER(S)			
6a. NAME OF PERFORMING ORGANIZATION  School of Engineering		6b. OFFICE SYMBOL (If applicable) AFIT/EN		7a. NAME OF MONITORING ORGANIZATION		
6c. ADDRESS (City, State and ZIP Code)  Air Force Institute of Technology Wright-Patterson AFB, Ohio 45433			7b. ADDRESS (City, State and ZIP Code)			
8a. NAME OF FUNDING/SPONSORING ORGANIZATION		8b. OFFICE SYMBOL (If applicable)		9. PROCUREMENT INSTRUMENT IDENTIFICATION NUMBER		
8c. ADDRESS (City, State and ZIP Code)			10. SOURCE OF FUNDING NOS.			
11. TITLE (Include Security Classification) See Box 19			PROGRAM ELEMENT NO.		PROJECT NO.	TASK NO.
			WORK UNIT NO.			
12. PERSONAL AUTHOR(S) Edmund G. Boy, Capt, USAF						
13a. TYPE OF REPORT MS Thesis		13b. TIME COVERED FROM _____ TO _____		14. DATE OF REPORT (Yr., Mo., Day) 1984 March		15. PAGE COUNT 173
16. SUPPLEMENTARY NOTATION  Approved for public release IAW AFM 100-19 John Wolaver John S. WOLAVER Dean for Research and Professional Development Air Force Institute of Technology (AFIT)						
17. COSATI CODES			18. SUBJECT TERMS (Continue on reverse if necessary)			
FIELD	GROUP	SUB. GR.	Aimpoints, Damage Expectancy, DGZs, Nonlinear, Optimization, Targeting			
15	07					
19. ABSTRACT (Continue on reverse if necessary and identify by block number)  Title: AN INVESTIGATION OF OPTIMAL AIMPOINTS FOR MULTIPLE NUCLEAR WEAPONS AGAINST INSTALLATIONS IN A TARGET COMPLEX  Thesis Advisor: Ivy D. Cook, Lt Col, USAF						
20. DISTRIBUTION/AVAILABILITY OF ABSTRACT UNCLASSIFIED/UNLIMITED <input checked="" type="checkbox"/> SAME AS RPT. <input type="checkbox"/> DTIC USERS <input type="checkbox"/>				21. ABSTRACT SECURITY CLASSIFICATION  UNCLASSIFIED		
22a. NAME OF RESPONSIBLE INDIVIDUAL  Ivy D. Cook, Lt Col, USAF			22b. TELEPHONE NUMBER (include Area Code) 513-255-3362		22c. OFFICE SYMBOL AFIT/ENS	

→ Strategic nuclear targeting studies generally include more target installations than there are weapons. Hence, a weapon is not assigned to an installation, but rather, to a Desired Ground Zero (DGZ). The objective of this study was to investigate optimal DGZs for multiple nuclear weapons against installations in a target complex. To accomplish this, it was necessary to develop the target Complex Expected Damage Function (CEDF) maximization algorithm. The algorithm locates optimal DGZs by maximizing the CEDF; the CEDF is a nonlinear function of  $2m$  variables, the  $(X_i, Y_i)$  DGZ coordinates for each of the  $m$  weapons.

The algorithm uses two CEDF models and two optimization techniques. These models use DIA Physical Vulnerability System probability of damage models. The CEP-Included model includes each weapon's CEP; the simpler CEP-Excluded model assumes each weapon's CEP equals 0. An analytical expression for the gradient of the CEP-Excluded model was calculated; the algorithm maximizes this CEDF using a conjugate gradient with restarts search technique. The algorithm maximizes the CEP-Included CEDF using a direct search technique, Powell's method of conjugate directions.

This investigation characterized three factors that affect the optimal DGZ locations for multiple nuclear weapons in a target complex. The first factor was gradient symmetry; this symmetry resulted from either a geographically symmetric target complex or collocated weapons. The second factor was weapon CEP. Maximization of the two CEDF models produced slightly different optimal DGZs; this difference depended on a weapon's CEP and the CEDF model. The third factor was the initial DGZ location prior to CEDF maximization. The algorithm located different CEDF local maximums depending on the initial DGZ condition. However, the investigation revealed that the most successful initial DGZ condition is to use the coordinates of the highest valued installations as the initial DGZ coordinates. ← too long

## Preface

My concept of and algorithm for locating optimal aimpoints for multiple nuclear weapons in a target complex were a synthesis of three analyst's ideas. Captain Mark Orlicky, Air Force Studies and Analysis, Major Steve Sperry, Joint Strategic Target Planning Staff, and Mrs. Adelaide Bialek, Academy for Interscience Methodology all contributed to my strategic targeting education. I thank each of them for the valuable suggestions that they provided to me. I also extend special thanks to Mr. Carol Strom of the Computer Sciences Corporation; he shared his ideas with me and provided me with results from the model NUCWAVE.

I am especially grateful to my adviser, Lt Col Ivy D. Cook, for his unending suggestions and guidance. I thank him for helping me complete my thesis project and discover the strengths and weaknesses of my analytic ability. I would also like to express my sincere appreciation to my reader, Lt Col Palmer W. Smith, for his ideas and enthusiasm.

Finally, I recognize and extend thanks to my most valuable thesis contributor -- my typist, my editor, my best friend, and my wife Mary. I thank you for your encouragement and because you, and our children, Greg, Becky, and Leanne, have endured more hardships than I have during the past 18 months.

## Table of Contents

	Page
Preface . . . . .	ii
List of Figures . . . . .	v
List of Tables . . . . .	vi
Abstract . . . . .	vii
I. Introduction . . . . .	1
Background . . . . .	1
Problem Statement . . . . .	6
DGZ Models . . . . .	7
Objectives . . . . .	12
Scope and Assumptions . . . . .	13
Overview . . . . .	14
II. Mathematical Formulation of the Complex Expected Damage Function and Gradient . . . . .	15
Conceptual Model . . . . .	15
Probability of Damage Models . . . . .	19
The CEDF Model . . . . .	27
Gradient of the CEP-Excluded Model . . . . .	29
III. Optimization of the Complex Expected Damage Function . .	37
Optimization . . . . .	38
Numerical Search Techniques . . . . .	39
Conjugate Directions and Quadratic Termination . . . . .	43
CEDF Optimization Methods . . . . .	45
IV. Computerization, Verification, and Validation of the CEDF Maximization Algorithm . . . . .	50
Computerization . . . . .	50
Verification . . . . .	56
Validation . . . . .	62
V. CEDF Maximization Algorithm Properties . . . . .	66
Convergence Criteria . . . . .	67
Symmetry Characteristics . . . . .	73
VI. Algorithm Results for Different Initial DGZ Locations . .	82
A Three Installation Complex . . . . .	83
The CEP Effect . . . . .	88
Larger Complexes . . . . .	92

	Page
VII. Conclusions and Recommendations . . . . .	96
Conclusions . . . . .	98
Recommendations . . . . .	100
Appendix A: Determination of the Distance Damage Sigma ( $\sigma_d$ ) and the Weapon Radius (WR) . . . . .	102
Appendix B: Formulation of $f(r)$ and Calculation of the Integration Limits . . . . .	106
Appendix C: Gauss-Legendre Quadrature to Integrate $f(r')$ . . .	110
Appendix D: Computer Code of the CEDF Maximization Algorithm .	113
Appendix E: User Guidelines and a Sample Problem . . . . .	147
Appendix F: Verification of the Gradient of the CEP-Excluded CEDF Model . . . . .	156
Bibliography . . . . .	163
Vita . . . . .	165

## List of Figures

Figure	Page
1. LAIR Intersections . . . . .	8
2. Conceptual Model of the CEDF . . . . .	16
3. Geometry of the Installation-Weapon Interaction . . . . .	20
4. A Probability of Damage Function $P_d(r)$ . . . . .	21
5. A Representative CEDF with Three Installations and Two Weapons . . . . .	28
6. Flowchart of the CEDF Maximization Algorithm . . . . .	51
7. CEDF Maximization Algorithm Subroutine Hierarchy . . . . .	52
8. The CEDF for a Two Weapon-Two Installation Geometry . . . . .	58
9. The CEDF for a One Weapon-Two Installation Geometry . . . . .	60
10. The One Weapon-Two Installation Geometry . . . . .	61
11. A Symmetric Two Installation Complex . . . . .	74
12. A Symmetric Four Installation Complex . . . . .	78
13. CEDF Values Along Line Segments U-U' and V-V' for the Symmetric Four Installation Complex . . . . .	81
14. A Three Installation Complex . . . . .	84
15. Pseudo-random Initial DGZ Conditions . . . . .	86
16. Multiple Local Optimal DGZs for a Two Weapon- Four Installation Complex . . . . .	92
B-1. Weapon-Installation Geometry to Determine a and b . . . . .	108
C-1. Quadrature Base Points . . . . .	111
E-1. The CEDF Maximization Algorithm Input File, INDATA, for a Two Weapon-Four Installation Complex . . . . .	148



List of tables

Table	Page
I. Steps to Calculate $Pd_{i,j}$ . . . . .	26
II. Comparison Between an Original Problem and a 1/10 Value Scaled Problem . . . . .	69
III. Comparison of ACC Convergence Criteria . . . . .	70
IV. Comparison of ZXM, PWM, and MXM Optimal DGZe . . . . .	90
A-1. Distance Damage Sigma and Target Type . . . . .	103
C-1. Quadrature Base Points and Coefficients . . . . .	112
F-1. The CEDF(x) and the Gradient of the CEDF(x) for a One Weapon-Two Installation Complex . . . . .	157

ABSTRACT

Strategic nuclear targeting studies generally include more target installations than there are weapons. Hence, a weapon is not assigned to an installation, but rather, to a Desired Ground Zero (DGZ). The objective of this study was to investigate optimal DGZs for multiple nuclear weapons against installations in a target complex. To accomplish this, it was necessary to develop the target Complex Expected Damage Function (CEDF) maximization algorithm. The algorithm locates optimal DGZs by maximizing the CEDF; the CEDF is a nonlinear function of  $2m$  variables, the  $(X_i, Y_i)$  DGZ coordinates for each of the  $m$  weapons.

The algorithm uses two CEDF models and two optimization techniques. These models use DIA Physical Vulnerability System probability of damage models. The CEP-Included model includes each weapon's CEP; the simpler CEP-Excluded model assumes each weapon's CEP equals 0. An analytical expression for the gradient of the CEP-Excluded model was calculated; the algorithm maximizes this CEDF using a conjugate gradient with restarts search technique. The algorithm maximizes the CEP-Included CEDF using a direct search technique, Powell's method of conjugate directions.

This investigation characterized three factors that affect the optimal DGZ locations for multiple nuclear weapons in a target complex. The first factor was gradient symmetry; this symmetry resulted from either a geographically symmetric target complex or collocated weapons. The second factor was weapon CEP. Maximization of the two CEDF models

produced slightly different optimal DGZs; this difference depended on a weapon's CEP and the CEDF model. The third factor was the initial DGZ location prior to CEDF maximization. The algorithm located different CEDF local maximums depending on the initial DGZ condition. However, the investigation revealed that the most successful initial DGZ condition is to use the coordinates of the highest valued installations as the initial DGZ coordinates.

AN INVESTIGATION OF OPTIMAL AIMPOINTS  
FOR MULTIPLE NUCLEAR WEAPONS AGAINST  
INSTALLATIONS IN A TARGET COMPLEX

I. Introduction

Effective U. S. targeting of an enemy's resources is an important part of U. S. military air power. One of the fundamental objectives of U. S. military forces is to sustain deterrence (Ref 8: para 1-6). Deterrence is an enemy's state of mind brought about by the existence of U. S. military power or the enemy's perception of U. S. resolve to use that power. Strategic nuclear targeting, an assignment process, is a key element of nuclear deterrence. The nuclear weapons planner must assign a weapon system to a specific target. Targeting consists of three interacting processes: the target intelligence process, the threat estimate process, and the operational planning process (Ref 7:2-2). This study investigates an important phase of the target intelligence process, nuclear weaponeering, and a weaponeering problem. Lee defines weaponeering as "the process that determines the physical vulnerabilities of targets, the optimum weapon type, the number of weapons, and sometimes the best system required to achieve a desired level of damage on a target or a target system" (Ref 18:122).

Background

Weapons planners allocate weapons to Desired Ground Zeros (DGZs) to achieve damage to installations within a target complex. A target

complex is a geographical area that includes different types and numbers of target elements or installations. Nuclear detonations within a complex will cause insignificant damage to installations within all adjacent complexes (Ref 20:6). A complex may contain one installation or a few hundred installations. For example, a 50-square-mile Air Force base may be a target complex. Similarly, the runway, the maintenance facility, the parked aircraft, and the headquarters command post are installations of this target complex. However, weapons planners do not allocate weapons to each installation. Instead, they allocate weapons to DGZs and plan to damage more than one installation with one weapon. A DGZ is a point on the surface of the earth at or vertically below the center of a planned weapon explosion (Ref 7:5-6). In this study, a DGZ refers to a nuclear weapon detonation at a specific geographical location. A DGZ may be located directly on an installation; or, if one weapon will sufficiently damage two or more installations, then the DGZ may be located between the installations.

Weapons analysts use the concept of a lethal aimpoint region (LAIR) to locate DGZs within a target complex (Ref 20:10; 21:4; and 25:2-6). The LAIR is a circular area whose center is the target installation. It represents a geographical region within which a weapon can detonate and achieve at least a minimum probability of damage (Pd) to a target. Pd is the probability that a desired level of damage (severe, moderate, light) will occur to a target (Ref 7:5-6). "The general definitions of the three damage levels are: (1) severe damage -- a level which requires essentially complete reconstruction or replacement of one or more critical major elements of the target, plus reconstruction, repair, or replacement of associated structures or equipment. Severe damage

precludes utilization of the target for any purpose, (2) moderate damage -- a level which requires major repairs to one or more critical major elements of the target, plus major reconstruction, repair, or replacement of associated structures or equipment. Moderate damage precludes effective utilization of the target for its intended purpose, (3) light damage -- a level which does not significantly impair the target function, but requires some repairs to restore the target to complete usefulness" (Ref 19:1-7).

The radius of the LAIR depends on specific weapon system and target parameters. The accuracy of the missile or aircraft system that delivers the weapon to the DGZ affects the LAIR. Also, the yield of the nuclear weapon affects the LAIR. Yield is a numeric value measured in kilotons (kt) and is a relative indicator of the explosive energy the weapon releases when it detonates. This explosive energy causes damage to installations. A nuclear weapon distributes its damage energy in several ways through damage mechanisms or weapon effects. For ground targets, the most prominent mechanism is the blast effect. The primary elements of blast are overpressure and dynamic pressure. Overpressure creates a force that crushes an installation; dynamic pressure creates a force from the resulting high wind velocity (Ref 11:80-82). But thermal effects, cratering, and impulse are other nuclear weapon effects that may contribute to target damage. The occurrence and intensity of these weapon effects vary for different weapon yields.

The LAIR also depends upon target characteristics, specifically, the vulnerability of the target to blast effects. The Defense Intelligence Agency (DIA) uses a Physical Vulnerability coding system to quantify a target's susceptibility to blast damage. Each installation is

characterized by a three-part Vulnerability Number (VN). The first part consists of a two-digit integer reflecting the target's relative hardness in terms of a 20-kt weapon and a specified damage level (severe, moderate, light). The second part is a letter indicating whether the target is predominantly sensitive to either overpressure (L,M,N,O,P) or dynamic pressure (Q,R,S,T,U). The third part is a K factor. This factor adjusts the target's relative hardness for weapon yields other than 20-kt (Ref 6:34 and 19:1-7).

In this paper, four factors characterize a nuclear weapon -- yield, accuracy, height of burst, and probability of arrival (Pa). Circular error probable (CEP) is a numeric value measured in units of length that represents a weapon's delivery accuracy. A 500-foot CEP indicates a weapon has a 50% chance of being delivered within 500 feet of the target. Similarly, height of burst is the weapon's distance above the ground when the weapon detonates. Pa is the probability that a delivery vehicle (bomber, missile) and its weapon arrive at the target and the weapon detonates as planned. Pa depends upon the delivery vehicle's pre-launch survivability (PLS), weapon and weapon system reliability (WSR), and probability to penetrate (PTP). Each of these factors is a probability (Ref 7:5-7).

The weapons analyst plans to damage installations within a target complex by assigning weapons to a prioritized list of DGZs. In addition to Pd and Pa, which are multiplied together to calculate an installation's Damage Expectancy (DE), the value of each installation is needed to develop the prioritized list. The value of an installation is a number that represents the value of the installation relative to all other

installations. Most value systems cardinally order targets over a range from the most valued target (highest value number) to the least valued target (Ref 7:6-19). The total complex expected target value damage is the sum of each installation's value multiplied by the installation's cumulative DE.

There is a shortfall in the nuclear weaponing process. The prioritized target list generally has more DGZs than there are weapons available to assign to the DGZs. The weapons analyst must determine not only the best weapon-DGZ combination to achieve the desired attack objectives, but also alternative combinations (Ref 7:5-6).

The method that strategic nuclear weapon targeting models use to address this problem depends on the specific objective of the model. One objective is to minimize the number of weapons required to achieve at least a minimum acceptable probability of damage to all installations in the complex. This method determines the minimum number of weapons when installation Pds are prespecified. A different objective is to achieve the maximum total expected target value damage for the complex. This method determines the Pd to each installation when the number of weapons available is prespecified.

As an example, suppose a preliminary target analysis indicates five DGZs are necessary to achieve a minimum acceptable Pd for each installation in a complex. However, after allocating weapons to the entire prioritized DGZ list (all complexes), only four weapons are actually available to this complex. Should the four weapons be targeted against the four highest expected target value DGZs or should an attempt be made to locate four new DGZs, perhaps unrelated to the five potential DGZs? The former choice will achieve a minimum acceptable Pd on some,



but not all, of the installations in the complex. The installations that would have been damaged by a weapon allocation to the unassigned DGZ probably will receive insignificant damage. Conversely, the latter choice may increase the total expected target value damage to the complex with either no decrease or a minimal decrease in the minimum acceptable Pd for each installation.

According to a 15 September 1983 literature review, AF Studies and Analysis, Command and Control Technical Center (CCTC), and the Single Integrated Operational Plan (SIOP) Simulation Branch, Joint Strategic Target Planning Staff (JSTPS) use different models for DGZ optimization studies (Ref 4; 13; 20; 22; and 28). Each of these mathematical models has a limitation. Initially, the algorithms generate a DGZ list for a complex using an unlimited supply of weapons. Then the algorithms assign weapons either to the minimum number of DGZs required to achieve an acceptable level of damage on all targets or, when the numbers of weapons are constrained, to the DGZs that achieve the best total expected target value damage for the preplanned DGZs. The second situation, limited weapon supply, is more realistic. However, the development of new DGZs in the constrained weapons case to maximize total expected target value damage is not attempted. In some algorithms, DGZs are relocated, but relocation is sequential. One DGZ is moved until its contribution to the total expected target value damage is maximized, then that DGZ is assigned, and a second DGZ is sequentially moved.

#### Problem Statement

After a weapon allocation for all target complexes is completed, not all complexes may be allocated enough weapons to achieve an

acceptable Pd for all installations.

An algorithm is needed that will optimally locate DGZs in a target complex for a fixed number of weapons, while maximizing the total expected target value damage to installations within the complex.

### DGZ Models

Multiweapon Optimizer for Strategic Targets (MOST), Seiler, and NUCWAVE are mathematical models that Air Force agencies use for strategic targeting studies (Ref 20; 21; and 25). The models locate DGZs within a target complex. Each of these models depends on the LAIR concept and uses either partial enumeration, or linear programming allocation, or sequential allocation to determine a set of DGZs for a complex.

MOST determines a DGZ list in two phases. Each phase satisfies an associated criteria. These phases allow MOST to achieve its objective -- determining the fewest number of weapons (DGZs) required to achieve at least a minimum acceptable Pd for each installation in a complex (Ref 21). There are several steps in the first phase. Initially, MOST generates a LAIR for each installation. These LAIRs satisfy the criteria to achieve a minimum acceptable Pd on all installations. Next, MOST compiles subsets of DGZs through a partial enumeration process; each subset contains a list of LAIR intersections. For one subset, all installations in the complex must be included in at least one intersection. Then MOST selects the subset that contains the fewest number of LAIR intersections; if several equivalent subsets require the fewest number of aimpoints, then the subset with the highest total expected target value damage is selected. As an example, consider the target complex

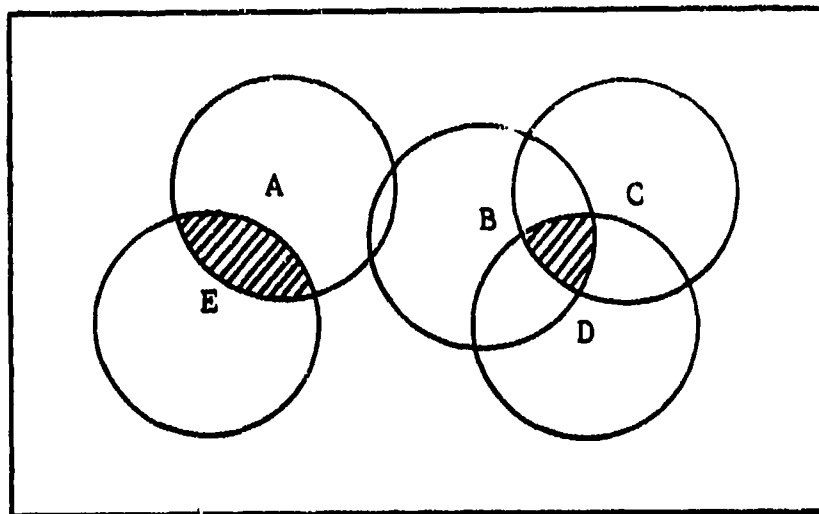


Figure 1. LAIR Intersections

in Figure 1. The algorithm would select the DGZ subset that contains the LAIR intersection of installations B, C, and D as one DGZ and the LAIR intersection of installations A and E as the second DGZ of this target complex (the shaded regions in Figure 1).

In the second phase, MOST adjusts the final DGZ locations within the LAIR intersection regions using a weighted installation value system. This process maximizes the total expected target value damage for all DGZs. If installation D was more valuable than B and C in Figure 1, then the actual DGZ would be moved proportionately closer to installation D. These adjustments to final DGZs are accomplished sequentially. First, the DGZ associated with the greatest number of LAIR intersections would be maximized (the DGZ associated with the intersection of target LAIRs B, C, and D). Then the DGZ associated with the second greatest number of LAIR intersections, etc. MOST was designed to find the minimum number of DGZs for Poseidon re-entry vehicles, irrespective of weapon supply constraints. If there are not enough weapons to

allocate to the complex, then the least valued DGZs would not be assigned weapons.

The objectives and purpose of the Seiler model are similar to MOST. Seiler was designed to study the assignment of nuclear weapon missile systems (ICBM and SLBM) to installations within many target complexes (Ref 20). Seiler also uses two phases to assign weapons to a prioritized list of DGZs. In the first phase, generation of aim-points, Seiler creates DGZs using the LAIR concept and a tiered DGZ system. The primary tier consists of the minimum number of DGZs that are required to achieve a minimum acceptable Pd to all installations when only the largest yield weapon is considered. For each subset of installations contained in a primary tier DGZ, supplementary DGZs are created for the next largest yield weapon. Supplementary DGZs are always subsets of a primary tier DGZ or a higher-tiered supplementary DGZ. Each DGZ, supplementary or primary, achieves a minimum acceptable Pd on a subset of the installations in a target complex and has an associated DGZ value. This value depends on the cumulative total expected target value damage of the associated installations.

In the second phase, Seiler uses a linear programming (LP) algorithm to determine an optimal (or near optimal) assignment of weapons. The LP objective is to maximize the total complex expected target value damage. Seiler accomplishes this assignment using the primary and supplementary tiered DGZs, missile delivery vehicle range capabilities, and constraints on the number of primary and supplementary tier weapons available. If there are not enough weapons available to allocate to the installations in the complex, then lower value DGZs (and hence

installations) remain untargeted just as in MOST.

NUCWAVE determines the number and the location of DGZs using a different approach (Ref 25). It is a one-sided nuclear weapons allocation war gaming model. The user can select one of two strategies -- (1) allocate a limited number of weapons to DGZs in order to maximize the total expected target value damage to all target complexes considered, or (2) determine the minimum number of DGZs required to achieve a minimum acceptable Pd to installations within all target complexes. NUCWAVE generates DGZs using the LAIR concept, similar to MOST and Sailer, for allocation strategy 2. Allocation strategy 1 is accomplished using a sequential algorithm and will be discussed later.

The NUCWAVE algorithm consists of three phases, irrespective of the allocation strategy chosen. The first phase, potential allocation, uses an unlimited supply of weapons to maximize the damage attained by each weapon until a sufficient number of potential DGZs are located to satisfy the strategy objective. In the second phase, an LP weapon selection program uses these potential DGZs and weapon supply constraints to select the number and the type of weapons to be assigned to each complex. In the final phase, real allocation, the specific number and types of weapons are "optimally allocated" against the installations in each complex (Ref 25:2-8). If allocation strategy 2 has been selected and the weapon selection program allocated fewer than the required number of weapons to a complex, then the lower valued DGZs and their associated installations would not be targeted. No relocation of the DGZs is attempted with strategy 2.

When allocation strategy 1, maximize total expected target value

damage, is selected, NUCWAVE determines DGZs sequentially in both the potential and real allocation phases. NUCWAVE starts by locating the first DGZ at the highest-valued installation in the complex. The algorithm then moves the DGZ to a location that maximizes the total complex expected target value damage. The algorithm may move the DGZ closer to several installations, thus increasing the Pd and expected target value damage for these installations. Similarly, the algorithm may move the DGZ farther away from other installations, thus decreasing the Pd and expected target value damage for these installations. When the optimal location is determined, two steps occur. First, a weapon-DGZ location, having been determined, is stored. Next, the surviving value of all installations is calculated by multiplying the previous value of the installation by the Pd of the installation from the current weapon-DGZ combination. NUCWAVE then selects the installation with highest surviving value and the entire process is repeated. DGZs are sequentially determined in this manner until the specified stopping condition is reached. In the potential allocation phase, the stopping condition is that a user-specified percent of the total expected target value damage has been achieved; in the real phase, the condition is no more remaining weapons.

After a weapon allocation is made for the entire target list, only a finite number of weapons may be assigned to a target complex. Only NUCWAVE attempts to locate new DGZs, but it uses a sequential optimization algorithm. When less than the desired number of weapons are allocated to a target complex, a simultaneous optimal solution specifying the location of the final DGZs should exist. In this study,

optimal means the best location of DGZs such that the total complex expected target value damage is maximized.

### Objectives

The primary objective of this study is to investigate the optimal DGZ locations within a target complex. In order to accomplish this, it is necessary to develop an algorithm. This algorithm will optimally locate the DGZs for fixed numbers of weapons in a target complex by maximizing the expected target value damage to all installations. The algorithm will not be restricted to one type of weapon; that is, different weapons may be included in the fixed number of weapons.

Also, it will be necessary to determine the sensitivity of the algorithm to two factors -- first, the mathematical technique used to locate the optimal DGZs; second, the initial starting conditions (latitude and longitude coordinates) for the DGZs.

The algorithm will consist of two elements. The first element is a mathematical model of the total complex expected target value damage. The second element is an optimization technique to determine the maximum total complex expected value damage and to locate the corresponding optimal DGZs. The following steps are an outline of the algorithm:

1. Specify target installation parameters. These include installation coordinates, VN numbers, and values.
2. Specify weapon parameters. These include yield, quantity, CEP, Pa, and height of burst.
3. Specify either the mathematical form or an acceptable approximation of the probability of damage function for an installation.
4. Determine the mathematical form of the Installation Expected

Damage Function (IEDF). This function represents the total expected target value damage to an installation from all weapons.

5. Specify the form of the Complex Expected Damage Function (CEDF). This function is a summation of all of the IEDFs.
6. Select a nonlinear optimization technique to maximize the CEDF and to locate the final coordinates of the DGZs.

### Scope and Assumptions

This study will develop an algorithm subject to certain restrictions that optimally locates DGZs in a target complex. Secondary damage will be assumed within the target complex; however, secondary damage from weapons detonated in adjacent complexes will not be considered. Also, the algorithm will not consider target avoidance areas.

Only military/industrial installations that can be modeled as point targets will be considered. Also, since blast is the primary damage mechanism for ground targets, other nuclear weapon effects will not be considered. Each installation's susceptibility to overpressure and to dynamic pressure will be specified with VN numbers. Also, the mathematical model of the probability of damage function developed by the Defense Intelligence Agency (DIA) will be used to specify the installation expected damage function (Ref 6).

The algorithm will consider weapon system delivery methods and accuracy since they will affect the expected target value damage. Delivery methods will be characterized by a specified Pa for each weapon. However, feasible delivery constraints will not be considered, for



example, Multiple Independent Reentry Vehicle (MIRV) footprinting and a weapon delivery system's range capability. A circular normal distribution will be assumed for weapon system accuracy, and a CEP will be specified for each weapon. Pa and CEP are a function of range for some weapons, but in this study they are prespecified numbers.

Different optimization techniques and initial DGZ conditions will be evaluated. These evaluations will characterize the properties, capabilities, and any limitations of the algorithm.

### Overview

This paper reports the methods and findings of a study that investigated the location of optimal aimpoints for multiple nuclear weapons against installations in a target complex. A CEDF maximization algorithm was developed to optimally locate DGZs for these weapons by maximizing the Complex Expected Damage Function (CEDF). The algorithm consists of two elements -- a mathematical model of the CEDF and an optimization technique. Chapter II presents the mathematical formulation of two CEDF models and the gradient for one of these models. Chapter III presents an overview of numerical search techniques; it also discusses the two techniques that are used to maximize the two CEDF models. Chapter IV contains the computerization of the algorithm and the verification and validation processes. Chapter V discusses the algorithm's convergence criteria, and specific properties of symmetric target complexes, and symmetric CEDF gradient elements. Chapter VI is an analysis of optimal DGZs for three, four, and seven installation target complexes. It also discusses and summarizes the three conclusions of this study. Finally, Chapter VII presents concluding remarks and recommendations.

## II. Mathematical Formulation of the Complex Expected Damage Function and Gradient

The algorithm determines the optimal DGZ locations within a target complex by maximizing the Complex Expected Damage Function (CEDF). Initially, the CEDF is developed from prespecified weapon and installation parameters; then the CEDF is maximized with an unconstrained, nonlinear optimization technique. One replication of the algorithm determines the optimal DGZ locations in a finite number of iterative steps. Each iterative step finds improved DGZ locations and an associated larger CEDF value as compared to the previous locations and CEDF value. The algorithm iterates until no significant increase in the CEDF is possible. This chapter explains the mathematical formulation of the CEDF and its gradient. Chapter III presents the unconstrained, nonlinear optimization techniques used to maximize the CEDF.

### Conceptual Model

The CEDF is a function of weapon and installation parameters and the coordinates of the DGZs. The conceptual model of the CEDF is shown in Figure 2. The  $i$  subscript of either a variable or a parameter refers to one of the  $m$  weapons; the  $j$  subscript refers to one of the  $n$  installations in the target complex. All parameters are constants (either prespecified or calculated values) except the  $(X_i, Y_i)$  DGZ coordinates for each of the  $m$  weapons. The basic element of the the CEDF is the  $Pd_{i,j}$  -- the probability of achieving a specified level of damage to installation  $j$  from weapon  $i$ . Similarly, the expected damage to installation  $j$  from weapon  $i$  is  $DE_{i,j}$  -- the product of  $Pd_{i,j}$  and

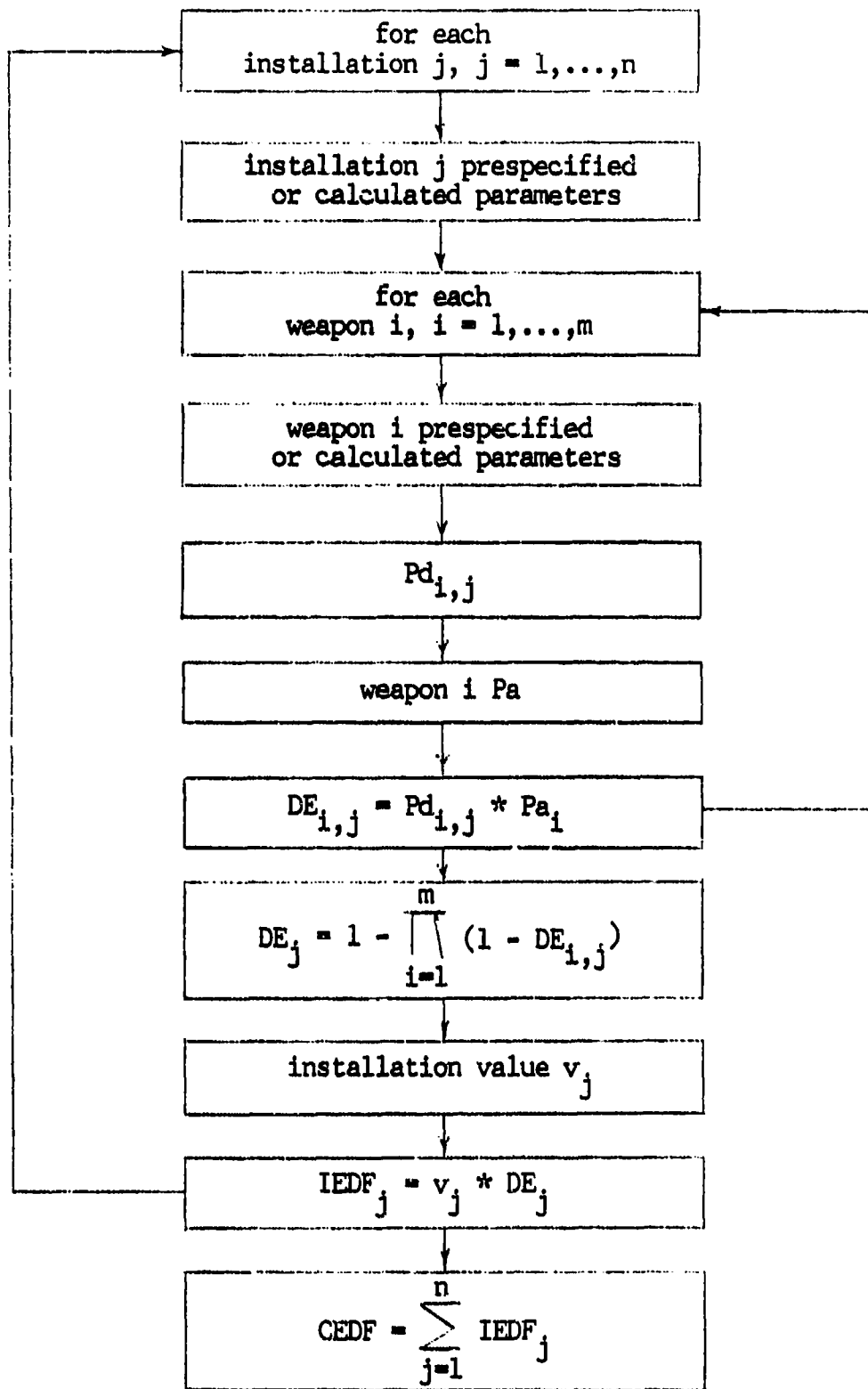


Figure 2. Conceptual Model of the CEDF

the probability of arrival for weapon  $i$ ,  $Pa_i$ . The cumulative expected damage to installation  $j$  from all  $m$  weapons is  $DE_j$ . This formulation for determining the cumulative damage to an installation from multiple bursts is similar to the formulation used in SIDAC and NUCWAVE (Ref 19:A-4 and 25:A-2). For each installation, the Installation Expected Damage Function, IEDF, is the product of its value  $v_j$  and  $DE_j$ . The CEDF is an unconstrained, nonlinear function; it is the summation of  $n$  IEDFs. The function is nonlinear because  $Pd_{i,j}$  is a nonlinear function. Again, all CEDF parameters are constants except the  $(X_i, Y_i)$  DGZ coordinates for each of the  $m$  weapons.

In order to determine the CEDF, the algorithm requires scenario dependent inputs, installation and weapon parameters. The minimum necessary installation parameters include:

1. The number of installations in the target complex -  $n$
2. The coordinates of each installation -  $(x_j, y_j)$
3. A VNTK code for each installation, indicating the installation's susceptibility to blast damage
4. A value from a relative installation value system -  $v_j$

The minimum necessary weapon parameters include:

1. The number of weapons available -  $m$
2. The height of burst for each weapon -  $HOB_i$
3. The yield in kilotons for each weapon -  $Y_i$
4. The CEP for each weapon -  $CEP_i$
5. The probability of arrival for each weapon -  $Pa_i$
6. The initial DGZ locations prior to optimization -  $(X_i, Y_i)$

The assignment of specific numeric values to these parameters was not a critical element of the study. Consequently, several hypothetical

target complexes were used. These complexes are described in Chapter IV.

Two mathematical forms of the CEDF are used; hence, there are two parallel algorithms, one for each form of the CEDF. The first CEDF is the CEP-Excluded version; the second CEDF is the CEP-Included version. These two versions are explained in the next section. The only difference between the two CEDFs is their respective forms of the probability of damage function. The Defense Intelligence Agency (DIA) developed these Pd models to provide analytical approximations to actual blast damage data. The CEP-Excluded CEDF uses a closed form analytical expression of an installation's Pd function that is independent of weapon delivery system accuracy, that is, weapon CEP = 0. The CEP-Included CEDF uses a more complicated analytical expression of an installation's Pd function that includes weapon CEP.

The two CEDF forms are used for three reasons. First, a closed form analytical expression for the gradient of the CEP-Included CEDF expression was not available; hence, this CEDF could only be maximized with an optimization technique that used function values. However, since gradient optimization techniques are generally more efficient than function value techniques (Ref 2:152; 5:321; and 10:286), a second form of the CEDF is desired. Therefore, an analytical expression for the gradient of the CEP-Excluded CEDF is calculated. This CEDF is maximized using gradient optimization techniques. Chapter III explains different optimization schemes and the optimization techniques used to maximize the two CEDFs. The second reason for using two CEDFs is verification. The results of the algorithm are compared to insure that they provide the same DGZ locations and complex expected damage value. The last reason for using two CEDFs is to investigate the

effect that the assumption of CEP = 0 has on the location of the optimal aimpoints.

### Probability of Damage Models

The CEDF is an unconstrained, nonlinear function of 2m variables -- the  $(X_i, Y_i)$  DGZ coordinates for each of the m weapons.

$$CEDF = \sum_{j=1}^n IEDF_j = \sum_{j=1}^n v_j * \left[ 1 - \prod_{i=1}^m (1 - Pd_{i,j} * Pa_i) \right] \quad (1)$$

The basic element of the CEDF is  $Pd_{i,j}$  -- the probability of achieving a specified level of damage to installation j from weapon i.  $Pd_{i,j}$  is a function of two independent variables, the  $(X_i, Y_i)$  coordinates of weapon i. Two forms of the  $Pd_{i,j}$  function used in this study are part of the DIA Physical Vulnerability (PV) System. They are not independent formulations. These formulations are described in Mathematical Background and Programming Aids for the Physical Vulnerability System for Nuclear Weapons (Ref 6). Therefore, only a useable, but limited, description will be presented here.

The  $Pd_{i,j}$  depends on the known distance s between  $DGZ_i$  and installation j. The coordinates of installation j are  $(x_j, y_j)$ . The geometry of the installation-weapon interaction is shown in Figure 3. The algorithm uses a flat earth approximation to calculate this distance, that is,

$$s = \left[ (X_i - x_j)^2 + (Y_i - y_j)^2 \right]^{1/2} \quad (2)$$

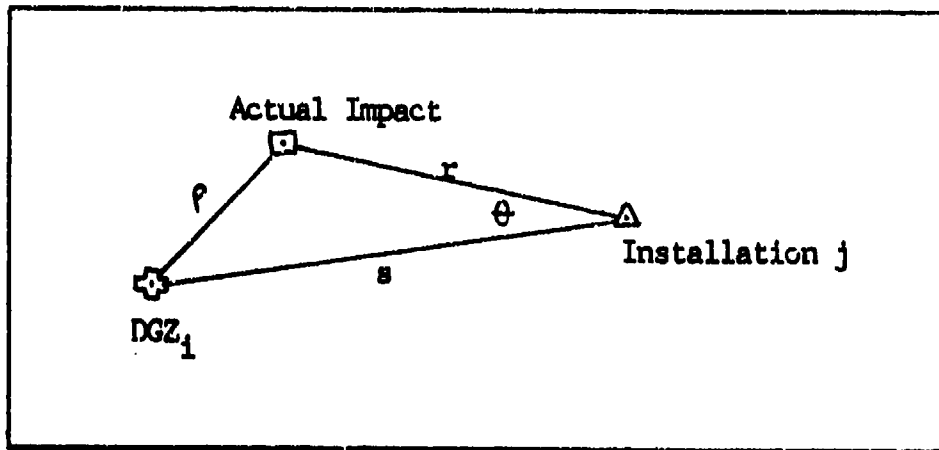


Figure 3. Geometry of the installation-weapon interaction (Ref 6:20).

The  $(X_1, Y_1)$  and  $(x_j, y_j)$  coordinates are measured in feet from a common origin. Comparatively, the distance  $r$  is the distance between installation  $j$  and the actual weapon impact point. When  $CEP \neq 0$ , the impact point and  $DGZ_1$  may not be the same point, and  $s$  will not equal  $r$ .

CEP-Excluded Model. If the CEP of the weapon delivery system can be assumed to equal 0, that is, the actual weapon impact point is the  $DGZ_1$ , then the distance  $r$  from installation  $j$  to the impact point is known. The distance  $r$  can be calculated from the  $(X_1, Y_1)$   $DGZ$  coordinates, the  $(x_j, y_j)$  installation coordinates, and Eq (2). The distance damage function,  $P_d(r)$ , is the DIA analytical approximation for the probability of damage function when weapon  $CEP = 0$ . It is based upon actual blast damage data.  $P_d(r)$  is the complement of the cumulative log normal distribution function. For this CEDF version, CEP-Excluded, the probability of damage function,  $P_{d_{1,j}}$ , is the distance damage function,  $P_d(r)$ . However, it will be referred as the distance damage function  $P_d(r)$  to parallel the DIA development. The shape of a  $P_d(r)$  function is shown

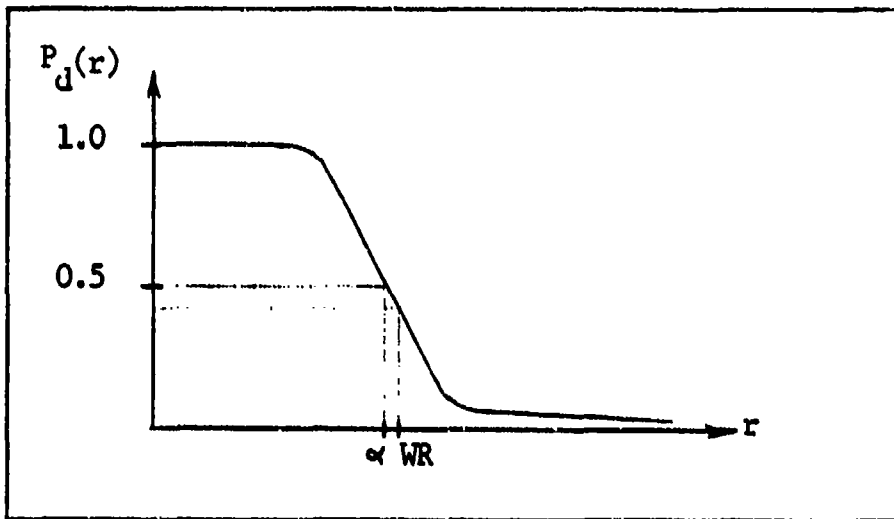


Figure 4. A probability of damage function  $P_d(r)$

in Figure 4. The independent variable is the distance  $r$  between the installation and the impact point.

The distance damage function is a nonlinear expression in integral form; it is specified by the location and dispersion parameters,  $\alpha$  and  $\beta$ .

$$P_d(r) = \frac{1}{\sqrt{2\pi}} \int_{-\infty}^{z(r)} e^{-1/2t^2} dt \quad (3)$$

$$z(r) = \frac{1}{\beta} \ln\left(\frac{\alpha}{r}\right) \quad (4)$$

The parameter  $t$  is a dummy variable of integration for the normal probability distribution. "The parameter  $\alpha$ , which is the median of the log normal density function, is the distance from ground zero at which there is a 50% chance of achieving a specified level of damage. The parameter  $\beta$  is the standard deviation of  $\ln(r)$ " (Ref 6:6,7). These parameters depend on the weapon radius ( $WR$ ) and distance damage sigma ( $\sigma_d$ ). If a weapon is detonated within a uniform distribution of targets, then the  $WR$  is



the radius of a circle centered at the weapon impact point. The circle contains as many targets undamaged to a specified level inside the circle as there are targets damaged to a specified level outside the circle. " $\sigma_d$  is a measure of the variance of the density function. A small  $\sigma_d$  indicates a relatively rapid fall off of the damage function; a large  $\sigma_d$  indicates a more gradual fall off" (Ref 6:11).

Prior to 1 September 1972, the analytical approximation of actual blast damage data was the circular coverage function with parameters WR and  $\sigma_d$ . However, before that date, DIA decided that the distance damage function with parameters  $\alpha$  and  $\beta$  provided a better fit to actual blast damage data. Since previously measured and calculated target vulnerability data depended on WR and  $\sigma_d$ , DIA developed mathematical transformations to determine  $\alpha$  and  $\beta$  from WR and  $\sigma_d$ .

$$\beta = \sqrt{-\ln(1 - \sigma_d^2)}$$

$$\alpha = WR e^{-\beta^2}$$

With these transformations, the distance damage function could specify the Pd for targets characterized by the Physical Vulnerability (PV) coding system.

Consequently, the probability of damage to installation j from weapon i,  $Pd_{i,j}$ , can be calculated using Eqs (3) and (4), after  $\sigma_d$ , WR, and r have been determined. WR and  $\sigma_d$  are parameters that are calculated using prespecified user values. WR depends on the weapon's yield and HOB and the installation's VNTK code. Hence, there is a unique WR for each weapon i-installation j interaction --  $WR_{i,j}$ .

Likewise,  $\sigma_d$  and  $\beta$  depend only on the installation's VNTK code. Hence, there is a unique  $\sigma_{d_j}$  and  $\beta_j$  for each installation --  $\sigma_{d_j}$  and  $\beta_j$ . Appendix A presents the calculation of  $\sigma_{d_j}$  and WR. The independent variable  $r$  is actually a function of two independent variables, the  $(X_1, Y_1)$  DGZ coordinates, and two constants, the  $(x_j, y_j)$  installation coordinates.

The  $P_d(r)$  cannot be expressed in closed form in terms of elementary functions; however, it can be calculated by use of the error function,  $\text{erf}(u)$  (Ref 6:21 and 1:298). The  $\text{erf}(u)$  specifies the probability that a standard normal random variable observation is within  $\pm u$  of the mean value.

$$\begin{aligned}
 P_d(r) = P_{d_{i,j}}(X_1, Y_1) &= 0.5 + 0.5 \text{erf} \left( \frac{|z(r)|}{\sqrt{2}} \right) && \text{for } z(r) \geq 0 \\
 &= 0.5 - 0.5 \text{erf} \left( \frac{|z(r)|}{\sqrt{2}} \right) && \text{for } z(r) < 0 \quad (5)
 \end{aligned}$$

where

$$\begin{aligned}
 z(r) = z(X_1, Y_1) &= \frac{1}{\beta_j} \ln \left( \frac{\alpha_{i,j}}{r(X_1, Y_1)} \right) \\
 &= \frac{1}{\beta_j} \ln \left( \frac{WR_{i,j}}{r(X_1, Y_1)} \right) - \beta_j \quad (6)
 \end{aligned}$$

A polynomial function of the independent variable  $u$  can approximate  $\text{erf}(u)$  (Ref 14:185).

In summary, if the CEP of the weapon can be assumed to equal 0, then the probability of damage  $P_{d_{i,j}}$  to installation  $j$  from weapon  $i$  can be calculated using Eqs (5) and (6). Prespecified target and weapon parameters are necessary to calculate  $WR_{i,j}$ ,  $\beta_j$ , and  $r(X_1, Y_1)$ .

CEP-Included Model If the CEP of the weapon delivery system cannot be assumed to equal 0, that is, the actual impact point of the weapon is unknown, then the distance  $r$  from the impact point to installation  $j$  is unknown. The geometry of the installation-weapon interaction is shown in Figure 3. The distance  $s$  from  $DGZ_1$  to installation  $j$  can be calculated from the  $(X_1, Y_1)$  DGZ coordinates, the  $(x_j, y_j)$  installation coordinates, and Eq (2). The unknown distance  $\rho$  from  $DGZ_1$  to the actual impact point is a function of  $s$  and the independent variables  $r$  and  $\theta$ .

The DIA model determines the probability of damage to installation  $j$  in the following way. First, for each possible impact point, the probability of damage is multiplied by the probability that the weapon arrives and detonates at that point (Ref 6:19). The sum of these products for all possible impact points specifies the probability of achieving the desired level of damage to installation  $j$  from weapon  $i$ ,  $Pd_{i,j}$ . This summation is a multiple integral over the area that contains all possible impact points.

$$Pd_{i,j} = \int_0^{2\pi} \int_0^{\infty} P_d(r) \frac{1}{2\pi\sigma^2} e^{-\frac{\rho^2(r,\theta)}{2\sigma^2}} r dr d\theta \quad (7)$$

where  $P_d(r)$  = distance damage function, Eq (3)

$$\sigma^2 = CEP/1.1774$$

$$\rho(r,\theta) = [r^2 + s^2 - 2rs \cos\theta]^{1/2}$$

For this CEDF model,  $Pd_{i,j}$  and  $P_d(r)$  are not the same function.  $Pd_{i,j}$

has two distinct, yet dependent, terms:  $P_d(r)$  and  $\frac{1}{2\pi\sigma^2} e^{-\frac{\rho^2(r,\theta)}{2\sigma^2}}$ .

(1)  $F_d(r)$  specifies the probability of damage to an installation from an impact point, and

(2)  $\frac{1}{2\pi\sigma^2} e^{-\frac{\rho^2}{2\sigma^2}}$  specifies the circular normal probability of the weapon arriving and detonating at the DGZ.

A closed form solution to Eq (7) does not exist; however, an analytical approximation does (Ref 6:23).

$$Pd_{i,j} = \int_a^b f(r) dr$$

The limits of integration, a and b, are selected such that when  $r < a$  or  $r > b$ ,  $f(r) = 0$ . They are functions of s, CEP, WR, and  $\sigma$ .

Appendix B presents the development of  $f(r)$ , the determination of a and b, and the calculation of  $Pd_{i,j}$ . The function  $f(r)$  has two different forms. Each form depends on the distance s between DGZ<sub>i</sub> and installation j, the distance r, and the weapon's CEP.

This integral can be evaluated using Gauss-Legendre quadrature, a numerical integration technique. This technique approximates a definite integral as a finite series. Each term in the series is a weighted function value.

$$Pd_{i,j} = \frac{(b-a)}{2} \sum_{k=1}^{10} ww_k * f(r_k) \quad (8)$$

$$\text{where } r_k = \frac{(b-a)}{2} zz_k + \frac{(a+b)}{2} \quad (9)$$

Gauss-Legendre quadrature differs from the more common trapezoidal numerical integration. In Gauss-Legendre, the distances between

TABLE I

Steps to Calculate  $Pd_{i,j}$ 

Step	Given Parameters or values	Results
1	VNIK	$\sigma_{dj}$
2	$\sigma_{dj}$	$\beta_j$
3	VNIK, Yield <sub>i</sub> , hob <sub>i</sub>	WR <sub>1,j</sub>
4	X <sub>i</sub> , Y <sub>i</sub> , x <sub>j</sub> , y <sub>j</sub>	r(X <sub>i</sub> , Y <sub>i</sub> ), s(X <sub>i</sub> , Y <sub>i</sub> )
5	$\beta_j$ , WR <sub>1,j</sub> , r	Pd <sub>1,j</sub> (CEP-Excluded)
5	$\sigma_{dj}$ , WR <sub>1,j</sub> , s, CEP <sub>i</sub>	a, b
6	$\beta_j$ , WR <sub>1,j</sub> , r, s, a, b, CEP <sub>i</sub>	Pd <sub>1,j</sub> (CEP-Included)

the  $r_k$  values along the abscissa are not equal. The values of the quadrature coefficients,  $w_k$ , and the base points,  $z_k$ , can be determined from the  $N^{\text{th}}$  Legendre polynomial. Gauss-Legendre quadrature is discussed in more detail in Appendix C.

In summary, if the CEP of the weapon cannot be assumed to equal 0, then the probability of damage to installation  $j$  from weapon  $i$ ,  $Pd_{i,j}$ , can be calculated using Eqs (8) and (9). Specific target and weapon parameters are necessary to calculate  $a$ ,  $b$ , and  $f(r_k)$ .

Each  $Pd_{i,j}$  is an integral part of a Complex Expected Damage Function (CEDF). Eqs (5) and (8) are used to calculate  $Pd_{i,j}$  for the CEP-Excluded and for the CEP-Included CEDF models. Table I lists a summary of the steps necessary to calculate  $Pd_{i,j}$ .

### The CEDF Model

The CEDF is an unconstrained, nonlinear function of the  $(X_i, Y_i)$  DGZ coordinates for each of the  $m$  weapons.

$$\text{CEDF} = \sum_{j=1}^n v_j * \left[ 1 - \prod_{i=1}^m (1 - Pd_{i,j} * Pa_i) \right] \quad (1)$$

The  $i$  subscript refers to one of the  $m$  weapons; the  $j$  subscript refers to one of the  $n$  installations. The  $2m$  independent variables of the CEDF are

$$(X_1, Y_1, X_2, Y_2, \dots, X_m, Y_m)$$

The  $2m$  elements of the DGZ coordinate vector,  $\underline{x}$ , are these  $2m$  variables in a revised order.

$$\underline{x} = (X_1, X_2, \dots, X_m, Y_1, Y_2, \dots, Y_m)$$

The  $(X_i, Y_i)$  DGZ coordinates of weapon  $i$  are  $(x_i, x_{i+m})$ . Similarly, the  $2n$  parameters specifying the  $(x_j, y_j)$  coordinates of the  $n$  installations are

$$(x_1, y_1, x_2, y_2, \dots, x_n, y_n)$$

The  $2n$  elements of the installation coordinate vector,  $\underline{xx}$ , are these  $2n$  parameters in a revised order.

$$\underline{xx} = (x_1, x_2, \dots, x_n, y_1, y_2, \dots, y_n)$$

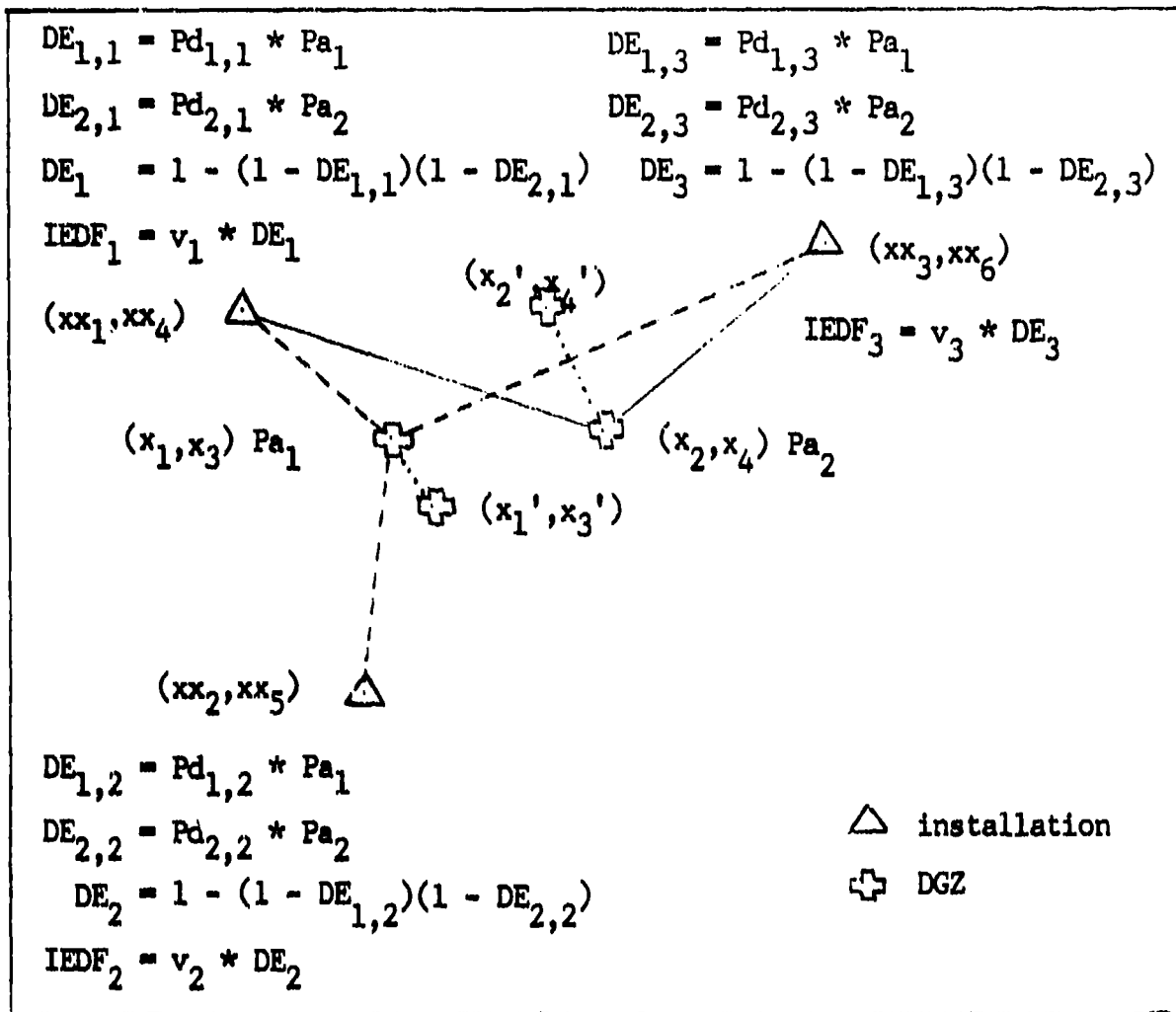


Figure 5. A representative CEDF with three installations and two weapons.

The  $(x_j, y_j)$  coordinates of installation  $j$  are  $(xx_j, xx_{j+n})$ .

Like the  $Pd_{i,j}$ , the damage expectancy for installation  $j$  from weapon  $i$  is a function of two independent variables  $DE_{i,j}(x_i, x_{i+m})$ . Similarly, like the CEDF, the cumulative damage expectancy for installation  $j$  from all weapons is a function of  $2m$  independent variables  $DE_j(x)$ .

A pictorial description of a representative CEDF is shown in Figure 5. The target complex consists of three installations and two weapons. Each installation is characterized by a value --  $v_j$ , a VNIK code, and  $(xx_j, xx_{j+3})$  coordinates. Each weapon is characterized

by a yield --  $Y_i$ , height of burst --  $HOB_i$ , probability of arrival --  $Pa_i$ , and  $(x_i, x_{i+2})$ . In order to determine all of the  $DE_{i,j}$ s, six  $Pd_{i,j}$ s are calculated according to the steps in Table I, one for each combination of  $i = 1, 2$  and  $j = 1, 2, 3$ . For the weapon coordinates  $(x_i, x_{i+2})$ ,  $i = 1, 2$

$$CEDF(\underline{x}) = v_1 * DE_1 + v_2 * DE_2 + v_3 * DE_3 \quad (1)$$

However, if the weapon coordinates are changed to  $(x_i', x_{i+2}')$ ,  $i = 1, 2$ , then  $DE_j$  may change for each of the  $j$  installations. That is,  $DE_j(\underline{x})$  may not equal  $DE_j(\underline{x}')$  for all  $j$ . If this is true, then the  $CEDF(\underline{x}')$  may be either greater than, equal, or less than  $CEDF(\underline{x})$ .

In order to maximize the CEDF, it is necessary to locate the  $\underline{x}^*$  DGZ coordinates such that

$$CEDF(\underline{x}^*) > CEDF(\underline{x}) \quad \text{for all } \underline{x}$$

One of the optimization techniques used to maximize the  $CEDF(\underline{x})$  and to locate the optimal  $\underline{x}^*$  DGZ coordinates required the gradient of the  $CEDF(\underline{x})$ .

#### Gradient of the CEP-Excluded Model

The Complex Expected Damage Function (CEDF) is a nonlinear function of  $2m$  variables -- the  $(x_i, x_{i+m})$  DGZ coordinates of the  $m$  weapons.

$$CEDF(\underline{x}) = \sum_{j=1}^n v_j * \left[ 1 - \prod_{i=1}^m (1 - Pd_{i,j}(x_i, x_{i+m}) * Pa_i) \right] \quad (1)$$

All parameters of the  $CEDF(\underline{x})$  are constants except the probability of



achieving a specified level of damage to installation j from weapon i,  $Pd_{i,j}$ . Each  $Pd_{i,j}$  is a function of two independent variables, the  $(x_i, x_{i+m})$  DGZ coordinates of weapon i. Therefore, to calculate the gradient of the CEDF, the  $Pd_{i,j}$  must be differentiable with respect to the two independent variables. A closed form analytical expression for the gradient of the CEP-Included  $Pd_{i,j}$ , Eq (7), was not available. This was one of the reasons for formulating the second version of the CEDF, the CEP-Excluded model. This section presents the calculation of the gradient of the CEP-Excluded CEDF.

The gradient of the CEDF( $\underline{x}$ ) is a vector of 2m elements.

$$\text{grad}(\text{CEDF}) = \frac{\partial \text{CEDF}(\underline{x})}{\partial \underline{x}} = \left( \frac{\partial \text{CEDF}}{\partial x_1} \quad \frac{\partial \text{CEDF}}{\partial x_2} \quad \dots \quad \frac{\partial \text{CEDF}}{\partial x_{2m}} \right) \quad (10)$$

where  $\text{CEDF}(\underline{x}) = v_1 * DE_1(\underline{x}) + v_2 * DE_2(\underline{x}) + \dots + v_n * DE_n(\underline{x})$

and  $DE_j(\underline{x}) = 1 - (1 - Pa_1 Pd_{1,j})(1 - Pa_2 Pd_{2,j}) \dots (1 - Pa_m Pd_{m,j})$

Since  $v_j$  is a constant, the  $k^{\text{th}}$  element of  $\text{grad}(\text{CEDF})$  is of the form

$$\begin{aligned} \frac{\partial \text{CEDF}}{\partial x_k} &= v_1 * \frac{\partial DE_1}{\partial x_k} + v_2 * \frac{\partial DE_2}{\partial x_k} + \dots + v_n * \frac{\partial DE_n}{\partial x_k} \\ &= \sum_{j=1}^n v_j * \frac{\partial DE_j}{\partial x_k} \end{aligned} \quad (11)$$

Each of the n terms of Eq (11) is of the form

$$v_j * \frac{\partial DE_j}{\partial x_k} = - v_j * \left[ \frac{\partial(1 - Pa_1 Pd_{1,j})}{\partial x_k} * \dots (1 - Pa_1 Pd_{1,j}) * \dots (1 - Pa_m Pd_{m,j}) \right. \\ \left. + \dots + (1 - Pa_1 Pd_{1,j}) * \dots \frac{\partial(1 - Pa_1 Pd_{1,j})}{\partial x_k} * \dots (1 - Pa_m Pd_{m,j}) \right. \\ \left. + \dots + (1 - Pa_1 Pd_{1,j}) * \dots (1 - Pa_1 Pd_{1,j}) * \dots \frac{\partial(1 - Pa_m Pd_{m,j})}{\partial x_k} \right]$$

However, since each  $Pd_{i,j}$  is a function of only two variables  $(x_i, x_{i+m})$ ,

for all i, all  $\frac{\partial(1 - Pa_i Pd_{i,j})}{\partial x_k}$  terms equal 0 except for  $k = i$  and  $i + m$ .

Hence, for  $k = i$  and  $i + m$

$$v_j * \frac{\partial DE_j}{\partial x_k} = - v_j * (1 - Pa_1 Pd_{1,j}) * \dots * \frac{\partial(1 - Pa_i Pd_{i,j})}{\partial x_k} * \dots (1 - Pa_m Pd_{m,j}) \\ = v_j * (1 - Pa_1 Pd_{1,j}) * \dots * Pa_i * \frac{\partial Pd_{i,j}}{\partial x_k} * \dots (1 - Pa_m Pd_{m,j}) \quad (12)$$

Now define

$$\text{factor}(j) = v_j \prod_{i=1}^m (1 - Pa_i Pd_{i,j})$$

and rewrite Eq (12) as

$$v_j * \frac{\partial DE_j}{\partial x_k} = \frac{\text{factor}(j)}{(1 - Pa_i Pd_{i,j})} * Pa_i * \frac{\partial Pd_{i,j}}{\partial x_k} \quad \text{for } k = i \text{ and } i + m \quad (13)$$

The gradient of the CEDF is a vector of  $2m$  elements. Eq (11) is the form of the  $k^{\text{th}}$  element. Similarly, each element is a summation of  $n$  terms. Eq (13) is the form of each of these  $n$  terms. Analytical expressions of  $\frac{\partial Pd_{i,j}}{\partial x_k}$  for  $k = i$  and  $i + m$  are needed to completely specify the gradient of the CEDF( $x$ ). The CEP-Excluded version of the  $Pd_{i,j}$  is

$$Pd_{i,j}(x_i, x_{i+m}) = 0.5 + 0.5 \operatorname{erf}\left(\frac{|z|}{\sqrt{2}}\right) \quad \text{for } z \geq 0 \quad (5)$$

$$= 0.5 - 0.5 \operatorname{erf}\left(\frac{|z|}{\sqrt{2}}\right) \quad \text{for } z < 0$$

where

$$z(r) = \frac{1}{\beta_j} \ln \frac{WR_{i,j} e^{-\beta_j^2}}{r} = \frac{1}{\beta_j} \ln(WR_{i,j} e^{-\beta_j^2}) - \ln(r) \quad (6)$$

First,  $\frac{\partial Pd_{i,j}}{\partial x_i}$  will be calculated for  $z \geq 0$ , that is, for  $r \leq WR_{i,j} e^{-\beta_j^2}$ .

Let  $u = \frac{|z|}{\sqrt{2}}$  and use the chain rule

$$\frac{\partial Pd_{i,j}}{\partial x_i} = 0.5 \frac{\partial \operatorname{erf}(u)}{\partial u} \left( \frac{\partial u}{\partial x_i} \right) \quad (14)$$

where

$$\frac{\partial u}{\partial x_i} = \frac{1}{\sqrt{2}} \frac{\partial |z|}{\partial x_i} \quad (15)$$

Now since  $r = \left[ (x_i - xx_j)^2 + (x_{i+m} - xx_{j+n})^2 \right]^{1/2}$  (2)

and  $z(r) = z(x_i, x_{i+m})$  from Eq (6), and again using the chain rule

$$\frac{\partial |z|}{\partial x_i} = \frac{\partial |z|}{\partial r} \frac{\partial r}{\partial x_i} \quad (16)$$

where

$$\frac{\partial |z|}{\partial r} = \frac{1}{\beta_j} \left( \frac{-1}{r} \right) = - \frac{1}{\beta_j r}$$

and

$$\frac{\partial r}{\partial x_i} = \frac{x_i - xx_j}{r} \quad (17)$$

hence

$$\frac{\partial u}{\partial x_i} = \frac{1}{\sqrt{2}} \left( \frac{-1}{\beta_j r} \right) \left( \frac{x_i - xx_j}{r} \right) \quad (18)$$

The derivative of  $\text{erf}(u)$  from the Handbook of Mathematical Functions with Formulas, Graphs, and Mathematical Tables (Ref 1:298,801) is

$$\frac{\partial \text{erf}(u)}{\partial u} = \frac{2}{\sqrt{\pi}} e^{-u^2} \quad (19)$$

Hence, combining Eqs (14), (18), and (19) specifies

$$\begin{aligned} \frac{\partial P_{d_{1,j}}}{\partial x_i} &= \frac{1}{2} \frac{2}{\sqrt{\pi}} e^{-u^2} \frac{1}{\sqrt{2}} \left( \frac{-1}{\beta_j r} \right) \left( \frac{x_i - xx_j}{r} \right) \quad \text{for } z \geq 0 \\ &= \frac{e^{-u^2}}{\sqrt{2\pi} \beta_j r^2} (xx_j - x_i) \end{aligned} \quad (20)$$

where 
$$u = \frac{1}{\sqrt{2}} \left| \frac{1}{\beta_j} \ln \left( \frac{WR_{i,j}}{r} \right) - \beta_j \right| \quad (21)$$

A similar mathematical development was used to calculate

$$\frac{\partial Pd_{i,i}}{\partial x_{i+m}} = \frac{e^{-u^2}}{\sqrt{2\pi} \beta_j r^2} (xx_{j+n} - x_{i+m}) \quad (22)$$

For  $z < 0$ , that is  $r > WR_{i,j} e^{-\beta_j^2}$ , then

$$\frac{\partial Pd_{i,i}}{\partial x_i} = -0.5 \frac{\partial \text{erf}(u)}{\partial u} \frac{\partial u}{\partial x_i} \quad (23)$$

The only difference between this development and the previous development for  $z > 0$  is the sign of  $\frac{\partial |z|}{\partial r}$ . This partial derivative is positive because  $r > WR_{i,j} e^{-\beta_j^2}$  and  $|z|$  is

$$|z| = \frac{1}{\beta_j} \left[ \ln(r) - \ln(WR_{i,j} e^{-\beta_j^2}) \right]$$

hence,

$$\frac{\partial |z|}{\partial r} = \frac{1}{\beta_j r} \quad (24)$$

Combining Eqs (15), (16), (17), and (24) yields

$$\frac{\partial u}{\partial x_i} = \frac{1}{\sqrt{2}} \left( \frac{1}{\beta_j r} \right) \left( \frac{x_i - xx_j}{r} \right) \quad (25)$$

Now Eqs (19), (23), and (25) specify

$$\begin{aligned} \frac{\partial Pd_{1,j}}{\partial x_1} &= -\frac{1}{2} \frac{2}{\sqrt{\pi}} e^{-u^2} \frac{1}{\sqrt{2}} \left( \frac{1}{\beta_{j,r}} \right) \left( \frac{x_1 - xx_j}{r} \right) \quad \text{for } z < 0 \\ &= \frac{e^{-u^2}}{\sqrt{2\pi} \beta_{j,r}^2} (xx_j - x_1) \end{aligned} \quad (26)$$

Hence, comparing Eqs (20) and (26),  $\frac{\partial Pd_{1,j}}{\partial x_1}$  is the same for all z.

A similar development indicates  $\frac{\partial Pd_{1,j}}{\partial x_{1+m}}$  is also the same for all z.

In summary, the gradient of the CEP-Excluded CDF( $\underline{x}$ ) is a vector of 2m elements. The  $k^{\text{th}}$  element of the gradient is

$$\frac{\partial \text{CEDF}}{\partial x_k} = \sum_{j=1}^n v_j * \frac{\partial DE_j}{\partial x_k} \quad (11)$$

where

$$v_j * \frac{\partial DE_j}{\partial x_k} = \frac{\text{factor}(j)}{(1 - Pa_1 Pd_{1,j})} * Pa_1 * \frac{\partial Pd_{1,j}}{\partial x_k} \quad \text{for } k = i \text{ and } i + m \quad (13)$$

Also, for  $k = i$

$$\frac{\partial Pd_{i,i}}{\partial x_k} = \frac{e^{-u^2}}{\sqrt{2\pi}\beta_j r^2} (xx_j - x_i) \quad (20)$$

and for  $k = i + m$

$$\frac{\partial Pd_{i,i}}{\partial x_k} = \frac{e^{-u^2}}{\sqrt{2\pi}\beta_j r^2} (xx_{j+n} - x_{i+m}) \quad (22)$$

where

$$u = \frac{|z|}{\sqrt{2}} = \frac{1}{\sqrt{2}} \left| \frac{1}{\beta_j} \ln \left( \frac{WR_{i,i}}{r} \right) - \beta_j \right| \quad (21)$$

and

$$r = \left[ (x_i - xx_j)^2 + (x_{i+m} - xx_{j+n})^2 \right]^{1/2} \quad (2)$$

### III. Optimization of the Complex Expected Damage Function

Two approaches are available to maximize a function of  $n$  variables-- analytical and numerical search. An analytical approach is preferred if the roots of the  $n$  equations defining the critical points of the function are easily determined and solved. These equations are the first partial derivatives of the function set equal to 0. However, if these analytical expressions are not easily determined or solved, then numerical search techniques are necessary to determine the maximum of the function. Numerical search techniques require an organized, efficient exploration of the solution space.

Numerical search techniques were used to maximize the Complex Expected Damage Function (CEDF) because of the complexity of the CEDF. This chapter presents a general methodology and overview of numerical search techniques that are used to maximize unconstrained functions. Also, this chapter discusses the two related techniques that were used to maximize the two versions of the CEDF -- the CEP-Included and the CEP-Excluded models. The primary difference between the two CEDF models is that there was a closed form expression for the gradient of the CEP Excluded model. Therefore, gradient search techniques could be used to maximize the CEP Excluded model. The CEP-Included model was maximized using Powell's conjugate directions method (Ref 23). This method maximizes a function using only function values. The CEP-Excluded model was maximized using a conjugate gradient with restarts method (Ref 24).



## Optimization

Optimization is a process that attains the best or most effective results for a problem, while satisfying any given conditions or constraints. Optimization can be either maximization or minimization. One part of this study was to maximize the CEDF( $\underline{x}$ ), a nonlinear function of  $2m$  independent variables -- the  $(x_1, x_{1+m})$  DGZ coordinates of each weapon. The CEDF( $\underline{x}$ ) is an unconstrained function. It can be maximized by minimizing  $-CEDF(\underline{x})$ . That is, the point  $\underline{x}^*$  in  $2m$  space, such that CEDF( $\underline{x}$ ) is a maximum, is the same point where  $-CEDF(\underline{x})$  is a minimum.

In this chapter, direct references to maximizing the CEDF are not made. Instead, all references concerning optimization reference minimizing an unconstrained, nonlinear function of  $n$  variables,  $f(\underline{x})$ ;  $\underline{x}$  is an  $n$  element vector in  $n$ -dimensional space,  $R^n$ . The gradient of  $f(\underline{x})$  is  $\nabla f(\underline{x})$ ; the Hessian matrix of  $f(\underline{x})$  is  $H(\underline{x})$ . A base point in  $R^n$  is  $\underline{x}^1$ ; the optimal point in  $R^n$  is  $\underline{x}^*$ .

There is an important difference between a strict local minimum and the global minimum of  $f(\underline{x})$ . The following two definitions are extracted from Avriel (Ref 3:10). A real valued function  $f(\underline{x})$  with domain  $D$  in  $R^n$  has a strict local minimum at  $\underline{x}^*$ , if there exists a number  $\delta$  such that

$$f(\underline{x}^*) < f(\underline{x}) \quad \text{for all } \underline{x} \in D \quad (27)$$

such that  $|\underline{x} - \underline{x}^*| \leq \delta$ . This definition states that  $\underline{x}^*$  is a local minimum over a region bounded by a number  $\delta$ . If Eq (27) holds for all  $\underline{x} \in D$ , that is,  $\underline{x}$  not contained within a bounded region, then  $\underline{x}^*$  is the global minimum. Optimization techniques locate the global minimum only

under special conditions. That is, the function is known to be unimodal. Generally, if a function is not known to contain a global minimum, an accepted procedure is to search D from a number of initial, separated base points to determine all local minimums. Beveridge and Schechter state "the only method of determining the global optimum is the direct comparison of the function values at various local optima" (Ref 5:357).

### Numerical Search Techniques

The numerical search for the minimum value of an unconstrained function  $f(\underline{x})$  with domain D in  $R^n$  is a sequential, iterative process. It includes the successive calculation of new objective function values,  $f(\underline{x}^1)$ , and the comparison of these values with the best value that has been obtained so far. It is necessary to determine  $\underline{x}^*$  by

$$f(\underline{x}^1) > f(\underline{x}^2) > \dots > f(\underline{x}^i) > \dots > f(\underline{x}^*) \quad \text{for all } \underline{x} \in D$$

While generating the sequence of  $\underline{x}^i$ , each unconstrained numerical search technique must consider three important elements -- the search direction, the distance to move, and the stopping criteria. From a base point  $\underline{x}^i$ , a search technique must select (1) a direction of movement  $\underline{d}$  and (2) a distance to move  $t$ . These values specify the next point in  $R^n$

$$\underline{x}^{i+1} = \underline{x}^i + t\underline{d}$$

If  $f(\underline{x}^{i+1}) < f(\underline{x}^i)$ , then  $\underline{x}^{i+1}$  is a better estimate of the local minimum

than  $\underline{x}^i$ . The stopping criteria for a search technique depends upon the values of either  $\underline{x}^{i+1}$ ,  $f(\underline{x}^{i+1})$ , or  $\nabla f(\underline{x}^{i+1})$ . That is, if either  $|\underline{x}^{i+1} - \underline{x}^i| \leq \delta_1$ , or  $|f(\underline{x}^{i+1}) - f(\underline{x}^i)| \leq \delta_2$ , or  $|\nabla f(\underline{x}^{i+1})| \leq \delta_3$ , then the technique stops iterating, and  $\underline{x}^* = \underline{x}^{i+1}$  is the optimal point in  $R^n$  such that  $f(\underline{x}^{i+1})$  is a minimum. Numerical search techniques use different methods to determine  $\underline{d}$  and  $t$ .

There are three categories of numerical search techniques (Ref 2:101). The first category includes direct search techniques. These techniques use only functional values to locate  $\underline{x}^{i+1}$  from  $\underline{x}^i$ . The second category includes gradient or first-order search techniques. These techniques use  $f(\underline{x}^i)$  and  $\nabla f(\underline{x}^i)$  to determine  $\underline{x}^{i+1}$ . Generally, gradient methods are more efficient and preferred to direct techniques (Ref 2:152; 5:321; and 10:386). However, when the gradient is not easily obtained, direct searches are more appropriate. The last category includes second-order techniques. These techniques use  $f(\underline{x}^i)$ ,  $\nabla f(\underline{x}^i)$ , and the Hessian,  $H(\underline{x}^i)$ , to locate  $\underline{x}^{i+1}$ . Detailed explanations of the following techniques can be found in most optimization books (Ref 2; 3; 5; and 10). Hence, only a brief explanation is presented here.

If an unconstrained objective function  $f(\underline{x})$  is not easily differentiated, then a direct search technique is necessary to minimize  $f(\underline{x})$ . These techniques use two stages, an exploratory and a pattern, to move from  $\underline{x}^i$  to  $\underline{x}^{i+1}$ . Two older techniques are the Hooke-Jeeves pattern search and Rosenbrock's method of rotating directions. In the exploratory stages, Hooke-Jeeves only searches along the axial coordinate directions; Rosenbrock searches along a set of mutually orthogonal directions that are determined from  $\underline{x}^i$  and  $\underline{x}^{i+1}$ . Both of these techniques

use a fixed step length when exploring around  $x^i$ . The exploratory function evaluations specify the direction  $d$  of the pattern move. A more efficient technique is Powell's method of conjugate directions (Ref 23). In the exploratory stage, Powell's method searches along conjugate directions that are determined from  $x^i$  and  $n - 1$  of the previous  $n$  exploratory search directions. Conjugate directions are a generalization of orthogonal directions. Also, Powell's method does not use a fixed step length. Rather, this method conducts a one-dimensional search in each of the conjugate directions from  $x^i$ . A more complete description of conjugate directions and Powell's method of conjugate directions is presented later in this chapter.

Gradient search techniques are separated into two categories, either those techniques that follow the gradient as closely as possible (the methods of steepest descent) or those techniques that use the gradient to guide the search (the conjugate gradient methods). Cauchy's steepest descent method uses the gradient to find the direction of greatest functional decrease from a base point. The greatest decrease in  $f(x)$  is in the direction of the largest negative gradient. That is,

$$d = -\nabla f(x^i)$$

$$x^{i+1} = x^i - t \nabla f(x^i)$$

The steepest descent method uses a one-dimensional minimization search in the direction of  $-\nabla f(x^i)$  to determine the step length  $t$  and to subsequently locate  $x^{i+1}$ .

$$\min_t f(x^i - t \nabla f(x^i))$$

Conversely, the method of conjugate gradients locates a new base point  $x^{i+1}$  by searching along a mutually conjugate direction  $d$  (Ref 9 and 24). The direction  $d$  is determined using the gradient at the current base point and the previous search direction. From  $x^i$ , the method uses a one-dimensional minimization search in this direction to determine the step distance  $t$ .

$$\min_t f(x^i - td)$$

This one-dimensional search establishes a new base point  $x^{i+1}$ . A more complete description of the conjugate gradient method is presented later in this chapter.

If first and second partial derivatives of  $f(x)$  are available, then Newton's method could be used to minimize the function. This technique uses the function's gradient and Hessian to specify the direction and the distance of the maximum decrease in  $f(x)$ .

$$x^{i+1} = x^i - H(x^i)^{-1} \nabla f(x^i)$$

Avrial states, "If there are a large number of variables, the function and derivative evaluations and especially the matrix inversions, are time-consuming and expensive operations" (Ref 3:288).

These are not the only techniques available to minimize unconstrained, nonlinear functions. However, they are representative of the three categories of techniques -- direct, gradient, and second-order. A detailed presentation and summary of numerical search techniques for each category is provided by Gill, Murray, and

Wright (Ref 10). In addition to the above techniques, several variations are available to minimize unconstrained nonlinear functions. The most powerful is the "variable metric" or quasi-Newton method. This algorithm differs from Newton's method. It does not use the Hessian matrix. Instead of calculating  $H(x^i)$ , the technique approximates the inverse of  $H(x^i)$  by using the gradient and the previous estimate of the inverse. There are other variations of Newton's method. Similarly, finite difference techniques are variations of gradient methods; they use function values to approximate  $\nabla f(x^i)$ . Generally, it is not possible to single out a method as the one to be used in every case.

Each form of the Complex Expected Damage Function (CEDF) was maximized using only one technique. Since an analytical expression for the gradient of the CEP-Included model was not available, it was maximized using a direct search technique -- Powell's method of conjugate directions. Conversely, since an analytical expression for the gradient of the CEP-Excluded model was calculated, it was maximized using a gradient search technique -- a conjugate gradient with restarts method.

#### Conjugate Directions and Quadratic Termination

Conjugate directions are a generalization of orthogonal directions. A set of  $n$  vectors  $d^1, d^2, \dots, d^n$  in  $R^n$  are orthogonal if their inner product is 0, that is,

$$d_i^T d_j = 0 \quad \text{for all } i \neq j \quad (28)$$

A set of  $n$  vectors  $d^i$  is mutually conjugate with respect to the  $n \times n$

symmetric, positive definite matrix A if

$$d_i^T A d_j = 0 \quad \text{for all } i \neq j \quad (29)$$

Thus, for every  $n \times n$  symmetric, positive definite matrix there is at least one set of  $n$  mutually conjugate directions. If the matrix A is the identity matrix, then Eq (29) becomes Eq (28), the definition of orthogonal directions.

Powell's method of conjugate directions and conjugate gradient methods depend upon the concept of quadratic termination. Powell proved the following theorem on quadratic termination (Ref 23).

Theorem: If  $d^1, d^2, \dots, d^m$ ,  $m < n$  are mutually conjugate directions, then the minimum of the quadratic function  $f(x)$  is a point in  $m$ -dimensional space,  $R^m$ , containing  $x^0$ , the initial point, and the directions  $d^1, d^2, \dots, d^m$ , and the minimum of  $f(x)$  may be found by searching along each of the directions only once. The required minimum is the point

$$x^* = x^0 + \sum_{i=1}^m t_i d^i$$

The distances  $t_i$  are determined by minimizing  $f(x)$  in each direction  $d^i$

$$\min_t f(x^0 + \sum_{i=1}^m t_i d^i)$$

where

$$f(x) = x^T A x + b x + c$$

and, A is a symmetric, positive definite Hessian matrix.

Powell's theorem proved that the minimum of a quadratic function  $f(\underline{x})$  with domain  $D$  in  $R^n$  and a symmetric, positive definite Hessian could be located in  $n$  steps. Each step is a search along one of the  $n$  mutually conjugate directions  $\underline{d}_j^1$ . However, since each direction  $\underline{d}_j^1$  has  $n$  component directions in  $R^n$ , each step requires  $n$  one-dimensional searches to minimize  $f(\underline{x})$ .

### CEDF Optimization Methods

Powell's theorem is the basis for the method of conjugate directions and conjugate gradient methods. If  $f(\underline{x})$  is quadratic, then the minimum can be located in a finite ( $\leq n$ ) number of steps. However, even if  $f(\underline{x})$  is not quadratic, the concept of quadratic termination can still be used to locate the minimum. When the method is applied to non-quadratic functions, it becomes iterative and a test of convergence is necessary to determine the minimum of  $f(\underline{x})$ . This section presents a brief explanation of these two optimization techniques. Detailed explanations of them are available in Refs 9, 23, and 24; also, most optimization books provide complete explanations of these techniques.

Powell's Method of Conjugate Directions. This section presents an algorithm for Powell's method of conjugate directions (Ref 17 and 23). This method assumes quadratic convergence of  $f(\underline{x})$ ; the method will not locate the local minimum in  $n$  steps unless the  $f(\underline{x})$  is quadratic. Instead, the method iterates from  $\underline{x}^i$  to  $\underline{x}^{i+1}$  until  $|\underline{x}^{i+1} - \underline{x}^i| \leq \epsilon$ . In this development, the superscript  $i$  refers to the iteration and the subscript  $j$  refers to one of the  $n$ -dimensional component directions of  $R^n$ . The starting point in  $R^n$  is  $\underline{x}^0$ ; the initial search directions  $\underline{d}_j^1$  are the  $R^n$  coordinate directions.



- An iteration process is used to locate  $\tilde{x}^*$  such that  $f(\tilde{x}^*)$  is a local minimum. For the  $i^{\text{th}}$  iteration,
1. From  $\tilde{x}^i$ , search each of the  $n$  directions  $\tilde{d}_j^i$  where  $j=1, \dots, n$ . These one-dimensional searches use functional values to locate a minimum in each direction. A quadratic approximation and unimodal behavior of  $f(\tilde{x})$  is assumed.
  2. These searches locate three specific points in  $R^n$  --  $\tilde{x}_n^i$ , the last point;  $\tilde{x}_t^i$ , an expanded point; and  $\tilde{x}_m^i$ , the point where the greatest decrease in  $f(\tilde{x}_j^i)$  occurred.
  3. The convergence test checks  $\tilde{x}_n^i$  to determine if  $f(\tilde{x}_n^i)$  is a local minimum. If  $\tilde{x}_n^i$  passes the convergence condition  $|\tilde{x}_n^i - \tilde{x}_n^{i-1}| \leq \delta$ , then  $\tilde{x}^* = \tilde{x}_n^i$ . If not, the algorithm continues.
  4. The modification test checks the decrease in  $f(\tilde{x})$  from  $\tilde{x}_1^i$  to  $\tilde{x}_n^i$ . These functional changes specify the set of directions  $\tilde{d}_j^{i+1}$  for the next iteration. The same mutually conjugate directions may be used again or a new set of mutually conjugate directions may be determined.

A Conjugate Gradient Method. This section presents an algorithm for a conjugate gradient with restarts method (Ref 9 and 24). Again, for functions which are not quadratic, the method will not locate the local minimum in  $n$  steps. Instead, the method iterates from  $\tilde{x}^i$  to  $\tilde{x}^{i+1}$  until  $|\nabla f(\tilde{x}^{i+1})| \leq \delta$ .

$$\tilde{x}^{i+1} = \tilde{x}^i + t_i \tilde{d}^i$$

The direction  $\underline{d}^i$  is mutually conjugate to the previous  $i - 1$  search directions; it is determined using the previous direction  $\underline{d}^{i-1}$  and  $\nabla f(\underline{x}^i)$ . The starting point in  $R^n$  is  $\underline{x}^0$ ; the initial search direction is the negative of the gradient,  $-\nabla f(\underline{x}^0)$ .

An iterative process is used to locate  $\underline{x}^*$  such that  $f(\underline{x}^*)$  is a local minimum. For the  $i^{\text{th}}$  iteration,

1. Calculate  $\nabla f(\underline{x}^i)$
2. From  $\underline{x}^i$ , use a one-dimensional minimization search in the direction  $\underline{d}^i$  to determine the step length  $t_i$  and to subsequently locate the point  $\underline{x}^{i+1}$ .

$$\underline{x}^{i+1} = \underline{x}^i + t_i \underline{d}^i$$

$$\min_{t_i} f(\underline{x}^i + t_i \underline{d}^i)$$

3. Calculate  $\nabla f(\underline{x}^{i+1})$
4. The convergence test checks  $\underline{x}^{i+1}$  to determine if  $f(\underline{x}^{i+1})$  is a local minimum. If  $\|\nabla f(\underline{x}^{i+1})\| < \delta$ , then  $\underline{x}^* = \underline{x}^{i+1}$ . If not, the algorithm continues.

5. Compute 
$$\beta_i = \frac{\|\nabla f(\underline{x}^{i+1})\|^2}{\|\nabla f(\underline{x}^i)\|^2}$$

6. Determine the next mutually conjugate search direction.

$$\underline{d}^{i+1} = -\nabla f(\underline{x}^{i+1}) + \beta_i \underline{d}^i$$

This algorithm locates the minimum of a quadratic function with a

symmetric, positive definite Hessian matrix in  $n$  or less iterations. However, for functions that are not quadratic, the minimum will generally not be determined in  $n$  steps. After the  $n$  steps,  $n$  mutually orthogonal directions have been searched.  $\underline{x}^n$  may or may not have converged rapidly towards  $\underline{x}^*$ .

For functions with slow rates of convergence, because of nearly parallel  $\underline{d}^i$  and  $\underline{d}^{i+1}$ , Fletcher and Reeves developed the restart procedure (Ref 9). After every  $n + 1$  steps, the method reverts to the direction of steepest descent, the largest negative gradient, for the next search direction. That is, following iteration  $i = n + 1$ , which located  $\underline{x}^{n+2}$ , the direction  $\underline{d}^{n+2}$  would not be specified as in step 6 above, but rather  $\underline{d}^{n+2} = -\nabla f(\underline{x}^{n+2})$ . "Thus the whole procedure is restarted from the current  $\underline{x}$ , discarding all previous experience that would normally be transmitted in the calculation of  $\underline{d}^i$ . The process remains quadratically convergent provided such restarts are not more frequent than every  $n$  steps" (Ref 9).

The CEDF models developed in Chapter II are maximized with these two techniques. Powell's method of conjugate directions maximizes the CEP-Included CEDF model; a conjugate gradient with restarts method maximizes the CEP-Excluded CEDF model. These methods require the vector of the  $2m$  independent variables  $\underline{x}$  and the function  $\text{CEDF}(\underline{x})$ ; the conjugate gradient technique also requires the gradient of  $\text{CEDF}(\underline{x})$ . The computerization of the algorithm that maximizes the two  $\text{CEDF}(\underline{x})$  models is presented in Chapter IV.

Greenwood developed a similar version of the  $\text{CEDF}(\underline{x})$  (Ref 12). His algorithm uses a different, yet related approach to determine

optimal DGZ locations. His function  $G(\underline{x})$  depends on the total expected target value undamaged. The  $2m$  first partial derivatives of  $G(\underline{x})$  are set equal to 0. Then these  $2m$  nonlinear equations are solved iteratively to yield a  $\underline{x}^*$  such that  $G(\underline{x}^*)$  is a minimum. NUCWAVE uses a modified Greenwood technique to determine optimal DGZ locations (Ref 25:4-3). It optimizes one weapon at a time. Hence, it iteratively solves 2 nonlinear equations to determine  $(X_i, Y_i)$  -- the coordinates of weapon  $i$ . Then it repeats the process for the next weapon.

#### IV. Computerization, Verification, and Validation of the CEDF Maximization Algorithm

The Complex Expected Damage Function (CEDF) maximization algorithm includes the CEDF models, CEP-Included and CEP-Excluded, and the optimization techniques, Powell's method of conjugate directions and the conjugate gradient with restarts method. The algorithm determines optimal DGZ locations for a finite number of nuclear weapons against installations in a target complex by maximizing the CEDF.

Evaluation of the algorithm consisted of three related stages -- construction, verification, and validation. These stages formed an iterative process that was necessary to develop user confidence in the capability of the algorithm. Construction is the formulation and computerization of a model. The computerization of the CEDF maximization algorithm used a modular approach. Smaller segments of the CEDF model were developed to accomplish lower level procedures. These segments became subprograms in the final computer code. Verification of the CEDF maximization algorithm used example problems to insure that the results of each subprogram were correct. Validation measures the relative agreement between the model and the system modeled (Ref 26:215). Validation of the CEDF maximization algorithm was a comparison of the results from the algorithm with the results from a current DGZ model. This chapter presents the evaluation of the CEDF maximization algorithm with respect to these three stages.

##### Computerization

A flow chart of the CEDF maximization algorithm is shown in Figure 6.

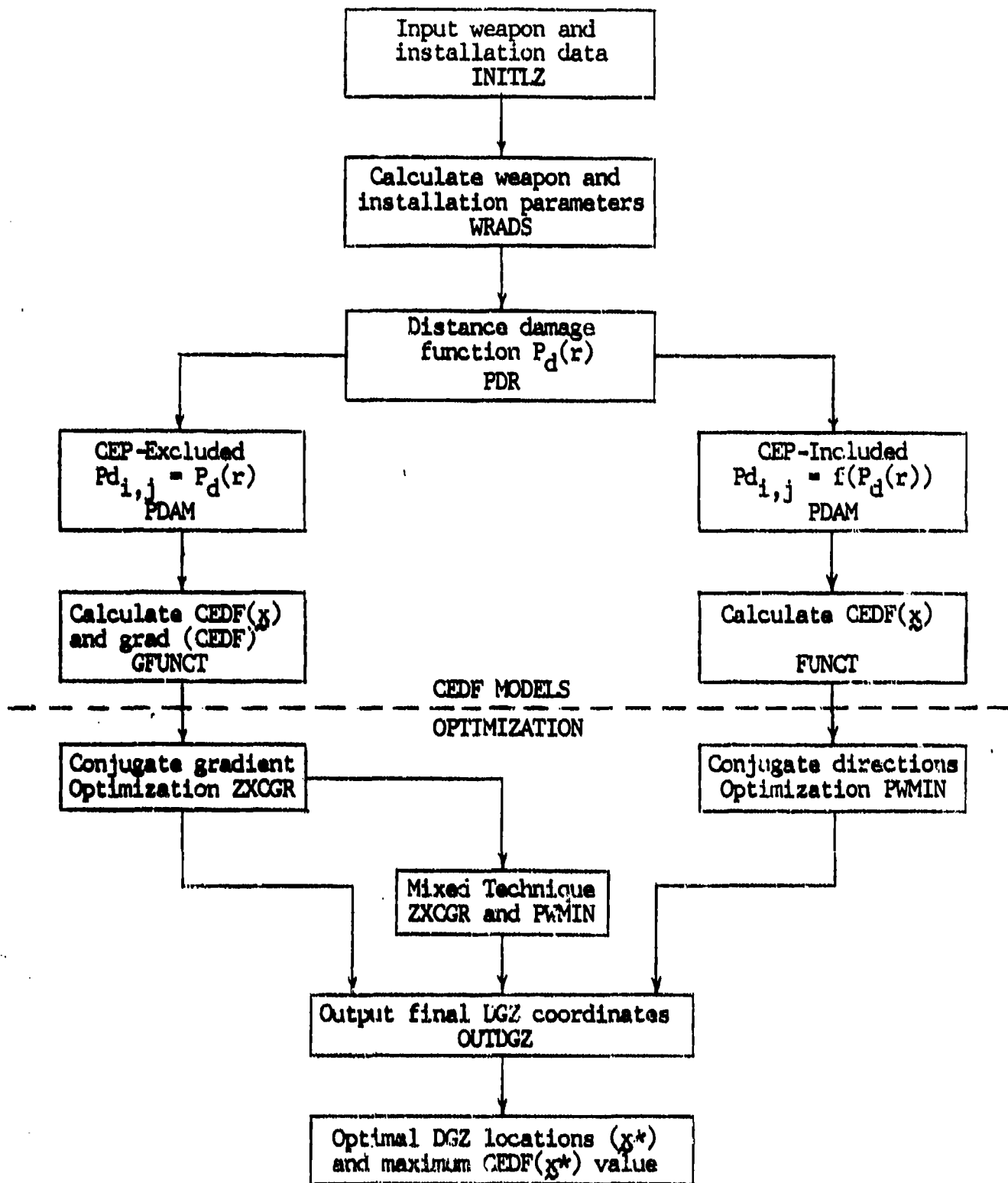


Figure 6. Flowchart of the CEDF Maximization Algorithm

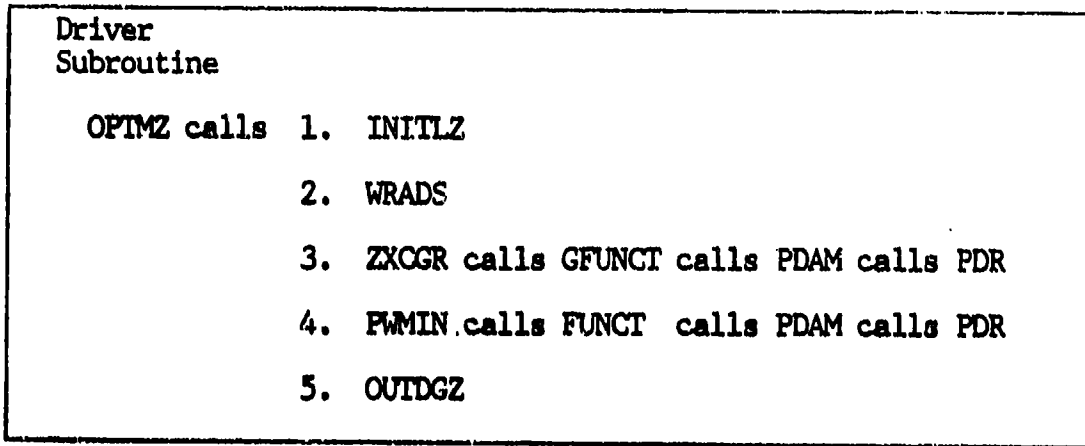


Figure 7. CEDF Maximization Algorithm Subroutine Hierarchy

The symmetry of Figure 6 illustrates several characteristics of the algorithm. The blocks above the dashed line correspond to the procedures that use weapon and installation parameters to develop the  $CEDF(x)$  and the gradient of the  $CEDF(x)$ . The lower blocks correspond to the optimization techniques that were used to maximize the respective CEDF. The left blocks correspond to the CEP-Excluded model; alternately, the right blocks correspond to the CEP-Included model. The upper three and lower three blocks are common to both CEDF models. Each block is a smaller segment of the CEDF maximization algorithm.

The computer code of the CEDF maximization algorithm was written using FORTRAN V. Appendix D contains a listing of the code and a glossary of the FORTRAN variables. The computer code includes a driver module, seven subroutines and two functions. The hierarchy of the algorithm's subprograms is shown in Figure 7. All program variables, including weapon and installation parameters, that are used in more than one subprogram, are stored in six named common blocks. Only the DGZ coordinate vector  $x$  is transferred between subprograms by the subprograms' argument lists.

The driver module OPTMZ controls the CEDF maximization algorithm. OPTMZ calls the five highest level subroutines. The primary functions of these subroutines are: (1) INITLZ inputs user-specified weapon and installation parameters, (2) WRADS calculates additional installation and weapon parameters, (3) ZXCGR is a conjugate gradient with restarts subroutine that maximizes the CEP-Excluded CEDF, (4) PDMIN is a conjugate directions subroutine that maximizes the CEP-Included CEDF, and (5) OUTDGZ outputs the final DGZ coordinates. ZXCGR calls GFUNCT, a subroutine that calculates the value of the  $CEDF(x)$  and the gradient of the  $CEDF(x)$ . PDMIN calls FUNCT, a subroutine that calculates the value of the  $CEDF(x)$ . GFUNCT and FUNCT call PDAM, a function that calculates the probability of achieving a specified level of damage to installation  $j$  from weapon  $i$ ,  $P_{d_{i,j}}$ . PDAM, in turn, calls PDR, a function that calculates the distance damage function,  $P_d(r)$ . More complete descriptions of these subroutines and functions are given below. WRADS, PDAM, and PDR are modifications of subprograms from Mathematical Background and Programming Aids for the Physical Vulnerability System for Nuclear Weapons (Ref 6).

INITLZ. This subroutine has four primary functions. First, it reads user-specified weapon and installation parameters from an external file, INDATA. Appendix E contains samples of an input file and an output data file. For each weapon  $i$ , the user specifies a yield, a hob, and a  $P_a$ ; the user may specify initial DGZ coordinates. Also, for each installation  $j$ , the user specifies coordinates, a VNTK code, and a value. The user inputs the weapon and installation latitude and longitude in degrees-minutes-seconds and the direction from either the prime meridian or the equator. Positive coordinates are east of the prime



meridian and north of the equator.

Second, INITLZ assigns the initial coordinates of the  $m$  weapons, prior to maximization. The user has three options: (1) provide independent estimates of the weapon coordinates; (2) let INITLZ assign the coordinates of the  $m$  highest valued installations to be the coordinates of the  $m$  weapons in decreasing order of yield, that is, the largest yield weapon is initially located at the highest valued installation; or (3) let INITLZ assign the coordinates of the  $m$  hardest installations to be the coordinates of the  $m$  weapons in decreasing order of yield, that is, the largest yield weapon is initially located at the installation with the largest VN number.

Third, INITLZ transforms all weapon and installation degrees-minutes-seconds into coordinates measured in feet and relative to a common origin in an XY coordinate system. The CEDF maximization algorithm assumes a flat earth model to locate all coordinates. Each minute of latitude equals 6080 feet. However, one minute of longitude equals 6080 feet only at the equator. When the latitude is not the equator, one minute of longitude is less than 6080 feet because of the merging of the meridian lines. The scale factor is the cosine of the latitude.

Lastly, INITLZ specifies accuracy requirements for ZXCGR and PWIN. These subroutines need prespecified values to test for the convergence of  $\chi$  to the maximum value of  $CEDF(\chi^*)$ .

WRADS. This subroutine calculates additional weapon and installation parameters from the user-specified parameters. For each installation  $j$ , it determines a distance damage sigma ( $\sigma_{d_j}$ ) and a  $\beta_j$ . Also, for each weapon  $i$ -installation  $j$  combination, it calculates a weapon radius,  $WR_{i,j}$ . These calculations are described in Appendix A.

PDR. This function calculates the distance damage function  $P_d(r)$ , the probability of achieving a specified level of damage to installation  $j$  from weapon  $i$  when the distance  $r$  between installation  $j$  and weapon  $i$  is known. See Eq (5).

PDAM. This function calculates the probability of achieving a specified level of damage to installation  $j$  from weapon  $i$ ,  $P_{d_{i,j}}$ . For the CEP-Excluded CEDF model,  $P_{d_{i,j}}$  is the distance damage function from PDR. For the CEP-Included CEDF model, the distance  $r$  between installation  $j$  and the impact point is unknown, and  $P_{d_{i,j}}$  is calculated using Gauss-Legendre quadrature and the distance damage function. See Eq (8).

GFUNCT. This subroutine calculates the  $CEDF(\underline{x})$  and the gradient of the  $CEDF(\underline{x})$ . One function and gradient evaluation requires  $m * n$  calls to function PDAM. These calls specify  $P_{d_{i,j}}$  for each weapon  $i$ -installation  $j$  combination using the CEP-Excluded model.  $CEDF(\underline{x})$  is calculated using Eq (1). Each element of the gradient is calculated using Eq (11).

FUNCT. This subroutine also calculates the  $CEDF(\underline{x})$  using Eq (1), and one function evaluation requires  $m * n$  calls to function PDAM. However, these calls specify  $P_{d_{i,j}}$  for each weapon  $i$ -installation  $j$  combination using the CEP-Included CEDF model.

ZXOGR. This subroutine minimizes  $-CEDF(\underline{x})$  for the CEP-Excluded model. It is a conjugate gradient with restarts routine from the International Mathematical and Statistical Libraries, Inc. (Ref 16:ZXOGR). ZXOGR requires function and gradient evaluations from GFUNCT and the DGZ coordinate vector  $\underline{x}$ . It uses two control parameters -- DFPRED and ACC. DFPRED specifies an estimate of the expected increase in the CEDF; ACC specifies the desired accuracy of the convergence check. This check

requires the sum of the squares of the gradient elements to be less than ACC.

PWMIN. This subroutine minimizes  $-CEDF(x)$  for the CEP-Included model. It is a conjugate directions routine from Optimization Techniques with FORTRAN (Ref 17:331-343). PWMIN requires function evaluations from FUNCT and the DGZ coordinate vector  $x$ . It also uses two control parameters -- ESCALE and E. ESCALE specifies the maximum step size multiplier for a single step of any  $x_k$ ; E specifies the accuracy of the convergence check. This check requires the absolute value of the differences between each element of  $x^i$  and  $x^{i+1}$  to be less than E.

OUTDGZ. This subroutine translates the XY coordinates of the final DGZs from feet into degrees-minutes-seconds and the direction from either the prime meridian or the equator. Then it outputs these coordinates to the external data file, 'TAPE6.

The CEDF maximization algorithm provides three sets of optimal DGZ locations. The first set is from the CEP-Excluded CEDF model and ZXCGR maximization; the second set is from the CEP-Included CEDF model and PWMIN maximization. The last set of DGZ locations is from both CEDF models and ZXCGR and PWMIN maximization -- a mixed technique.

### Verification

The verification of the CEDF maximization algorithm included four phases. Each phase verified the subprograms of the algorithm using example problems. For each computer program, the results of each example problem, including the values of intermediate variables, were calculated independently of the respective computer program. Then the computer program solved the example problem. PRINT statements in the

program printed values of most FORTRAN variables. These values were compared with the values calculated by pencil and paper to verify that the computer program calculated the correct values.

The first phase verified five lower level subprograms -- PDR, PDAM, WRADS, INITLZ, and OUTDGZ. Each of these modules was coded and debugged as a small FORTRAN program. Mathematical Background and Programming Aids for the Physical Vulnerability System for Nuclear Weapons includes example problems. Fifteen of these problems were used to check PDR, PDAM, and WRADS. These programs calculated the same values as the example problems. The outputs of INITLZ for several example problems were compared with results that were calculated independently of the computer program. These comparisons indicated INITLZ was properly forming the XY coordinate system and the installation and DGZ coordinate vectors. Similarly, the outputs of OUTDGZ for several test cases were compared with pencil and paper calculated results. These comparisons indicated OUTDGZ was correctly translating the final DGZ coordinate vector from feet into degrees-minutes-seconds and the direction from either the prime meridian or the equator. These five subprograms were merged into one program and became the foundation of the next verification phase.

The second phase verified the subroutine FUNCT. The small programs, PDAM and PDR, became FORTRAN functions; the programs WRADS, INITLZ, and OUTDGZ, became FORTRAN subroutines. FUNCT calculates the value of the CEDF(x) using Eq (1). The pencil and paper calculated results from several example problems were compared with the results from FUNCT. One example included two identical installations. Each installation's value and VNTK code were 15.0 and 15P2. The distance between the two installations was 6000 feet. Two identical weapons

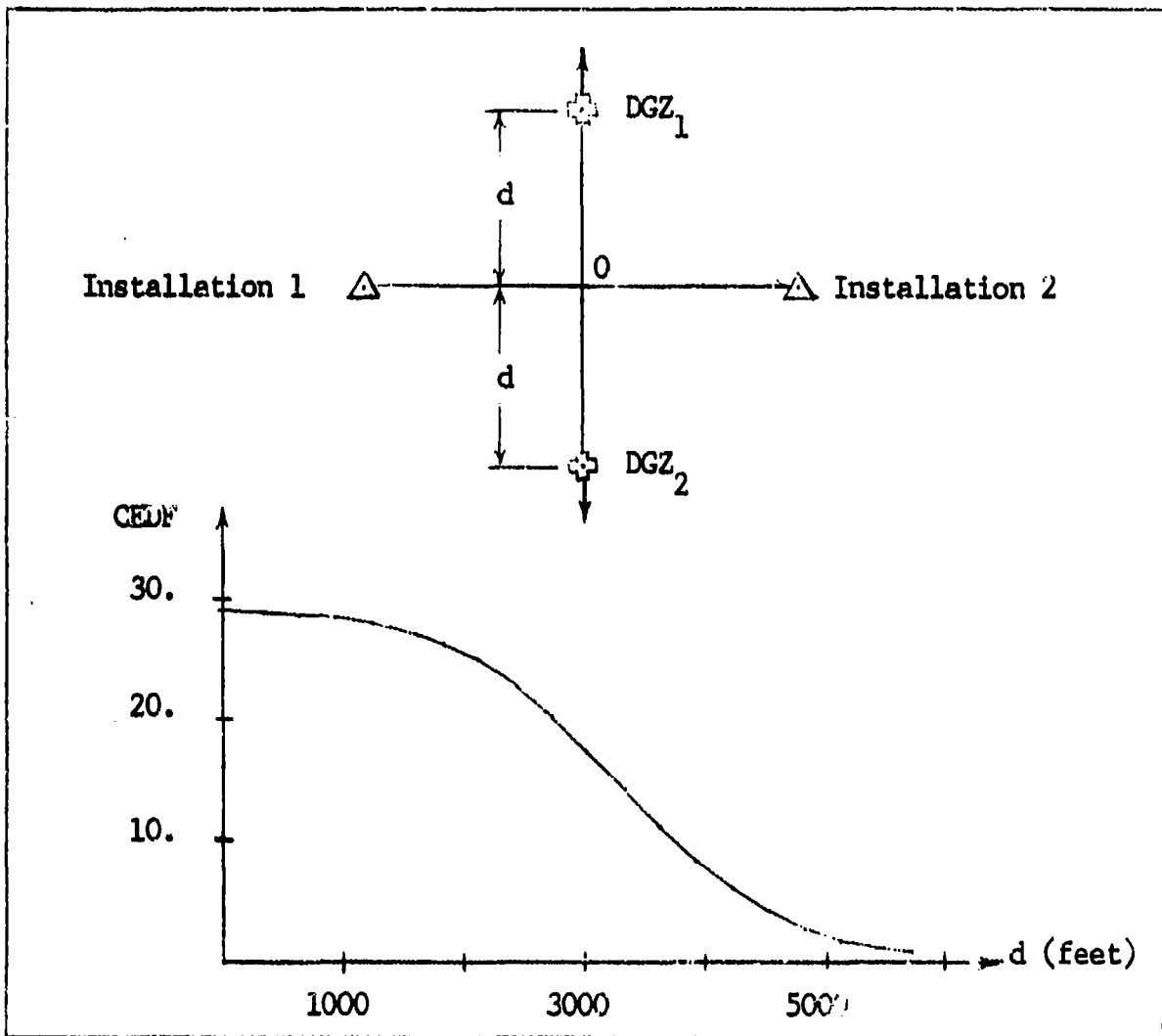


Figure 8. The CEDF for a two weapon-two installation geometry.

were collocated halfway between the two installations. Each weapon's yield, height of burst, and CEP were 100-kt, 1000 feet, and 600 feet. The independent calculation of the CEDF for this complex was 29.15; the CEDF value from FUNCT was 29.1492. These example problems indicated FUNCT was properly calculating the  $CEDF(x)$ .

This two weapon-two installation complex was used to investigate the results of moving the two collocated DGZs. The geometry of this complex is shown in Figure 8. Initially, the two 100-kt weapons were collocated at point 0, and the CEDF value was 29.15. The CEDF value

decreased as the two DGZs were moved in opposite directions a distance  $d$  from point 0. A graph of CEDF versus  $d$  for this problem is also included in Figure 8. This example indicated the existence of a CEDF maximum, on the line considered, as the distances between the DGZs and the installations varied.

The third phase verified the gradient calculation of the CEP-Excluded CEDF in the subroutine GFUNCT. GFUNCT also calculates the CEDF( $x$ ) using Eq (1). The gradient vector from GFUNCT was checked using two weapon-installation geometries. Appendix F includes the table and calculations used to verify the gradient of the CEDF( $x$ ) for these two examples.

The first example included one weapon and two installations. The first installation's value and VNIK code were 5000 and 11P2; the second installation's value and VNIK code were 12000 and 15P2. The weapon's yield and height of burst were 100-kt and 1000 feet, and the CEP was 0 feet. Forty values of the CEDF( $x$ ) were calculated for different DGZ locations. The  $x$  direction was along the line connecting the two installations. These 40 values were then plotted. Figure 9 is a plot of CEDF( $x$ ) versus  $x$  for this example. A DGZ between the two installations was selected ( $x = 63500$ ) and the gradient calculated using two methods. In this example, the gradient had only one element because the  $y$  variable was constant, and only the  $x$  variable was allowed to vary. The gradient values for the two calculation methods were compared with the gradient from GFUNCT. The first method used a difference equation  $\frac{\Delta \text{CEDF}}{\Delta x}$  to approximate the gradient. For the DGZ selected, the difference equation approximation of the gradient was 3.939. The second method was pencil and paper calculations of all the steps necessary to determine

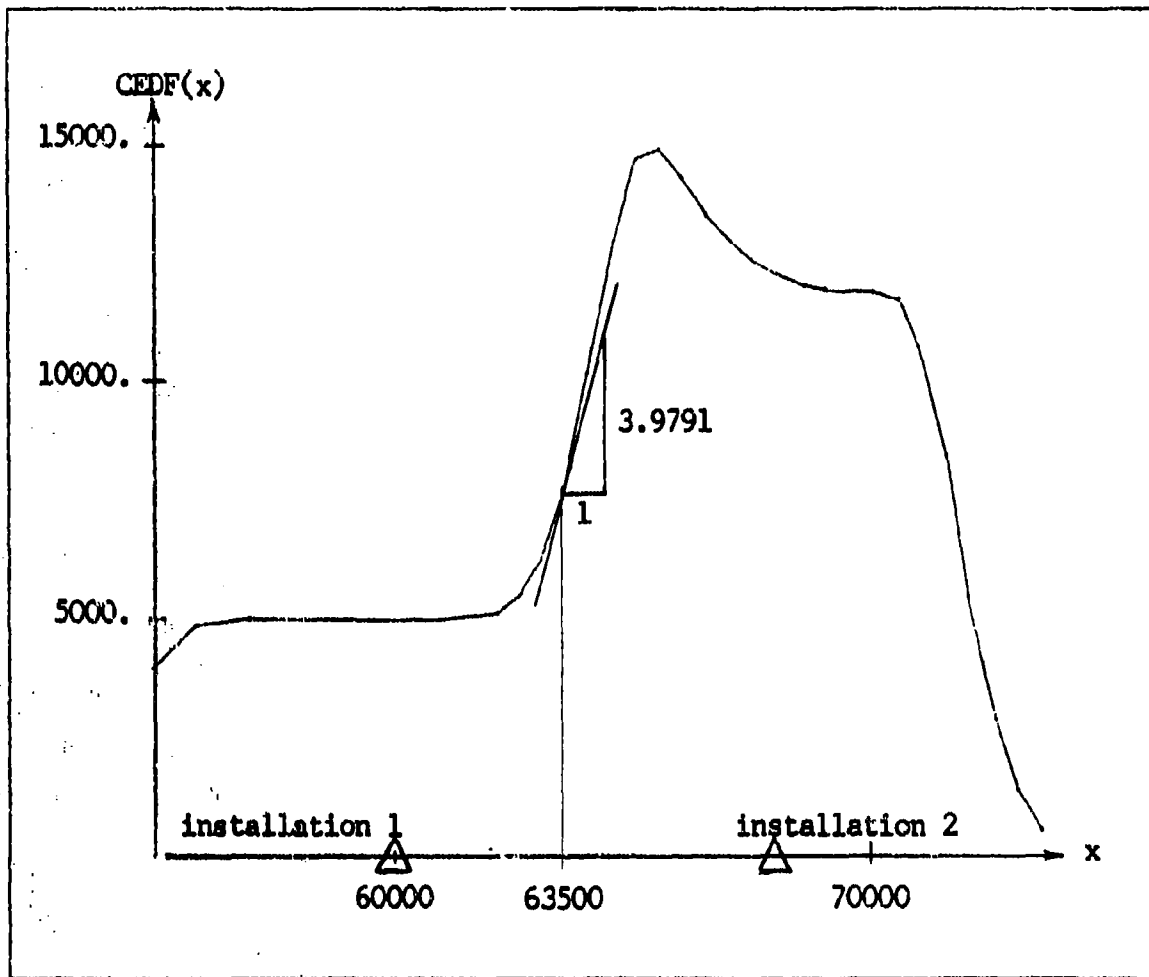


Figure 9. The CEDF for a one weapon-two installation geometry.

the gradient. Chapter II presented these steps. For the DGZ selected, the pencil and paper calculation of the gradient was 3.9791. The value of the gradient from GFUNCT for the DGZ selected was 3.9791. These comparisons indicated the subprogram GFUNCT was properly calculating the gradient of the CEDF(x).

The second example included two weapons and three installations. The gradient of the CEDF(x) in this example has 2m or four elements. Only one element was completely checked by pencil and paper calculations. A location for each DGZ within the three-installation complex was selected.

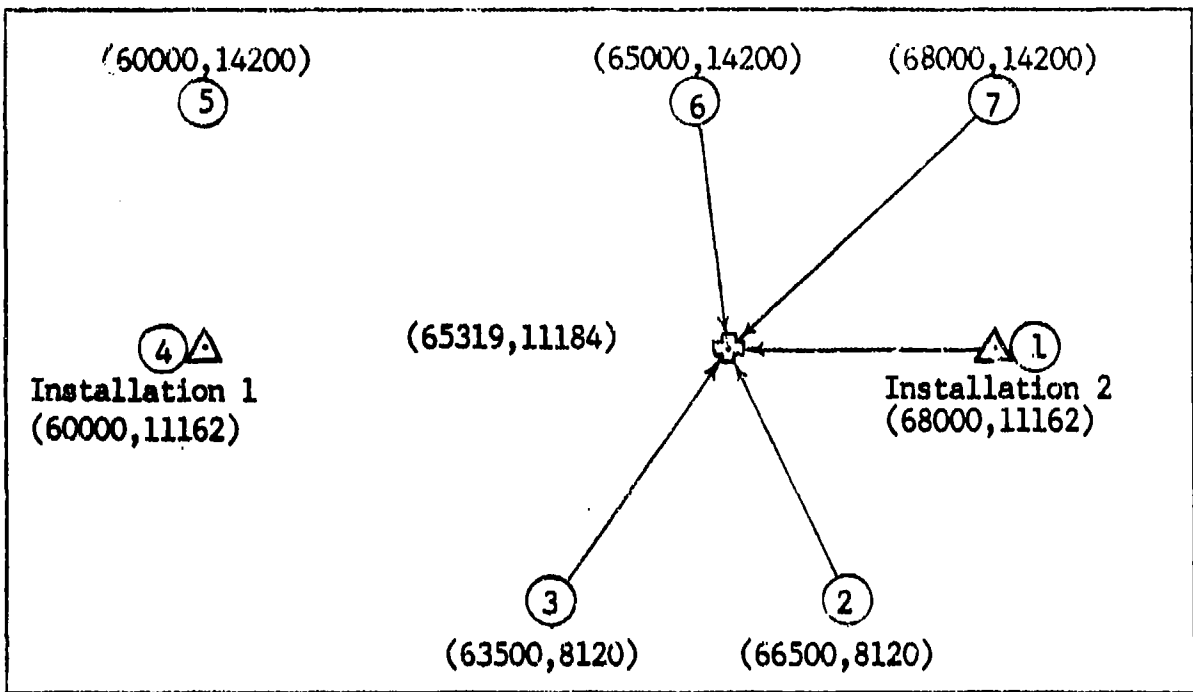


Figure 10. The one weapon-two installation geometry.

Then  $\frac{\partial \text{CEDF}(x)}{\partial x_2}$  was calculated to be 0.192548; the subsequent value from GFUNCT was 0.19255136. These comparisons indicated GFUNCT was correctly forming the gradient of the  $\text{CEDF}(x)$ .

The last phase verified the CEDF maximization algorithm's ability to locate a local maximum of the CEDF. All subprograms, the subroutines ZXOGR and PWIN, and the driver module OPTMZ were merged into one program -- the CEDF maximization algorithm. The two installation-one weapon complex described above to verify GFUNCT was also used to verify the algorithm. Figure 10 presents this complex, several initial starting points for the DGZ, and the mean location  $x^*$  for the local maximum of the  $\text{CEDF}(x)$ . In this simple example, the local maximum is also the global maximum. The graph of the  $\text{CEDF}(x)$  versus  $x$  in Figure 9 indicated the maximum CEDF value was approximately 15000 for  $65000 < x < 66000$ .

The CEDF maximization algorithm was run with seven different



initial DGZ. From the initial locations 1, 2, 3, 6, and 7, the algorithm converged to a maximum CEDF value and an optimal DGZ. The algorithm did not move the DGZ from the initial locations 4 and 5. For these locations, the ZXOGR and PWIN convergence criteria were satisfied, and the CEDF value was 4950. The algorithm did not move the DGZ from these locations because there were no indications of a CEDF increase. Chapter VI explains this result in more detail.

The mean optimal DGZ location and CEDF value were calculated for the other five initial DGZ locations. For the CEP-Excluded model using ZXOGR, the mean location of the optimal DGZ was (65319,11184). The standard deviation for x was 8 feet; for y it was 15 feet. The mean value of the  $CEDF(\underline{x})$  was 15019; the standard deviation was 4.3. For the CEP-Included model using PWIN, the mean location of the optimal DGZ was (65300,11172). The standard deviation for x was 58 feet; for y it was 98 feet. The mean value of the  $CEDF(\underline{x})$  was 15006; the standard deviation was 16.6. PWIN is a slower optimization routine; hence, less restrictive convergence criteria were established for PWIN. This could account for PWIN's smaller CEDF value and larger standard deviations for x and y.

The results from both CEDF models were compared to the values from Figure 9. These comparisons indicated that the CEDF maximization algorithm located an optimal DGZ location by maximizing the  $CEDF(\underline{x})$  for this simple two installation-one weapon complex. More detailed complexes are considered in the next section and the next two chapters.

### Validation

Validation measures the relative agreement between the model and

the system modeled. It is not possible to make comparisons between the CEDF maximization algorithm and the real world. Similarly, validation is not a yes or a no answer; it is a qualitative, relative measure. The CEDF maximization algorithm results for two example problems were compared with the results from NUCWAVE (Ref 29). NUCWAVE is a one-sided nuclear weapons allocation war gaming model. It optimizes the damage to a set of targets using a preselected set of weapons.

Two of the primary differences between the CEDF maximization algorithm and NUCWAVE are NUCWAVE's starting solution and optimization technique. It optimizes sequentially by starting the largest yield weapon at the highest valued installation. It optimizes over the (X,Y) coordinates of this weapon. Then it stores the final coordinates of this weapon, calculates the damage of all affected installations, and determines the remaining values for all installations. Then it optimizes the next largest yield weapon by starting it at the highest remaining valued installation. NUCWAVE continues to iterate through the entire weapon set until no further movement of a DGZ results in an increase in the total expected target value damage. Chapter I includes a description of NUCWAVE methodology. For these comparisons, the CEDF maximization algorithm assigned the initial DGZ locations to the highest valued installations.

The first problem included one weapon and two installations. This complex was very similar to the complex in Figure 10. The first installation's coordinates were 46°03'15" N - 45°10'00" E; its VNIK code and value were 11P2 and 5000. The second installation's coordinates were 46°03'25" N - 45°11'20" E; its VNIK code and value were 15P2 and 12000. The weapon's yield, height of burst, and CEP were 100-kt, 1000 feet,

and 0 feet. The coordinates of NUCWAVE's optimal DGZ were 46°03'22" N - 45°10'58" E; the total expected target value damage was 16579 or 97.52% of the complex value. The coordinates of the CEDF maximization algorithm's optimal DGZ were 46°03'21" N - 45°10'50" E; the CEDF was 16788 or 98.75% of the complex value. This represents a difference of approximately 575 feet and an increase in CEDF value of approximately 1%. Then the final DGZ coordinates from NUCWAVE were used as starting coordinates for the CEDF maximization algorithm. The CEDF value at these coordinates was 16647. The final coordinates for this run of the algorithm were also 46°03'21" N - 45°10'50" E. These results indicate that the CEDF maximization algorithm achieves comparable results with an existing model, NUCWAVE.

The second problem included two weapons and five installations. The installations' VNTK codes ranged from 14P3 to 20P3; the installations' values ranged from 3000 to 12000. The total complex value was 33000. Both weapons' yield, height of burst, and CEP were 100-kt, 1000 feet, and 0 feet. The coordinates of NUCWAVE's optimal DGZs were 46°01'58" N - 45°09'55" E and 46°00'48" N - 45°09'42" E; the total expected target value damage was 28730 or 87.06% of the complex value. The coordinates of the CEDF maximization algorithm's optimal DGZs were 46°01'58" N - 45°09'54" E and 46°00'45" N - 45°09'38" E; the CEDF value was 29543 or 89.52% of the complex value. This represents a difference of approximately 70 feet in the first DGZ and 415 feet in the second DGZ and an increase in CEDF value of approximately 3%. Again, the final DGZ coordinates from NUCWAVE were used as starting coordinates for the CEDF maximization algorithm. The CEDF value at these coordinates was 29018. The final coordinates from this run

were also  $46^{\circ}01'58''$  N -  $45^{\circ}09'54''$  E and  $46^{\circ}00'45''$  N -  $45^{\circ}09'38''$  E; the CEDF value was also 29543.

The comparisons between the results from the CEDF maximization algorithm and the results from NUCWAVE for the two examples indicate that the algorithm correctly determines the same local maximum as NUCWAVE. The results from these two examples do not validate the algorithm, but because the DGZ locations were consistent between NUCWAVE and the CEDF maximization algorithm, the algorithm's results are not invalid. These results provide the user confidence in the capability of the CEDF maximization algorithm.

## V. CEDF Maximization Algorithm Properties

The Complex Expected Damage Function (CEDF) maximization algorithm determines optimal DGZ coordinates for multiple nuclear weapons against installations in a target complex by maximizing the CEDF. The previous chapter presented the computerization and evaluation of the algorithm. The flowchart in Figure 6 summarizes the algorithm's modules. It also presents the algorithm's three CEDF maximization techniques: (1) ZXCGR, a conjugate gradient with restarts optimization method that maximizes the CEP-Excluded CEDF model; (2) PWSIN, Powell's method of conjugate directions that maximizes the CEP-Included CEDF model; and (3) a mixed technique that uses both CEDF models.

The ZXCGR and the mixed techniques each consist of two stages. The first stage of the ZXCGR technique has a less restrictive convergence criteria than the second stage, and its DGZ coordinates are used as initial DGZ coordinates for the second stage of the ZXCGR maximization algorithm. These optimal DGZ coordinates from the first stage of the ZXCGR algorithm also are used as the initial DGZ coordinates for the second stage of the mixed technique. Mixed maximization has an initial ZXCGR stage and then a PWSIN stage. For brevity and completeness, the following nomenclature will be used throughout this report. ZXCGR conjugate gradient maximization will be referred to as ZXM. Powell's method of conjugate directions will be referred to as PWM. Finally, the mixed technique will be referred to as MXM.

This chapter contains two sections. Each section presents characteristics of the algorithm's three CEDF maximization techniques. Differences and similarities between ZXM, PWM, and MXM are discussed.

Similarly, some capabilities and limitations are presented. The first section discusses convergence criteria, installation value scaling, user guidelines and user cautions. Also, it presents comparisons of CEDF results for different convergence values. The second section presents characteristics and optimization results for specific, geometrically symmetric, two and four-installation target complexes. It also discusses the effects of symmetric gradient elements on ZXM maximization.

### Convergence Criteria

The optimal DGZ coordinates and CEDF values from the CEDF maximization algorithms, ZXCGR using the CEP-Excluded model and PWMIN using the CEP-Included model, were sensitive to the convergence control parameters.

The ZXCGR control parameters are ACC and DFPRED. ACC specifies the desired accuracy of the convergence check. This check requires the norm of the gradient to be less than ACC. The norm of the gradient,  $\|\nabla F\|$ , is the sum of the squares of the gradient elements. When ZXCGR locates a point  $x^*$  in  $2m$  space, such that the norm of the gradient is less than the prespecified value of ACC, the optimization routine stops iterating. DFPRED is an estimate of the expected increase in the CEDF. ZXCGR uses it to determine the size of the initial change in each  $x$ .

The values of the installations affected the choice of values for ACC and DFPRED. This is because the installation values directly scale the CEDF and the magnitude of the gradient elements. Eqs (1) and (11) in Chapter II present this relationship. Most of the example problems in this report used installation values between 0 and 10000 ( $10^4$ ). If

installation values are within this range, then the most versatile parameter values for second stage ZXM maximization of two optimal DGZs are  $ACC = 0.001$  and  $DFPRED = 1000$ . If the installation values are not within this range, then a heuristic guideline is suggested to assist the user in estimating reasonable parameter values. For either case, the first stage value of  $ACC = 0.01$  determined acceptable DGZ coordinates for a wide range of installation values and number of weapons.

A general guideline to determine ACC for two weapons depends on the highest valued installation in the target complex. The highest value is rounded up to the largest power of the base 10. Then ACC equals  $10^{-7}$  times this adjusted value. For example, for a four-installation complex with installation values between 2500 and 7000, the adjusted value would be the 7000 rounded up to 10000 ( $10^4$ ). Then ACC would equal  $10^{-3}$ . This heuristic implies that a smaller ACC is needed for complexes with overall lower valued installations. Intuitively, this makes sense because the scaling effect of smaller installation values decreases the CEDF and the magnitudes of the gradient elements. When more than two weapons are used, a larger ACC value is needed to account for the additional gradient elements.

As an example, Table II presents the results of two ZXM optimizations for a two weapon-four installation target complex. Weapon and installation parameters, except the installation values, were the same for both optimizations. In the original problem, the most valuable installation's value was 7000, and an ACC of 0.001 was used. The CEDF maximum value was 15436. In the 1/10 value scaled problem, the most valuable installation's value was reduced by a factor of 10 to 700, and a smaller ACC of 0.0001 was used. The CEDF maximum value was 1543. Each of the

TABLE II

CEDF Comparison between an Original Problem  
and a 1/10 Value Scaled Problem

Parameters		Original Problem	Scaled Problem
Target	VNIK	Value	Value
1	16P2	3500	350
2	22P2	2500	250
3	21P4	5000	500
4	19Q3	7000	700
ACC		0.0010	0.00010
$\ \nabla F\ $ at convergence		0.0004	0.00002
CEDF at convergence		15436	1543

ZXM CEDF maximizations located essentially the same coordinates for both DGZs. Comparing the two optimization results, the coordinates of the first DGZ were within one foot of each other, and the coordinates of the second DGZ were within five feet of each other. Hence, the original and the scaled optimization problems located the same DGZ coordinates without regard for the magnitude of each installation's value.

Another heuristic is suggested for estimating the value of DFPRED. For the  $m$  weapons, sum the values of the  $m$  highest valued installations. If the  $m$  weapons were assigned to these  $m$  highest valued installations, then this sum would be an approximate value for the CEDF. Next determine the total value of all the installations. Then subtract the value sum of the  $m$  highest installations from the complex's total value. This difference is the maximum possible CEDF increase. An estimate for DFPRED



TABLE III

## Comparison of ACC Convergence Criteria

Parameter	ACC		
	0.0100	0.0010	0.0005
$\ \nabla F\ $ at convergence	0.0095	0.0006	0.0004
Number of function evaluations	14	18	19
CEDF at convergence	15433.	15434.	15437.
DGZ 2 final coordinates	(44840,23075)	(44851,23090)	(44850,23089)

is one-half of this difference. Again, this guideline implies that for lower installation values DFPRED, the estimated increase in the CEDF, should be smaller.

Generally, by decreasing ACC, ZXGR can determine better estimates of the CEDF maximum and its respective optimal DGZ coordinates. For the original two weapon-four installation complex of Table II, ZXGR was used to compare the CEDF maximum value and  $\|\nabla F\|$  for three values of ACC. DFPRED equaled 1000 for these three examples. Table III presents the results and the DGZ 2 optimal coordinates for these examples. The results of these ZXM maximizations indicated that, by decreasing ACC, ZXM can determine a better estimate of a CEDF local maximum. That is, ZXM can achieve a larger CEDF value and a smaller  $\|\nabla F\|$ . The final

coordinates for DGZ 1 were the same for the three cases. Only DGZ 2 coordinates were different; Table III indicates this difference was barely noticeable. Since the final DGZ 2 coordinates were within 17 feet of each other, a less restrictive ACC is acceptable. That is, a value of ACC smaller than  $10^{-7}$  times the adjusted highest installation value is unnecessary.

The results of a similar experiment using the same two weapon-four installation target complex indicated that the value of DFPRED also did not significantly affect the CEDF maximum value or the optimal DGZ coordinates. Five values of DFPRED, 100, 1000, 2500, 5000, and 6000, were compared using a constant ACC of 0.001.

Occasionally, ZXCGR will not converge satisfactorily and locate an optimal point in 2m space. The IMSL subroutine will return an IER = 129 error message. This message indicates that the subroutine abandoned a line search; this was probably because of conflicting information. The gradient may indicate that a point is not optimal; that is,  $\|\nabla F\| > \text{ACC}$ . However, each additional iteration may be on either side of the optimal point and the algorithm is unable to terminate satisfactorily. For most of the occurrences of this error message, the point located by the subroutine actually was a good estimate to the local CEDF maximum. Three options are available to the user when the algorithm terminates with this error message. First, select another ACC value and rerun the same problem. Second, select another DFPRED value and rerun the problem. Third, compare the DGZ locations and the CEDF maximum value with the results of PWM and MXM. Again, for most occurrences of this message, the third option indicated that the point located was a good estimate of

the CEDF maximum value and the respective optimal DGZ coordinates.

Just as ZXCGR maximization results depended on the values of the convergence control parameters, ACC and DFPRED, PWIN maximization results depended on the values of E and ESCALE. E specifies the desired accuracy of the convergence check. This check requires the absolute value of the differences between each element of  $\underline{x}$  for iteration i and each element of  $\underline{x}$  for iteration i - 1 to be less than E. When PWIN locates a point  $\underline{x}^*$  in 2m space, such that all element differences are less than the prespecified value of E, the optimization routine stops iterating. ESCALE is the maximum step size multiplier for a one-dimensional search. PWIN will not increment each x by more than ESCALE\*E.

The effect of E and ESCALE on the maximum CEDF value and the optimal DGZ locations was not as evident as the ZXCGR convergence control variables. Accordingly, an indepth sensitivity analysis of these parameters was not accomplished. Preliminary investigations indicated that ESCALE/E values of 10000/0.1 were the most effective in maximizing the CEP-Included CEDF model. E values of 1, 5, and 10 often resulted in computer runs that exceeded 60 seconds of computer processing (CP) time. These incomplete runs generally aborted after the third or fourth PWM iteration. Also, ESCALE values of 1000 and 5000 were examined.

The most promising values of ESCALE/E were 5000/0.1 and 10000/0.1. These two combinations were used for more than 143 CEDF maximization algorithm evaluations using 3, 4, 5, and 7-installation target complexes. Eighty of 83 runs (96%) using the ESCALE/E values of 5000/0.1 converged to a solution; similarly, 54 of 60 runs (90%) using the ESCALE/E values of 10000/0.1 converged to a solution. The other nine runs were terminated because of excessive CP time. Twenty-eight CEDF maximization runs

were identical except that 14 used the ESCALE/E values of 5000/0.1 and 14 used the values of 10000/0.1. Differences between the two parameter pairs for two criteria, CEDF maximum value and CP time, were evaluated. The results of a sign test indicated that there was no difference between the parameter pairs.

The four convergence control parameters need to be specified prior to a CEDF maximization algorithm run. The subroutine INITLZ initializes the ACC value for the first stage of ZXM to 0.01. The user provides the ACC value for the second stage of ZXM through the external file, INDATA. Similarly, the user provides the DFPRED value through INDATA. Appendix E discusses the necessary input procedures. The subroutine INITLZ also initializes the values of ESCALE/E to 5000/0.1. If the user desires different PWM convergence control parameters, then only two lines of the code need to be changed.

The norm of the gradient,  $\|\nabla F\|$ , will be used as a relative indicator of convergence for all ZXM maximizations. For a two-weapon complex with a maximum installation value of 10000,  $\|\nabla F\| = 0.001$  implies that the mean value for each of the four gradient elements is approximately 0.015. That is, a change of 1000 feet in any of the 4 spatial directions would change the CEDF by only 15 value points.

### Symmetry Characteristics

Two simple target complexes were investigated to characterize the CEDF models and their respective maximization techniques. Initial DGZ locations were selected to emphasize special features of ZXM and PWM optimization techniques. The examples included either symmetric target

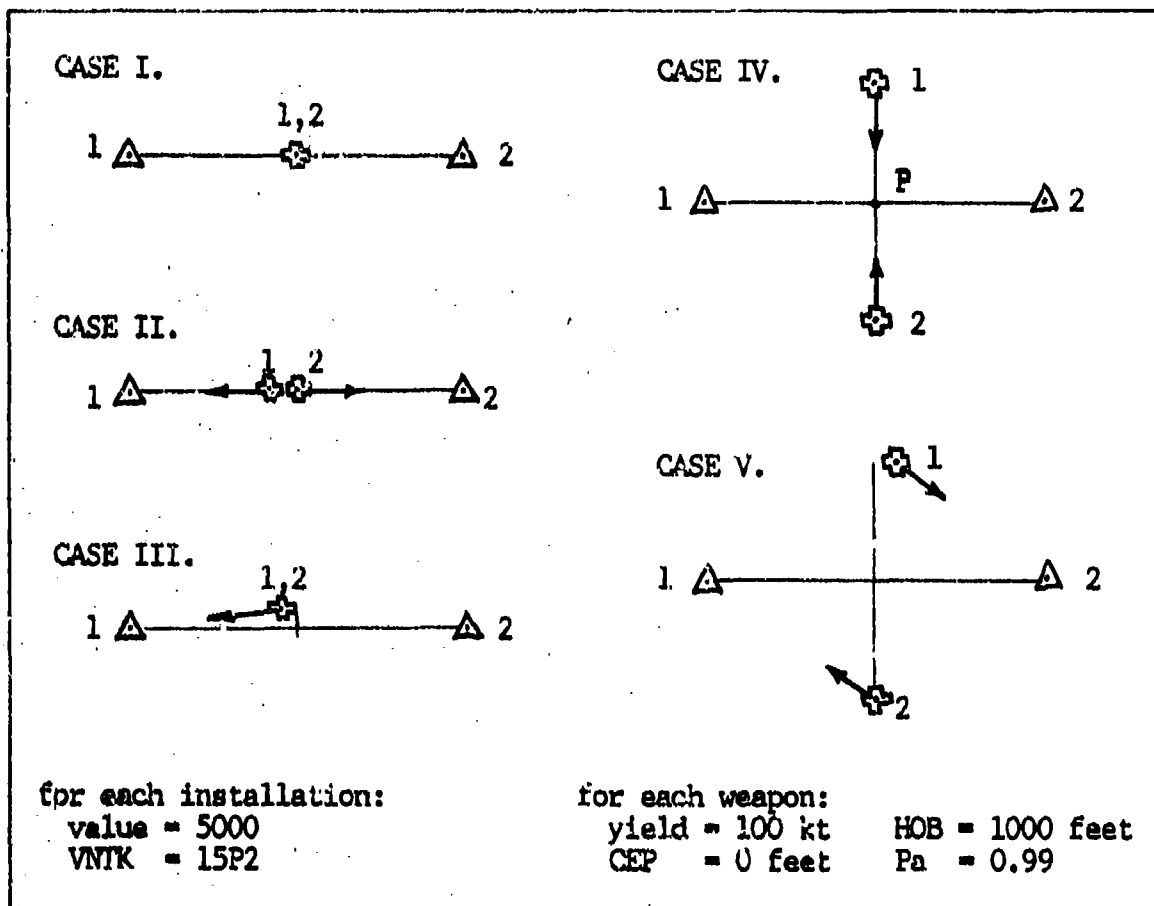


Figure 11. A symmetric two-installation complex.

complexes or a CEDF with symmetric gradient elements.

A two weapon-two installation complex was analyzed to determine the consequences of symmetric gradient elements on the ability of ZXM to locate a CEDF maximum value and optimal DGZ coordinates. Figure 11 presents the complex geometry, weapon and installation parameters, initial DGZ locations, and the ZXM direction of DGZ movement for five cases. Each of these cases had either a geometrically symmetric weapon-installation complex or a CEDF with symmetric gradient elements. The  $x_1$  and  $x_2$  directions were along the line segment connecting the two installations; the  $x_3$  and  $x_4$  directions were perpendicular to this line segment. For

each of these cases, PWM converged to a maximum CEDF value of 9900. This was each weapon's Pa times the total value of both installations. PWM also separated collocated DGZs. The results of the five cases provided further insight into the capability of the ZXM maximization technique.

CASE I. The initial DGZ locations for two identical weapons were collocated halfway between two identical targets. ZXM neither separated nor moved the two weapons. This was because all four of the CEDF gradient elements equaled 0. The  $x_3$  and  $x_4$  gradient elements were 0 because all y values were equal; the  $x_1$  and  $x_2$  elements were 0 because weapons 1 and 2 were halfway between the installations. That is, one installation's contributions to the  $x_1$  and  $x_2$  gradient elements cancelled the other installation's contributions. ZXM made the initial DGZ coordinates the optimal DGZ coordinates with a CEDF value of 3465.

CASE II. The collocated identical weapons in CASE I were separated. Weapon 1 was moved one minute of longitude west (approximately 70 feet). With this move from the complex's geometric center, the  $x_1$  gradient element was no longer 0; ZXM separated the two DGZs and moved weapon 1 towards installation 1 and weapon 2 towards installation 2. ZXM converged to a maximum CEDF value of 9900 and two optimal DGZs with a  $\|\nabla F\| = 10^{-9}$ .

CASE III. The two identical weapons were again collocated. However, the initial DGZ location was neither halfway between the two identical installations nor along the line segment connecting the installations. The gradient elements were all non-zero. The  $x_1$  and  $x_2$  elements were equal and positive; the  $x_3$  and  $x_4$  elements were equal and also positive. In this case, ZXM did not separate the two weapons because their respective gradient elements were the same; however, it did move

the two weapons together towards installation 1. That is, ZXM kept the two weapons collocated with a CEDF value of 5737 and  $\|\nabla F\| = 7.7 \times 10^{-5}$ .

Next, a variation of this case was examined. The same initial DGZ location was used, but the yield of weapon 2 was reduced from 100-kt to 95-kt. This yield reduction altered the gradient elements. The  $x_1$  and  $x_2$  elements were no longer equal; similarly, the  $x_3$  and  $x_4$  gradient elements were no longer equal. The two different weapons separated from the same initial DGZ location. ZXM moved weapon 1 towards installation 2 and weapon 2 towards installation 1. ZXM converged to a maximum CEDF value of 9900 and two optimal DGZs with  $\|\nabla F\| = 1.2 \times 10^{-8}$ .

CASE IV. The two identical weapons were separated along a line segment that was perpendicular to the line segment connecting the two identical installations. Figure 11 displays this geometry. The two weapons were each equidistant from the two installations. Again, because of the symmetry of the target complex, the identical weapons, and the identical installations, the gradient elements were symmetric. The  $x_1$  and  $x_2$  gradient elements were 0. That is, each installation's contributions to the  $x_1$  and  $x_2$  gradient elements negated each other. The  $x_3$  and  $x_4$  gradient elements were equal in magnitude, but opposite in direction; the  $x_3$  element was positive and the  $x_4$  element was negative. Because the  $x_1$  and  $x_2$  gradient elements were equal to 0, this restricted the DGZ movements to only the  $x_3$  and  $x_4$  directions. With the  $x_3$  and  $x_4$  gradient elements with equal magnitude but opposite direction, ZXM moved the DGZs directly towards each other to point P in Figure 11. This point was along the line segment connecting the two installations and halfway between the installations. ZXM converged to a local maximum CEDF value of 5729 and one collocated DGZ with  $\|\nabla F\| = 0.00028$ .

CASE V. A variation of CASE IV was examined. The initial DGZ location of weapon 1 was moved one minute of longitude east (approximately 70 feet). The  $x_1$  gradient element was no longer 0; ZXM moved weapon 1 towards installation 2 and weapon 2 towards installation 1. ZXM converged to a maximum CEDF value of 9895 and two optimal DGZs with  $\|\nabla F\| = 0.00085$ .

The algorithm located CEDF local maximums for this two weapon-two installation complex. However, the algorithm's optimal DGZ coordinates were not exactly the coordinates of the two installations. For this complex, the optimal DGZ locations would be one weapon on each installation, since the weapons and the installations were identical. Nevertheless, these examples demonstrate two important features, an operational characteristic and a limitation, of the CEP-Excluded CEDF model using ZXM maximization. Both of these are a result of the symmetry of the CEDF gradient elements. These cases indicated that there are two types of gradient symmetry. There is symmetry from weapons at symmetrical, initial DGZ locations (CASES I and IV) and from identical weapons at the same initial DGZ location (CASE III). The first type of symmetry is an operational characteristic; the second type, collocation of initial DGZ locations, is a minor limitation. This limitation means that the ZXM maximization algorithm cannot use collocated initial DGZ locations. The PMW maximization algorithm did not have this limitation.

A unique one weapon-four installation target complex also exhibited symmetric gradient properties. Figure 12 presents the complex geometry, weapon and installation parameters, and CEDF values for different potential DGZ locations.



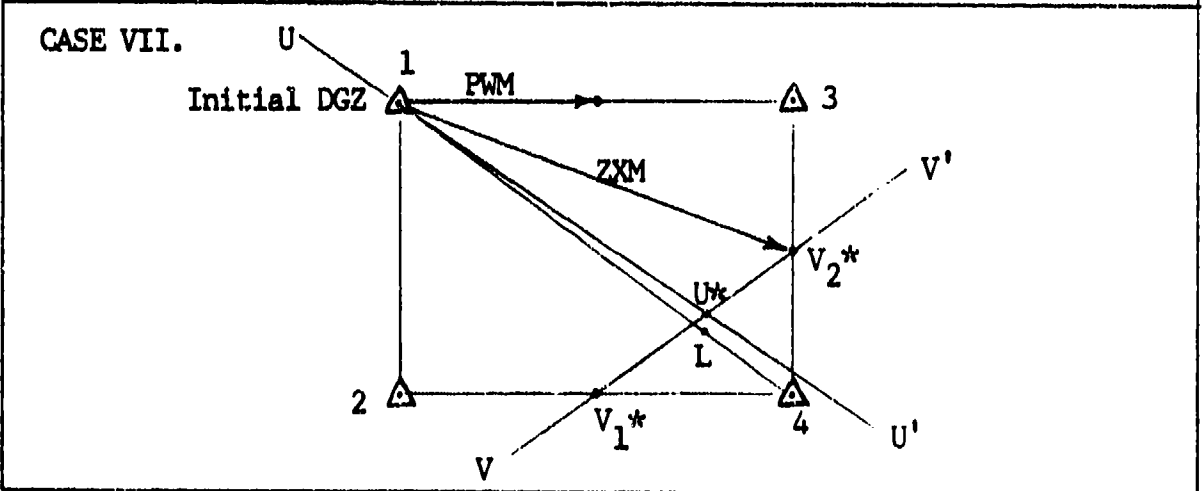
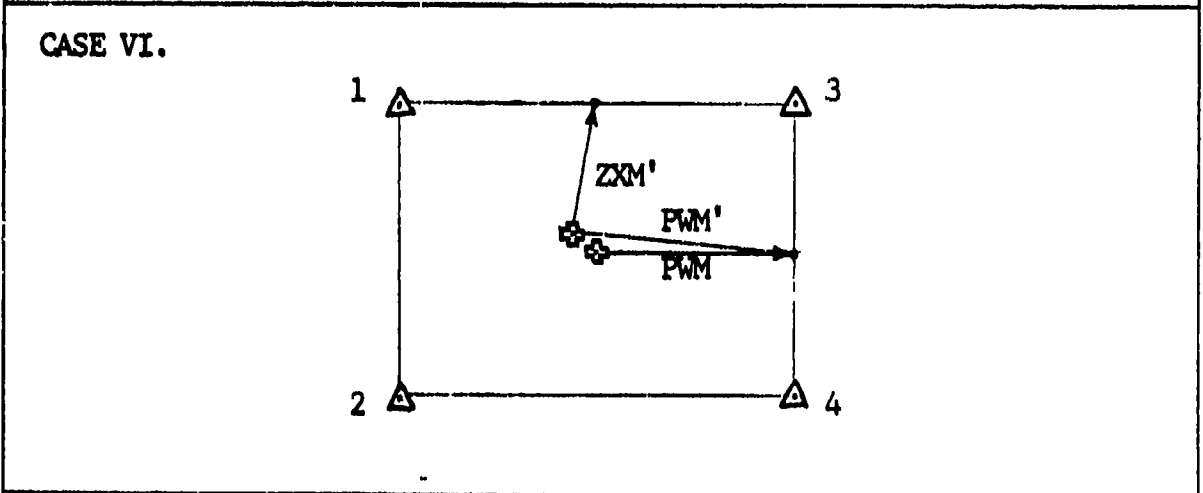
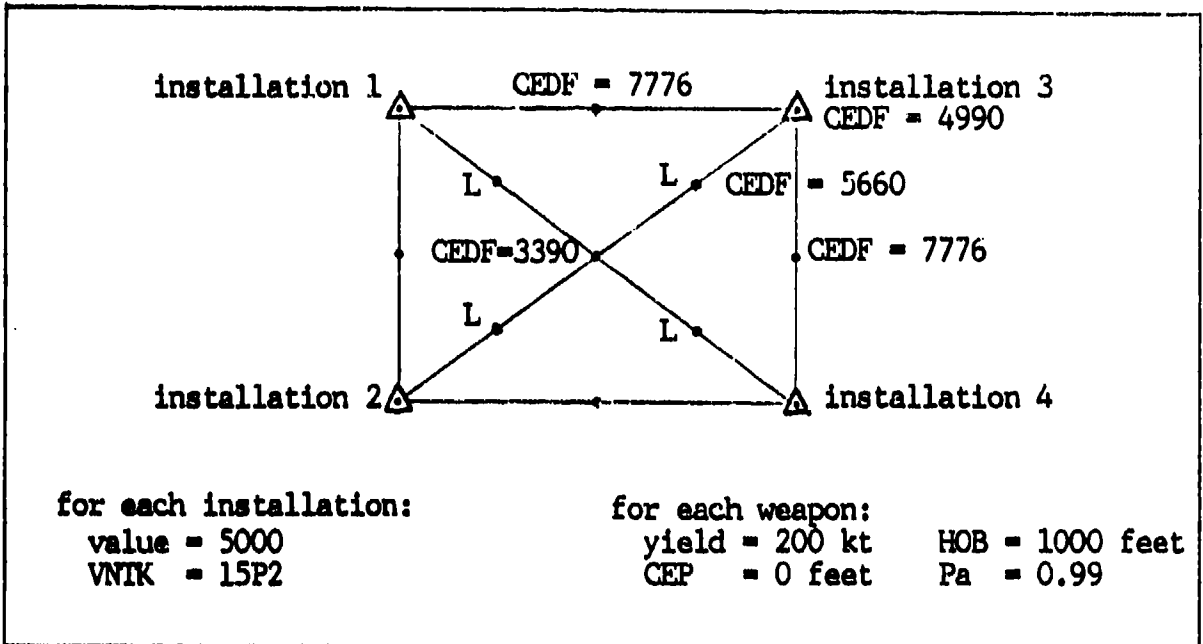


Figure 12. A symmetric four-installation complex.

The geometric shape of the complex was not a square, but rather, a rectangle. The north-south distance between the installations was 8511 feet; the east-west distance was 8448 feet. There were four local maximums or potential DGZ locations for this target complex; one at each midpoint of the four line segments of the rectangular perimeter. The CEDF value at each local maximum was 7776. The CEDF value for a DGZ located at the center of the target complex was 3390. The CEDF value for a DGZ located at one of the installations was 4990. Lastly, for a DGZ located halfway between an installation and the complex center along one of the complex's two diagonals at one of the points L in Figure 12, the CEDF value was 5660.

CASE VI. The initial DGZ was the geometric center of the target complex. Figure 12 also presents this location and the optimal DGZ location for PWM. At the initial DGZ location, the damage expectancy (DE) for each installation was less than 0.17. PWM moved the DGZ in the +x direction and converged to a maximum CEDF value of 7776 and an optimal DGZ location between installations 3 and 4. The DE for these installations from this optimal DGZ was approximately 0.78; the DE for installations 1 and 2 was approximately 0.001. ZXM did not move the DGZ; the two gradient elements were 0 because the initial DGZ was at the geometric center of the complex.

Next, a variation of this example was examined. The initial DGZ was moved one minute of longitude west and one minute of latitude north (approximately 120 feet). PWM moved the DGZ in the +x direction as before. However, the gradient elements were no longer 0 because the initial DGZ was not at the geometric center of the complex. ZXM

converged to a CEDF maximum value of 7776 and an optimal DGZ location between installations 1 and 3 with  $\|\nabla F\| = 0.0008$ . A possible explanation as to why ZXM moved to this optimal DGZ is presented in the next case.

CASE VII. The initial DGZ location was installation 1. Figure 12 also presents this location and the optimal DGZ locations. PWM again moved the DGZ in the +x direction to a CEDF maximum value of 7776 and an optimal DGZ location between installations 1 and 3. ZXM did not move the DGZ towards the closest local maximum as it did in CASE VI. Instead, ZXM moved the DGZ to a CEDF maximum value of 7643 at an optimal DGZ location between installations 3 and 4 with  $\|\nabla F\| = 0.0017$ .

Investigation of the first 20 iterations of ZXM for this complex provided a plausible explanation as to why ZXM converged to this optimal DGZ instead of the closest DGZ. The geometry of the complex was not a square, but rather, a rectangle. Hence at the initial DGZ, the two gradient elements were not exactly equal. The  $x_1$  gradient element was 0.0352. This was larger than the  $x_2$  gradient element which was 0.0310. Hence, the first iteration's search direction was above the diagonal of the complex along the line U-U' in Figure 12. Figure 13 shows an approximate curve of CEDF values, using seven known points, along U-U'. ZXM located the point U\*. ZXM next searched along the line segment V-V' through the point U\* and the two potential local maximums  $V_1^*$  and  $V_2^*$ . Again, Figure 13 shows an approximate curve of CEDF values, using five known points, along V-V'. From U\*, ZXM located the optimal DGZ  $V_2^*$ . In summary, ZXM does not always move the initial DGZ towards the closest local maximum.

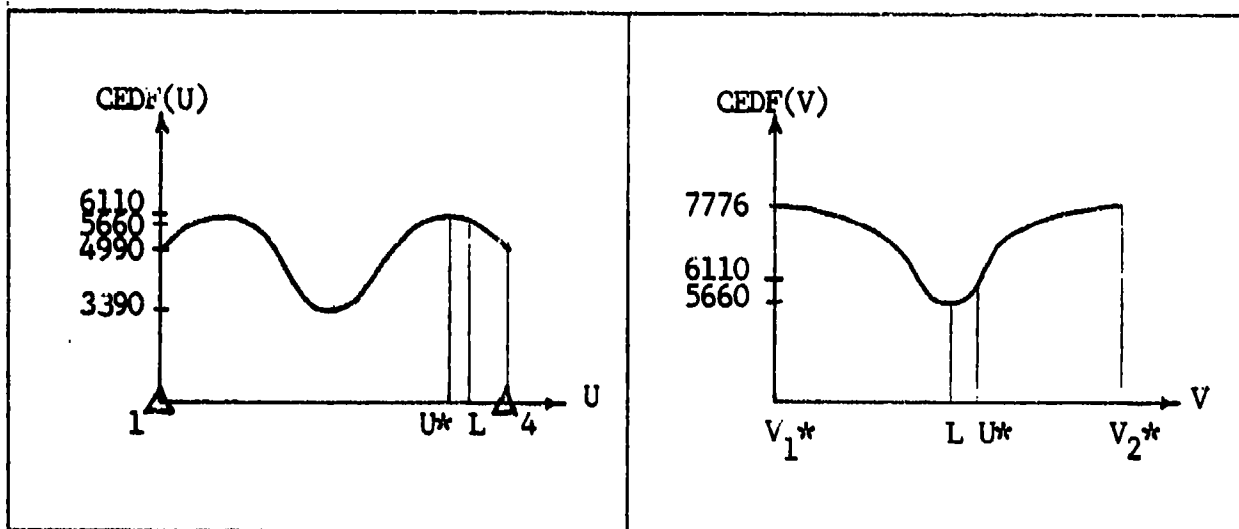


Figure 13. CEDF values along line segments U-U' and V-V' for the symmetric four-installation complex.

These seven cases demonstrated two important ZXM maximization characteristics. These characteristics depend on symmetry of the CEDF gradient elements. This symmetry is a result of either the geometrical symmetry of the target complex or the collocation of two or more similar weapon types. This second characteristic, a minor limitation, prohibits the CEDF maximization algorithm from using collocated initial DGZs. The next chapter provides a description of initial DGZ locations for more typical, nonsymmetric target complexes.

## VI. Algorithm Results for Different Initial DGZ Locations

This chapter presents results of the CEDF maximization algorithm using different initial DGZ conditions. The important results are the maximum CEDF value and the optimal DGZ coordinates. The three algorithm maximization techniques are: ZXM, conjugate gradient optimization of the CEP-Excluded model; PWM, conjugate directions optimization of the CEP-Included model; and MXM, a mixed technique.

Four initial DGZ conditions were evaluated using three target complexes. However, all four conditions were not matched with each of the complexes. The four initial DGZ conditions for  $m$  weapons against a target complex were: (1) locating the weapons at the  $m$  highest valued (HV) installations, (2) locating the weapons at the  $m$  hardest installations, (3) locating the weapons at the complex's centroid, and (4) locating the weapons at  $m$  pseudo-random points.

Intuitively, the most logical initial DGZ condition was the highest valued installations, and the least logical condition was random locations. The HV condition was a greedy condition; it started with the maximum damage on the  $m$  most valuable installations and then searched for other DGZs that provided an increase in the CEDF value. The random locations condition was not completely evaluated. Instead, for a two-weapon complex, six pairs of initial DGZs were evaluated, and the six CEDF values and optimal DGZs were compared to each other. The coordinates of one of the initial DGZs in each pair were fixed and common to all pairs. The coordinates of the other initial DGZ were changed for each of the six pairs and the respective six runs of the CEDF maximization

algorithm. The results of these pseudo-random initial DGZ locations provided additional insight concerning different initial DGZ locations.

The three target complexes included three, four, and seven installations. The CEDF maximization algorithm located optimal DGZs for one, two, or three weapons against these complexes. However, each complex was not matched with each of these number of weapons. That is, the three-target complex was only evaluated using one and two weapons, not three. The highest valued installation in any of the complexes was 9000. Hence, for the convergence control parameters, the algorithm generally used values of  $ACC = 0.001$ ,  $DFPRED = 1000$ ,  $E = 0.1$ , and  $ESCALE = 5000$ .

Three conclusions were made from the results of these examples. First, the algorithm requires some indication of a potential increase in CEDF value in order to move a DGZ. Second, there is a difference between the optimal DGZ coordinates from the CEP-Excluded model using ZXM maximization and those from the CEP-Included CEDF model using PWM maximization. This difference depends on a weapon's CEP and the CEDF model and not on the optimization technique. Third, the initial DGZ coordinates that the algorithm uses can affect the maximum CEDF value and the optimal DGZ coordinates. Statistical evidence of these conclusions is not presented. Rather, specific examples are presented that indicate the conclusions are not invalid.

#### A Three-Installation Complex

CEDF maximization algorithm results were analyzed for one and two weapons against a three-installation complex using different initial DGZ conditions. Figure 14 shows the geometry and specific parameters of the

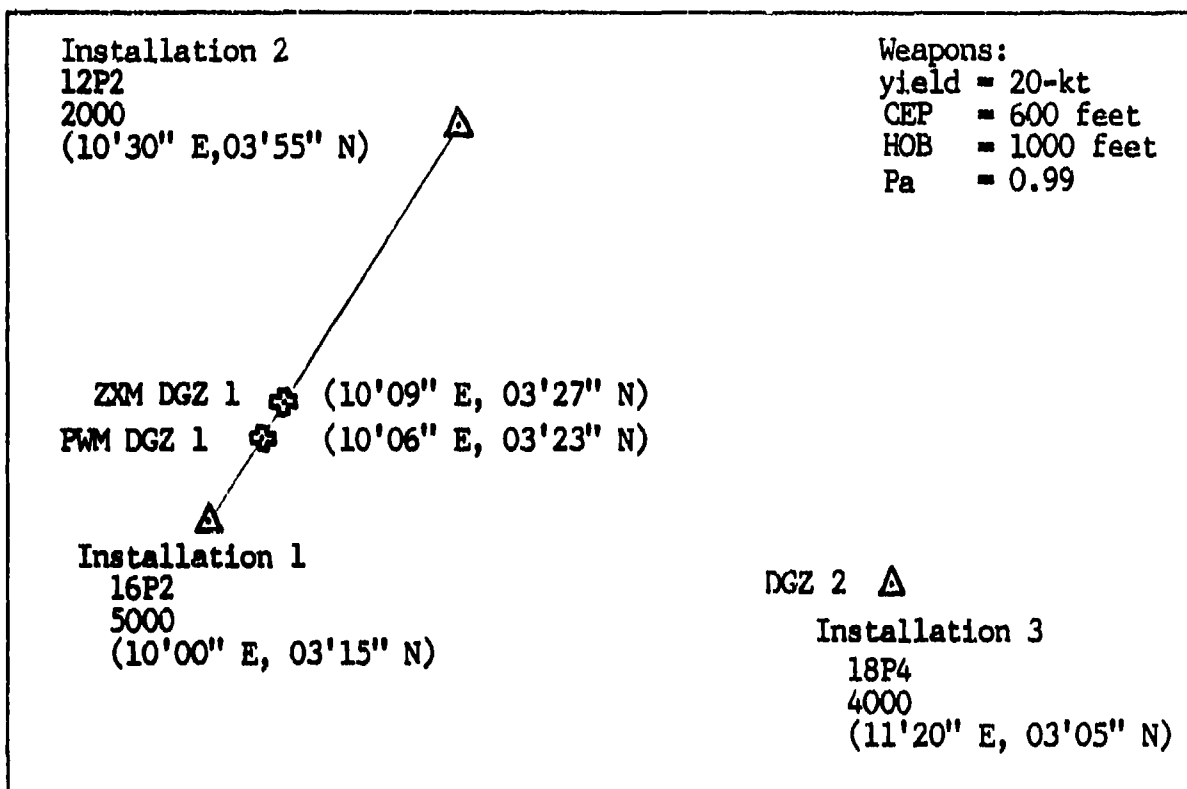


Figure 14. A Three-Installation Complex.

target complex. The total available target value for the complex, reduced by each weapon's Pa, was 10890. Figure 14 also shows the optimal DGZ coordinates for the highest valued (HV) initial DGZ condition using ZXM and PWM maximization. DGZ 2 was installation 3. The ZXM algorithm converged to a maximum CEDF value of 9812 or 90% of the complex value and to optimal DGZ coordinates with  $\|\nabla F\| = 0.00036$ . Similarly, PWM converged to a maximum CEDF value of 9223 or 85% of the complex value. The damage expectancy (DE) for installations 1, 2, and 3 from ZXM maximization were 0.96, 0.53, and 0.99. The algorithm did not move DGZ 2 from installation 3 and moved DGZ 1 from installation 1 towards installation 2. However, the two algorithms located the optimal DGZ 1 coordinates 480 feet apart. This difference was less than the CEP of 600 feet and initially appeared

insignificant. However, the differences between ZXM and PWM maximum CEDF values and DGZ 1 coordinates were important; these differences do not indicate ZXM is a better algorithm. These differences depended on the CEDF model and are discussed in more detail in the next subsection.

The CEDF maximization algorithm also converged to a local CEDF maximum for the centroid initial DGZ condition. ZXM converged to a CEDF value of 6932 and to optimal DGZ coordinates with  $\|\nabla F\| = 0.00003$ ; PWM converged to a CEDF value of 6910. However, these optimal DGZ locations were not the same locations as determined using the HV initial DGZ condition. Instead, ZXM and PWM moved the DGZs towards installations 1 and 2 until the DE for each installation were greater than 0.99. The final DE for installation 3, the second most valuable installation, was less than 0.001. The total available target value for installations 1 and 2, reduced by each weapon's  $P_a$ , was 6930; this was the same CEDF value as determined by ZXM maximization. These optimal coordinates, which were different and less valuable than the HV initial DGZ condition's optimal coordinates, were also identified by three pairs of the pseudo-random initial DGZ condition.

Six pairs of the pseudo-random initial DGZ condition were also evaluated. Figure 15 shows the initial DGZ locations and the respective optimal DGZ locations for ZXM maximization for two cases. It also shows the approximate weapons radius (WR) for each installation. For all six pairs, PWM maximization, using the CEP-Included CEDF model, converged to the same optimal DGZ locations as determined by the highest valued initial DGZ condition. The pictorial results in Figure 15 are for ZXM maximization using the CEP-Excluded CEDF model.



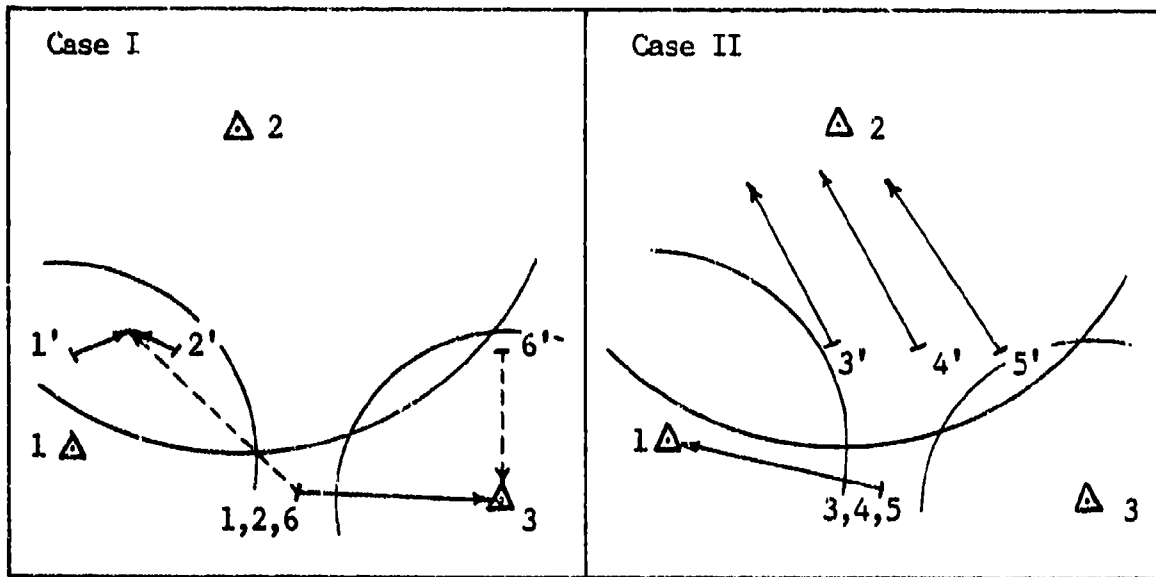


Figure 15. Pseudo-random initial DGZ conditions.

Case I. For the initial DGZ locations -- 1-1', 2-2', and 6-6' -- ZXM converged to a maximum CEDF value of 981.0 or 90% of the complex value and to optimal DGZ coordinates with  $\|\nabla F\| < 0.004$ . This was the same CEDF local maximum that the HV initial DGZ condition located.

Case II. For the initial DGZ locations -- 3-3', 4-4', and 5-5' -- ZXM converged to a maximum CEDF value of 693.2 or 64% of the complex value and to optimal DGZ coordinates with  $\|\nabla F\| < 0.0004$ . This was the same CEDF local maximum that the centroid initial DGZ condition located. Each of the optimal DGZ locations are slightly different locations; however, each of the locations are equivalent. ZXM moved from 3-3', 4-4', and 5-5' towards installations 1 and 2 until the DE for these installations was greater than 0.99.

A possible explanation exists for the difference between the two CEDF local maximums for the two cases. The Case I initial DGZ locations

each had one initial DGZ (1', 2', and 6') within the WR of one of the two highest valued installations. The other initial DGZ (1, 2, and 6) was outside the WR of all installations. Alternately, the Case II initial DGZ locations had neither of the initial DGZs within the WR of the two highest valued installations. Hence, for Case II, the algorithm moved one initial DGZ location (3', 4', and 5') towards installation 2 and the other initial DGZ location (3, 4, and 5) towards installation 1, the most valuable one. Figure 4 shows that the probability of achieving a specified level of damage to an installation at the WR is less than 0.5. Using WR to interpret CEDF local maximums is not a definitive technique. However, the relationship between the location of an initial DGZ and an installation's WR does provide insight and a possible explanation for the two CEDF local maximums.

In summary, these results point out the first of three conclusions of this study. The CEDF maximization algorithm requires some indication of a potential increase in the CEDF in order to move a DGZ. That is, if there is no indication of a CEDF increase in the direction of a valued installation and there is an indication of a CEDF increase in the direction of a lesser valued installation, then the algorithm may move the DGZ towards the lesser valued installation. Eventually, the algorithm will converge to a less valuable CEDF local maximum.

Using the CEDF maximization algorithm to evaluate one weapon against this three-installation complex produced similar results for three initial DGZ conditions. For the highest valued condition, ZXM started from installation 1 and converged to a CEDF maximum value and an optimal DGZ with  $\|\nabla F\| = 0.00030$ . The coordinates of this DGZ coincided with the

coordinates of one of the two-weapon HV condition DGZs. Similarly, PWM converged to the same optimal DGZ location as one of the two-weapon HV condition DGZs. This result indicated that the two weapons against the three installations were not dependent but rather, unrelated DGZs. The fact that DGZ 2 never moved from installation 3 for the two-weapon example also indicated that the two DGZs were independent.

A comparison between the one-weapon centroid initial DGZ condition results and the two-weapon HV initial DGZ condition results indicated the sensitivity of the gradient. Both of these examples located an optimal DGZ at 10'09" E - 03'27" N. However, when the optimal coordinates in feet were compared, the two DGZs were approximately 30 feet apart. For one DGZ, the  $\|\nabla F\| = 0.00031$ ; for the other DGZ, only 30 feet away,  $\|\nabla F\| = 0.00760$ .

For the hardest initial DGZ condition, neither ZXM nor PWM moved the one weapon initial DGZ. The DGZ started at installation 3 and remained there. The  $\|\nabla F\| = 10^{-5}$  at this point. The CEDF value for ZXM was 3962 or 99% of the value of installation 3; the CEDF value for PWM was 3918 or 98% of the value of installation 3. The difference in these CEDF values depended on the CEDF model and are discussed next.

#### The CEP Effect

CEDF maximization algorithm results for the three-installation complex using different initial DGZ conditions point out the second conclusion of this study. Both a weapon's CEP and the CEDF model used to maximize the CEDF affect the maximum CEDF value and the optimal DGZ coordinates. Specific results from three previous three installation examples provide evidence to support this conclusion.

First, the results from the one weapon-three installation complex using the hardest installation initial DGZ condition highlight this difference between the two CEDF models. The CEP-Excluded CEDF model, using ZXM maximization, converged to a CEDF value of 3962; the CEP-Included CEDF model, using PWM maximization, converged to a CEDF value of 3918. The optimal DGZ coordinates for these algorithms were within 1 foot of each other. The difference in CEDF values was attributed to the CEDF models. The  $P_{d_{i,j}}$  for the CEP-Excluded model does not include weapon accuracy or CEP. This probability is the distance damage function value,  $P_d(r)$ . The  $P_{d_{i,j}}$  for the CEP-Included model does include weapon CEP. Hence, this probability is less than  $P_d(r)$ . Consequently, the PWM damage expectancy for an installation is less than the ZXM damage expectancy for the same installation.

The second example that supports the conclusion was the two weapon-three installation complex using the highest valued initial DGZ condition. Analysis of this example's results provided an explanation for the CEDF differences between ZXM and PWM. Figure 14 shows the optimal DGZ coordinates for these algorithms. Only DGZ 1 coordinates are considered; DGZ 2 coordinates were the same for both algorithms. PWM converged to optimal DGZ 1 coordinates approximately 480 feet closer to installation 1 than ZXM. Two additional initial DGZ conditions were necessary to further investigate this difference. For the initial DGZ coordinates, the first condition used the PWM optimal coordinates; the second condition used the ZXM optimal coordinates. Table IV presents the final coordinates and CEDF values from these initial DGZ conditions. The coordinates are in feet and, even though they appear different within the three optimization categories, they are not. The ZXM coordinates were

TABLE IV  
Comparison of ZXM, PWM, and MXM Optimal DGZs

Initial DGZ Condition	ZXM CEDF Values		ZXM Final Location	PWM CEDF Values		PWM Final Location	MXM CEDF Values		MXM Final Location
	Start	End		Start	End		Start	End	
Highest Value	8985	9812	858,1039	8972	9220	585,642	9009	9223	664,627
PWM Optimal	9480	9813	837,1055	9222	9222	643,629	9008	9218	660,593
ZXM Optimal	9812	9812	824, 976	9073	9223	627,632	9009	9223	639,638
Mean Values		9812	840,1023		9222	618,634		9221	654,619

10'09" E - 10'27" N and the PWM and MXM coordinates were 10'06" E - 03'23" N.

Using PWM optimal DGZ coordinates as the initial DGZ coordinates, the algorithm produced three results. First, the PWM optimal DGZ location was the initial DGZ location. Second, the PWM optimal DGZ coordinates, the initial coordinates, were not optimal for ZXM. At these initial DGZ coordinates, the ZXM CEDF value was 9480. ZXM maximization moved the DGZ from 10'06" E - 03'23" N back to 10'09" E - 03'27" N and a maximum CEDF value of 9813. ZXM optimal coordinates are initial DGZ coordinates for the mixed technique, MXM. Third, these initial MXM coordinates were not optimal for MXM. At these DGZ coordinates, the MXM CEDF was 9008. MXM maximization moved the DGZ from 10'09" E - 03'27" N back to 10'06" E - 03'23" N, the PWM optimal DGZ coordinates, and a maximum CEDF value of 9218.

The algorithm produced three similar results when it used the ZXM

optimal DGZ coordinates as the initial DGZ coordinates. First, the ZXM maximization optimal DGZ location was the initial DGZ location. Second, the ZXM optimal DGZ coordinates, the initial coordinates, were not optimal for PWM. At these initial DGZ coordinates, the PWM CEDF value was 9073. PWM maximization moved the DGZ from this initial DGZ back to 10'06" E - 03'23" N and a maximum CEDF value of 9223. Third, the initial coordinates, 10'09" E - 03'27" N, again were not optimal for MXM. At these coordinates, the MXM CEDF value was 9009. MXM maximization moved the DGZ from this initial DGZ location back to 10'06" E - 03'23" N and a maximum CEDF value of 9223.

Finally, analysis of a third three-installation complex provided further insight into the capability of the CEDF models. In the previous example, the mixed technique moved the DGZs from the ZXM optimal DGZ coordinates to the PWM optimal DGZ coordinates. However, this readjustment did not occur in all examples. For instance, ZXM maximization for the pseudo-random initial DGZ pairs, 3-3', 4-4', and 5-5', converged to optimal coordinates that were different from the PWM optimal coordinates. The PWM optimal coordinates were the HV coordinates; the ZXM optimal locations were near installations 1 and 2. The mixed technique was unable to move the DGZs from these ZXM optimal coordinates to the PWM optimal coordinates. The  $\|\nabla F\| < 0.004$  for each ZXM local maximum.

These CEDF maximization algorithm results indicated that each CEDF model located a unique set of optimal DGZs. This occurred because of the difference in  $Pd_{i,j}$  for the two models.  $Pd_{i,j}$  is larger for the CEP-Excluded model than it is for the CEP-Included model.

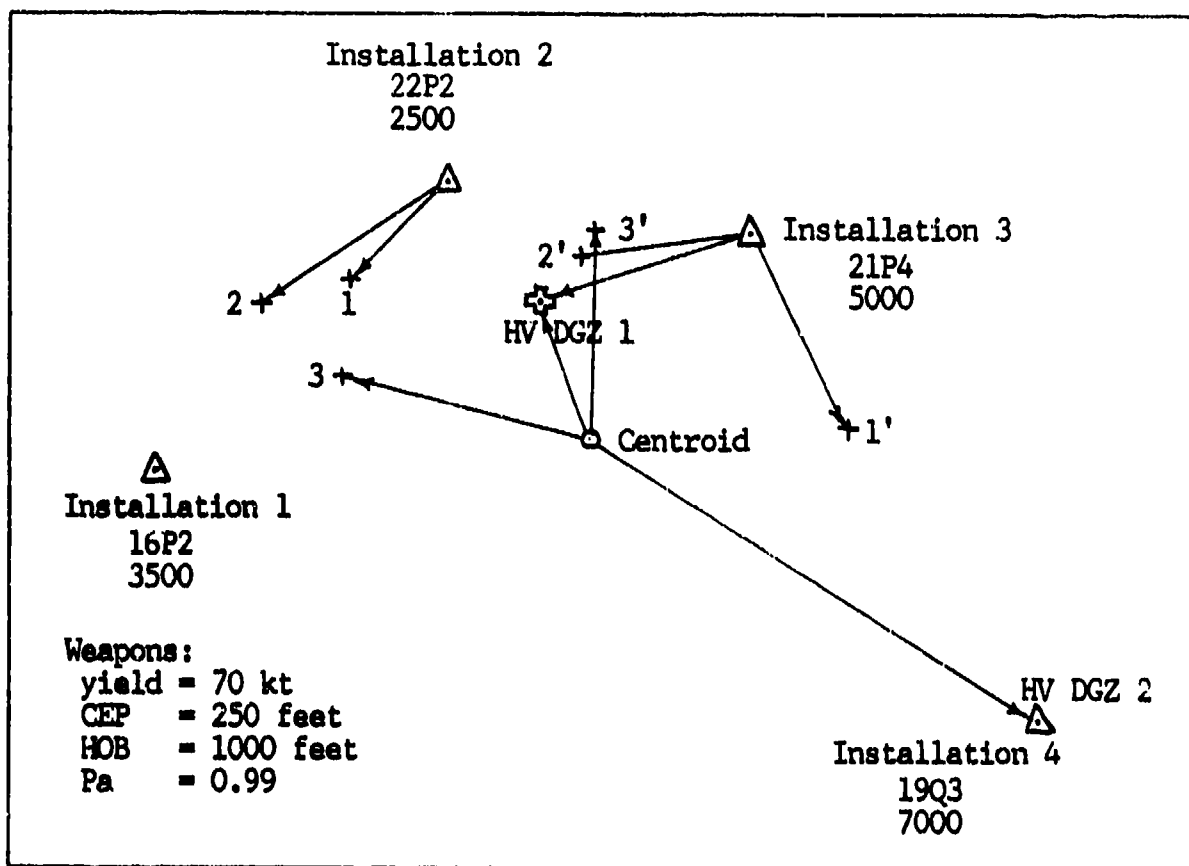


Figure 16. Multiple local optimal DGZs for a two weapon four installation complex.

### Larger Complexes

For a four-installation complex using the four initial DGZ conditions, the CEDF maximization algorithm produced results similar to the results for the three-installation complex. Figure 16 shows the geometry and specific parameters of the target complex. The total available target value for the complex, reduced by each weapon's  $P_a$ , was 17820. Figure 16 also shows the optimal DGZ locations for several initial DGZ conditions. Four local CEDF maximums and their respective optimal DGZ pairs were located for this complex: the HV (highest valued) DGZs, 1-1', 2-2', and 3-3'.

Again, ZXM and PWM located their highest valued DGZ 1 at slightly

different coordinates. The difference between the two locations was 90 feet. ZXM converged to a CEDF maximum value of 15434 or 87% of the complex value and to optimal DGZ coordinates with  $\|\nabla F\| = 0.00056$ . As with the three-installation complex, the ZXM optimal DGZ coordinates were not optimal for PWM. The mixed technique moved DGZ 1 from the ZXM optimal DGZ to the PWM optimal DGZ and a CEDF maximum value of 15142 or 85% of the complex value.

The three remaining local CEDF maxima appear to be related. When the initial DGZ condition was two weapons at the complex's centroid, ZXM converged to a local CEDF maximum value of 10921 and to the optimal DGZ pair 3-3' with  $\|\nabla F\| = 0.0007$ . Similarly, when the initial DGZ condition was the two hardest installations, PWM converged to a local CEDF maximum value of 10798 and to the optimal DGZ pair 2-2'. ZXM and the same initial DGZ condition produced a third local CEDF maximum.

When the initial DGZ condition was the hardest installations, ZXM converged to a CEDF maximum value of 11431 and to the optimal DGZ pair 1-1' with  $\|\nabla F\| = 0.0027$ . This optimal DGZ pair had a larger CEDF value than the pairs 2-2' and 3-3'. Yet, it had a smaller CEDF value than the pair of highest valued DGZs.

The local CEDF maximum for PWM, when the initial DGZ condition was two weapons at the complex's centroid, was the same local maximum as determined using the highest valued initial condition. Additionally, this local maximum was located by all eight of the pseudo-random initial DGZ conditions.

Results of the CEDF maximization algorithm using only one weapon against this four-installation complex were examined. ZXM and PWM, using the centroid initial DGZ condition, converged to the highest



valued DGZ 1 in Figure 16. This is one of the two optimal DGZ locations determined by the two weapon evaluation. ZXM converged to a CEDF maximum value of 8547 or 78% of the value of installations 1, 2, and 3 and to an optimal DGZ location with  $\|\nabla F\| = 0.0015$ . PWM achieved a CEDF maximum value of 8252. Next, the algorithms used the highest valued initial DGZ condition for one weapon. Neither algorithm moved the optimal DGZ from the initial DGZ, installation 4. ZXM and PWM terminated with a CEDF maximum value of 6930.

The CEDF maximization algorithm's results for the three and four-installation complexes point out the last conclusion of this study. The most likely to succeed initial DGZ condition is to use the coordinates of the  $m$  highest valued installations as the initial DGZ coordinates. For all examples considered, the other three initial DGZ conditions located at least one local CEDF maximum that was less valuable than the local CEDF maximum determined from the highest valued initial DGZ condition. However, there is always an exception. The CEDF results of the simple one weapon-four installation complex indicated the HV initial DGZ is not always the best. For this reason, the CEDF maximization algorithm does not include a decision structure to determine the initial DGZ condition to use. Sometimes, one condition may be more likely than another to succeed and to achieve the most valuable local CEDF maximum.

The results of a three weapon-seven installation complex were analyzed to further define the CEP effects of the two CEDF models. Only three CEDF maximization algorithm runs were made with this complex. For the three runs, all weapon and installation parameters remained constant except each weapon's CEP, and the algorithm used the highest valued initial DGZ condition. Using each weapon's CEP = 0 feet, the algorithm

converged to a CEDF maximum value and optimal DGZ coordinates for the three weapons. Each weapon's CEP equaled 250 feet for the algorithm's second run. For this example, the ZXM optimal DGZ coordinates remained the same, as they should have. The PWM optimal DGZs were along line segments between the highest valued initial DGZs and the optimal DGZs from the first run when each CEP was 0 feet. However, because each weapon's CEP > 0, each of the second run optimal DGZs were slightly closer to their respective highest valued initial DGZ. Similarly, each weapon's CEP was 400 feet for the algorithm's final run. Again, the PWM optimal DGZs were along the same line segments as the optimal DGZs of examples one and two. These optimal DGZs were even closer to their respective highest valued initial DGZ. Thus, the effects of each weapon's CEP need to be included in locating optimal DGZ coordinates in a target complex.

## VII. Conclusions and Recommendations

The primary objective of this study was to investigate optimal DGZ locations within a target complex. In order to accomplish this, it was necessary to develop the Complex Expected Damage Function (CEDF) maximization algorithm. The algorithm locates optimal DGZ coordinates for multiple nuclear weapons against installations in a target complex. It does this by maximizing the expected target value damage for all installations. The two subobjectives of this study were to determine the sensitivity of the algorithm's results, the maximum CEDF value and the optimal DGZ coordinates, to two factors: first, the mathematical technique used to locate the optimal DGZs; second, the initial DGZ locations prior to CEDF maximization. This chapter discusses these objectives and their associated conclusions.

The CEDF maximization algorithm contains two related algorithms, and both of these include two elements. The first element is the CEDF, a mathematical model of the total complex expected target value damage. The CEDF is an unconstrained, nonlinear function of  $2m$  variables -- the  $(X_i, Y_i)$  DGZ coordinates for each of the  $m$  weapons. There is a CEDF model for each of the related algorithms. The basic element of each model is  $Pd_{i,j}$  -- the probability of achieving a specified level of damage to installation  $j$  from weapon  $i$ . This study used two forms of the  $Pd_{i,j}$  function; both forms depend on the DIA Physical Vulnerability system.

The major difference between the two CEDF models is their respective  $Pd_{i,j}$  expressions. The CEP-Excluded CEDF model assumes each weapon's CEP is 0 feet. This simplifying assumption results in two conditions: a less complicated mathematical expression for the CEDF and a closed-

form analytical expression for the gradient of the CEP-Excluded CEDF. The CEP-Included CEDF model includes each weapon's CEP; it is a more complicated expression.

The second element of the algorithm is a nonlinear optimization technique that maximizes the CEDF models and locates the corresponding optimal DGZs. Since an analytical expression for the gradient of the CEP-Included CEDF model was not available, the algorithm maximizes this CEDF using a direct search technique -- Powell's method of conjugate directions, PWM. This numerical search technique requires only function evaluations to locate a local maximum. Conversely, an analytical expression for the gradient of the CEP-Excluded model was calculated. The algorithm maximizes this CEDF using a gradient search technique -- a conjugate gradient with restarts method, ZGM. The algorithm also contains a third CEDF maximization technique -- a mixed technique, MXM. This technique consists of two stages, an initial ZGM stage and a PWM stage. The optimal DGZ coordinates from the ZGM stage become the initial DGZ coordinates for the PWM stage.

The CEDF maximization algorithm was verified and validated using two, three, and five-installation target complexes. The CEDF maximum value and optimal DGZ locations for two example problems were also compared with results from NUCWAVE. NUCWAVE is a one-sided nuclear weapons allocation war gaming model. It also optimizes the damage to a set of installations using a finite number of weapons. However, NUCWAVE determines a sequential optimal solution; it optimizes one weapon at a time until no increase in complex damage is possible. The comparisons between the results from the CEDF maximization algorithm and from NUCWAVE for two and five-installation target complexes indicated that the

algorithm determines the same local maximum as NUCWAVE.

A symmetric one weapon-four installation complex was designed to have four local maximums. CEDF results from this complex were analyzed and pointed out two ZXM maximization features, an operational characteristic and a limitation. These features depend on the two types of gradient symmetry. There is gradient symmetry from either geometrical symmetry of the target complex or collocation of two or more similar weapon types. The second type of symmetry is a limitation and prohibits ZXM maximization from using collocated initial DGZs.

Further analysis of three and four-installation target complexes indicated the presence of multiple local CEDF maximums. A two weapon-three installation target complex was analyzed using CEDF algorithm results. There were two distinct local CEDF maximums and two corresponding pairs of optimal DGZs. Similarly, a two weapon-four installation complex was analyzed. There were three distinct local CEDF maximums and three corresponding pairs of optimal DGZs. The CEDF maximization algorithm located these local maximums using different initial DGZ conditions. For both complexes analyzed, one local maximum was definitely the highest valued local maximum for the complex.

### Conclusions

The first subobjective was to determine the sensitivity of the results of the CEDF maximization algorithm to the mathematical technique used to locate the optimal DGZs. Two conclusions of the study emphasize the differences in CEDF results for the two CEDF models and their respective optimization techniques -- ZXM and PWM.

First, the algorithm requires some indication of a potential

increase in CEDF value in order to move a DGZ. That is, if there is no indication of a CEDF increase in the direction of a valued installation and there is an indication of a CEDF increase in the direction of a lesser valued installation, then the algorithm will move the DGZ towards the lesser valued installation. Eventually, the algorithm may converge to a less valuable CEDF local maximum.

The second conclusion is that a weapon's CEP and the CEDF model affect the CEDF maximum value and the respective optimal DGZ coordinates. All three, four, five, and seven-installation target complexes analyzed, that used weapons with  $CEP > 0$ , confirmed this conclusion. ZXM optimal DGZ coordinates were not optimal for PWM; similarly, PWM optimal DGZ coordinates were not optimal for ZXM. Results indicated that each CEDF model located a unique set of optimal DGZs; however, the distance difference between a ZXM and a PWM optimal DGZ was less than the weapon's CEP. This difference occurred because of the difference in  $Pd_{i,j}$  for the two models. For a weapon  $i$ -installation  $j$  interaction,  $Pd_{i,j}$  is larger for the CEP-Excluded model than it is for the CEP-Included model. This is because the CEP-Included  $Pd_{i,j}$  is reduced by a factor that depends on the weapon's CEP.

The second subobjective was to determine the sensitivity of the results of the CEDF maximization algorithm to the initial DGZ locations prior to optimization. Four initial DGZ conditions were evaluated using three and four-installation target complexes. The four initial conditions for an  $m$ -weapon complex were: (1) locating the weapons at the  $m$  highest valued installations, (2) locating the weapons at the  $m$  hardest installations, (3) locating the weapons at the complex's centroid, and (4) locating the weapons at  $m$  pseudo-random points. The algorithm

using these initial DGZ conditions located more than one local CEDF maximum for three and four-installation complexes. Thus, the last conclusion of the study emphasizes that no single initial DGZ condition always locates the most valuable local CEDF maximum. Hence, the algorithm does not include a decision structure to determine the correct initial DGZ condition. However, this conclusion also indicates that the most likely to succeed initial DGZ condition is to use the coordinates of the  $m$  highest valued installations as the initial DGZ coordinates.

This investigation characterized three factors that affect the optimal DGZ locations for multiple nuclear weapons in a target complex. The first factor was gradient symmetry; this symmetry resulted from either a geographically symmetric target complex or collocated weapons. The second factor was weapon CEP. Maximization of the two CEDF models produced slightly different optimal DGZs; this difference depended on a weapon's CEP and the CEDF model. The third factor was the initial DGZ location prior to CEDF maximization. The algorithm located different CEDF local maximums depending on the initial DGZ condition.

### Recommendations

The weapons analyst can use the algorithm to solve large targeting problems that include many complexes and different types and numbers of weapons. The algorithm can be a valuable sensitivity analysis tool to investigate weapon allocation tradeoffs. The analyst can evaluate the changes in total complex expected target value damage as a result of an increase or decrease in the number of weapons available to a target complex. Similarly, the analyst can estimate the effects that changes in a weapon's yield, CEP, or Pa can cause to the optimal DGZs.

The CEDF maximization algorithm does have some limitations. However, there is a specific improvement or recommendation associated with each limitation. The following recommendations would provide a more capable algorithm for strategic targeting studies:

1. Currently, the algorithm accomplishes only two-dimensional location of optimal DGZs; the user provides each weapon's height of burst. Optimization of each weapon's height of burst could be added to the algorithm.

2. Currently, the algorithm only allows military/industrial targets that are modeled as point targets. The algorithm could be modified to include area targets, equivalent area targets, and target avoidance areas.

3. In an analogous manner, the algorithm only includes blast damage effects for these point targets. Other nuclear weapon damage effects could be added to the model.

4. Similarly, other optimization techniques could be used to further investigate and characterize the CEDF local maximums for a target complex.

5. User-specified constraints that establish a minimum acceptable Pd for some or all installations could be included. This addition would provide a new initial DGZ condition. That is, locate the weapons at the installations with the largest minimum Pd.



Appendix A: Determination of the Distance  
Damage Sigma ( $\sigma_d$ ) and the Weapon Radius (WR)

The parameters  $\sigma_d$  and WR are necessary to calculate the probability of achieving a specified level of damage to installation j from weapon i.

1. Distance damage sigma,  $\sigma_d$ . The value of  $\sigma_d$  depends on the T factor of an installation's VNTK code. Table A-1 lists the T factors and their associated  $\sigma_d$  values. This table was extracted from NUCWAVE Model Methodology Analysis (Ref 25:3-4).

2. Weapon Radius, WR = f(weapon and installation parameters). The calculation of a WR depends on the concept of yield scaling. The following information on yield scaling is based upon Glasstone and Dolan's presentation in The Effects of Nuclear Weapons (Ref 11:100).

"In order to calculate the characteristic properties of the blast wave from an explosion of any given energy if those of another energy are known, appropriate scaling laws are applied" (Ref 11:100). A 1-kiloton nuclear explosion is the reference explosion for nuclear weapon calculations. Pressure vs range data have been tabulated and graphed for the 1-kt reference explosion. Also, the distance scaling laws use the cube root of the weapon's yield as the scaling factor. That is, if a pressure is experienced at a ground distance  $d_1$  from a 1-kt reference explosion, then this same pressure value will be experienced at a distance  $d_w$  from a w-kiloton explosion.

$$d_w = d_1(w)^{1/3}$$

The needed pressure vs range ( $d_w$ ) data for a w-kiloton explosion can

TABLE A-1

## Distance Damage Sigma and Target Type

T Factor		$\sigma_d$
P Targets	Q Targets	
L	R	0.1
P	S	0.2
M	Q	0.3
N	T	0.4
O	U	0.5

be determined using the scaled distance  $d_1$ . Therefore, to determine either the overpressure or dynamic pressure from an explosion of w-kt, all distances need to be transformed to the 1-kt scaled reference frame. The amount of pressure an installation experiences is the primary determinant of the installation's probability of damage.

Weapon and installation parameters are needed to determine the WR. The weapon parameters needed are the yield (Y) and the height of burst (HOB). The HOB and the subsequently calculated scaled weapon radius (SWR) are the two distances that need to be yield scaled. HOB is scaled to start the formulation; after the SWR is calculated, it is inversely scaled to specify the WR. The only installation parameter necessary to calculate the WR is the VNIK code. The following presentation is based upon the material in Mathematical Background and Programming Aids for the Physical Vulnerability System for Nuclear Weapons (Ref 6:57-61).

$$WR = SWR \frac{c}{1 - \sigma_d^2} (Y)^{1/3} \quad (A.1)$$

The parameter  $c$  is a constant that equals either 0.96 for overpressure sensitive installations or 0.91 for dynamic pressure sensitive installations. The SWR is calculated from the scaled height of burst (SHOB) and the adjusted VN number ( $VN_{adj}$ ).

$$SHOB = \frac{HOB}{(Y)^{1/3}}$$

$$VN_{adj} = VN + \Delta VN$$

$\Delta VN = 5.485 \ln(R)$  for overpressure sensitive installations

$= 2.742 \ln(R)$  for dynamic pressure sensitive installations

An iterative procedure is used to calculate the VN adjustment factor  $R$

$$R = 1 - \frac{K}{10} + \frac{K}{10} \left( \frac{20}{Y} \right)^{1/3} R^e$$

$K$  is the installation's  $K$  factor and the exponent  $e$  equals either 1/2 for overpressure sensitive installations or 1/3 for dynamic pressure sensitive installations.

$$SWR = \exp^{f(VN_{adj}, SHOB)}$$

The function,  $f(VN_{adj}, SHOB)$ , is a polynomial expression whose coefficients are available at 100-foot increments of the SHOB between 0 and 900 feet. Hence, the SWR is derived by linearly interpolating between a low SWR, that is calculated from a low SHOB, and a high SWR, that is calculated from a high SHOB. For example, for a SHOB of 632 feet, a SWR low is calculated for a SHOB of 600 feet and a SWR high is calculated for a SHOB of 700 feet. The actual SWR is a linear interpolation of the high and

low SWRs. Other algorithms use a table look-up with parameters, SHOB and  $VN_{adj}$ , to specify the SWR (Ref 19 and 25). The SWR is inversely yield scaled using Eq (A.1) to determine the WR.

Appendix B: Formulation of f(r) and  
Calculation of the Integration Limits

This information is based on material in Mathematical Background and Programming Aids for the Physical Vulnerability System for Nuclear Weapons (Ref 6:69-75).

The probability of achieving a specified level of damage to installation j from weapon i depends on weapon and installation parameters.

$$P_{d_{i,j}} = \int_0^{\infty} \int_0^{2\pi} P_d(r) \frac{1}{2\pi\sigma^2} e^{-\frac{\rho^2}{2\sigma^2}} r dr d\theta \quad (B.1)$$

where  $P_d(r)$  = distance damage function

$$\sigma = CEP/1.1774$$

$$\rho(r, \theta) = (r^2 + s^2 - 2rs \cos\theta)^{1/2}$$

A closed form solution to Eq(B.1) does not exist; however, an analytical approximation does.

$$P_{d_{i,j}} = \int_0^{\infty} f(r) dr \quad (B.2)$$

$$\text{where } f(r) = P_d(r)r \int_0^{2\pi} \frac{1}{2\pi\sigma^2} e^{-\frac{(r^2 + s^2 - 2rs \cos\theta)}{2\sigma^2}} d\theta \quad (B.3)$$

Eq(B.3) can be rewritten using a zeroth order modified Bessel Function,  $I_0(x)$  (Ref 19:378).

$$I_0\left(\frac{rs}{\sigma^2}\right) = \frac{1}{2\pi} \int_0^{2\pi} e^{\frac{rs \cos\theta}{\sigma^2}} d\theta$$

$$f(r) = P_d(r) \frac{r}{\sigma^2} e^{-\frac{(r^2 + s^2)}{2\sigma^2}} I_0\left(\frac{rs}{\sigma^2}\right) \quad (B.4)$$

$P_{d_{1,j}}$  is calculated using normalized distance variables and Eq (B.1). That is,  $r$ ,  $s$ , and  $WR$  are divided by  $\sigma$ , the standard deviation of the circular normal distribution.

Let  $r' = \frac{r}{\sigma}$  = the normalized distance between the installation and the impact point

$dr' = \frac{1}{\sigma} dr$  = the normalized differential element of  $r$

$s' = \frac{s}{\sigma}$  = the normalized distance between the installation and the DGZ

$WR' = \frac{WR}{\sigma}$  = the normalized weapon radius

Then Eqs (B.2) and (B.4) become

$$P_{d_{1,j}} = \int_0^{\infty} f(r') dr' \quad (B.5)$$

$$\text{where } f(r') = P_d(r') r' e^{-\frac{(r')^2 + (s')^2}{2}} I_0(r's') \quad (B.6)$$

A polynomial approximation of the zeroth order modified Bessel function,  $I_0(r's')$ , specifies a value of  $f(r')$  for a given  $r'$  (Ref 1:378).

Eq (B.5) can be rewritten as a definite integral with limits of integration,  $a$  and  $b$ , such that  $f(r') = 0$  for  $r' < a$  or  $r' > b$ .

$$P_{d_{1,j}} = \int_a^b f(r') dr' \quad (B.7)$$

Therefore, it is necessary to determine  $a$ , the smallest possible value

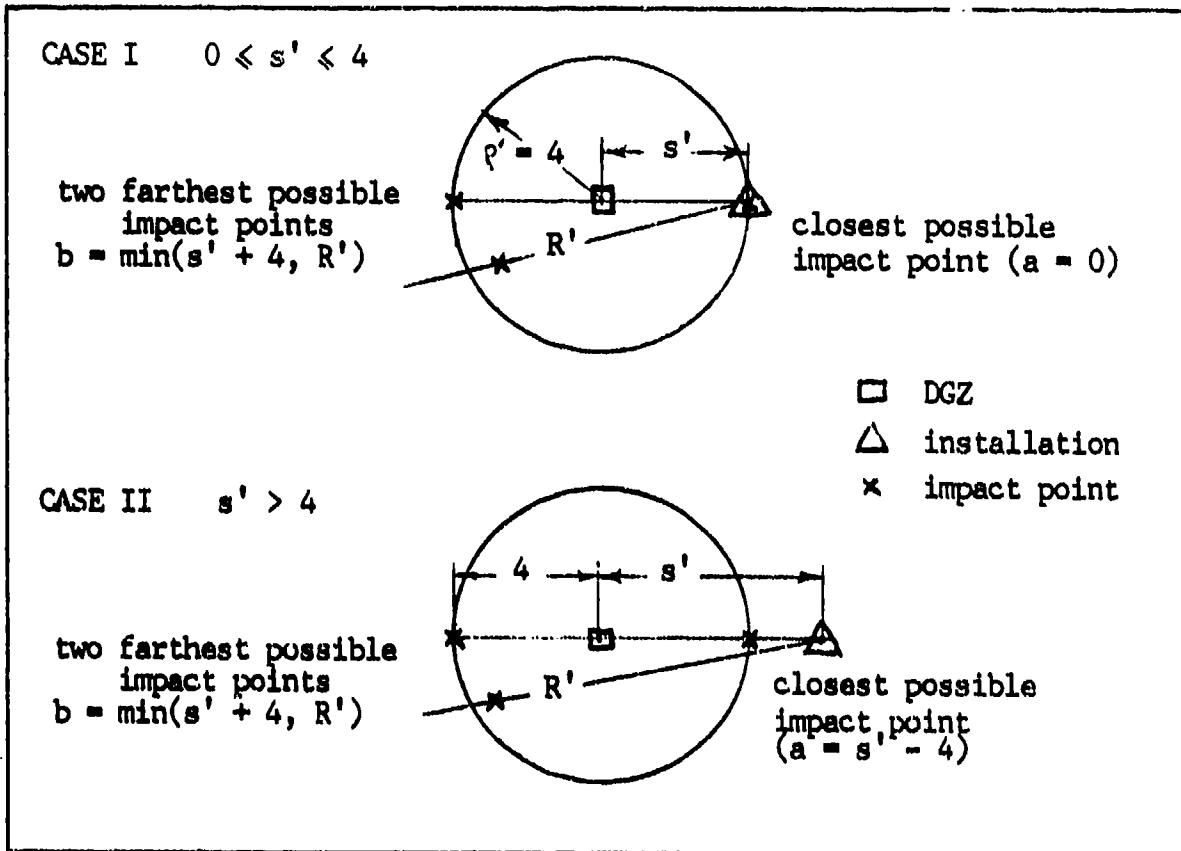


Figure B-1 Weapon-installation geometry to determine a and b

of  $r'$ , and  $b$ , the largest possible value of  $r'$ . These limits depend on weapon accuracy limitations and distance damage limitations. The weapon-installation geometry necessary to determine the limits of integration,  $a$  and  $b$ , is shown in Figure B-1. Two cases are examined.

Case I. The normalized distance between the installation and the DGZ is less than 4 ( $0 \leq s' \leq 4$ ). The distance between the closest possible impact point and the installation is  $r' = 0$ . The distance between the farthest possible impact point and the installation is the minimum of either  $r' = s' + 4$  or  $r' = R' = 1.06WR' \exp(2.86\sigma_d)$ . The point at  $r' = s' + 4$  corresponds to

the maximum distance from the DGZ,  $\rho'$ , that a weapon could be expected to impact. The probability that a weapon would impact farther than  $\rho = 4\sigma$  is less than 0.00005. Similarly, the point at  $r' = R'$  corresponds to the maximum distance from the installation,  $r'$ , that the weapon could detonate and expect to damage the installation. The  $P_d(r)$  for  $r' > R'$  is less than 0.0005.  $R'$  may be either greater than, equal, or less than  $s' + 4$ .

Case II. The normalized distance between the installation and the DGZ is greater than 4 ( $s' > 4$ ). The distance between the closest possible impact point and the installation is  $r' = s' - 4$ . The distance between the farthest possible impact point and the installation is again the minimum of either  $r' = s' + 4$  or  $r' = R'$ .

Therefore,  $a = \max(0, s' - 4)$  and  $b = \min(s' + 4, R')$  (Ref 6:73).

Eq (B.7) can be evaluated using Gauss-Legendre Quadrature between the limits,  $a$  and  $b$ ,

$$P_{d_{i,j}} = \frac{(b-a)}{2} \sum_{k=1}^{10} w w_k * f(r'_k) \quad (B.8)$$

where  $r'_k = \frac{(b-a)}{2} z z_k + \frac{(a+b)}{2}$

and  $f(r'_k)$  is Eq (B.6). Gauss-Legendre, the quadrature points,  $z z_k$ , and the coefficients,  $w w_k$ , are explained in Appendix C.

Eq (B.8) is evaluated to determine the probability of achieving a specified level of damage to installation  $j$  from weapon  $i$ .



Appendix C: Gauss-Legendre  
Quadrature to Integrate f(r')

Gauss-Legendre quadrature is a numerical integration technique that approximates a definite integral as a finite series (Ref 27:125). Each term is a weighted function value.

The series to approximate a definite integral along the interval  $[-1,1]$  by Gauss-Legendre is

$$\int_{-1}^1 f(y)dy = \sum_{k=1}^n ww_k * f(y_k) + R_n \quad (C.1)$$

where  $ww_k$  = quadrature coefficients  
 $y_k$  = quadrature base points  
 $R_n$  = remainder (negligible)  
 $n$  = number of quadrature points

Gauss-Legendre integration differs from symmetric, trapezoidal numerical integration. In Gauss-Legendre, the distances between the  $y_k$  base points along the abscissa are not equal. The points are spaced symmetrically, yet unequally, with respect to the midpoint of the interval  $[-1,1]$ , the origin. See Figure C-1. This method is more efficient than equal spacing trapezoidal methods because it requires fewer function evaluations to achieve comparable accuracy (Ref 15:378). The quadrature coefficients  $ww_k$  are positive numbers between 0 and 1; they are weights for the  $f(y_k)$  values.

The quadrature coefficients and weights are calculated from the nth

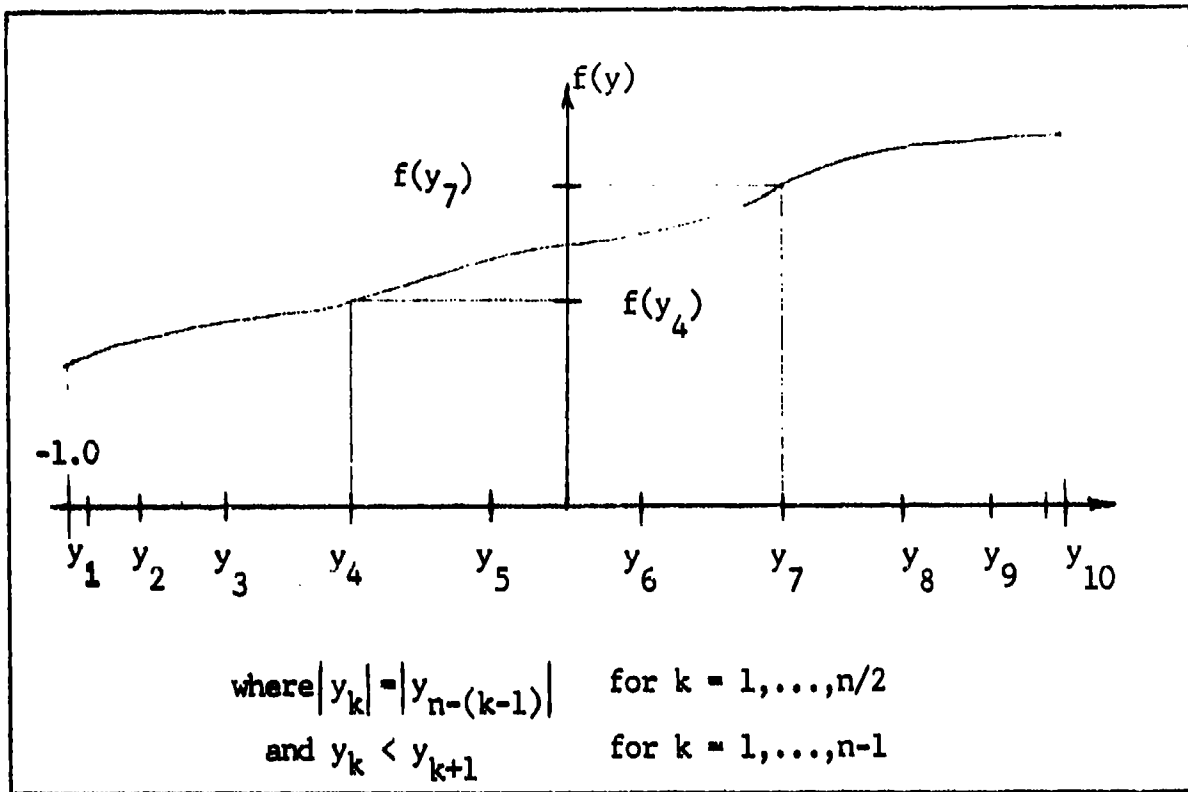


Figure C-1. Quadrature base points

Legendre polynomial,  $P_n$ . The base points,  $y_k$ , are the  $k = 1, \dots, 10$  zeros of  $P_n(y)$ . Similarly, the coefficients,  $w_k$ , are calculated from  $P_n(y)$  and the  $y_k$  (Ref 1:888). Table C-1 lists the base points and coefficients for  $n = 10$  (Ref 6:74 and 27:131).

However, to calculate  $Pd_{i,j}$  the interval of integration is not  $[-1,1]$ , but rather, it is  $[a,b]$ . For this interval of integration, the quadrature base points, coefficients, and limits of integration specify the transformed variables,  $w_k$  and  $r_k$  (Ref 1:887). Eq (C.1) becomes

$$\int_a^b f(y)dy = \sum_{k=1}^{10} w_k * f(r_k)$$

TABLE C-1

## Quadrature Base Points and Coefficients

n	$y_k$	$ww_k$
1, 10	0.9739065285	0.0666713433
2, 9	0.8650633667	0.1494513442
3, 8	0.6794095683	0.2190863625
4, 7	0.4333953941	0.2692667193
5, 6	0.148874339	0.2955242247

where  $w_k = \frac{(b-a)}{2} ww_k$

$$r_k = \frac{(b-a)}{2} y_k + \frac{(a+b)}{2}$$

This finite series is used to calculate  $Pd_{i,j}$ . For each  $k = 1, \dots, 10$ , an  $r_k$  and associated  $f(r_k)$  is calculated.

$$f(r_k) = f(r') = P_d(r') r' \exp \frac{(r')^2 + (s')^2}{2} I_0(r's')$$

Then  $f(r_k)$  is weighted by  $w_k$  and summed to form  $Pd_{i,j}$ .

Appendix D: Computer Code of the  
CEDF Maximization Algorithm

This appendix presents a glossary of the FORTRAN variables and lists the FORTRAN V source code of the CEDF maximization algorithm. The algorithm has the capacity to handle a target complex with up to ten weapons and ten installations. These capacities can be increased by changing the array dimension variables, MXM, MXN, MIM, MIN, MSQ, and M12. Parameter statements assign values to these variables; the glossary describes these variables.

The algorithm has several options. The user can specify one of three initial DGZ conditions and convergence parameters for ZXOGR. Chapters IV and V discuss user guidelines in selecting a particular option. Also, appendix E provides instructions in how to create an input data file.

The subroutine INITLZ assigns values to the two PVMIN maximization convergence control parameters, E and ESCALE. Chapter V discusses these parameters. Minor code changes would be required to modify either of the parameters.

A typical two weapon-four installation CEDF maximization problem requires approximately 3.0 seconds of execution time. The current program requires 50,000 words of core memory on a Control Data Corporation (CDC) 6600 Cyber computer.

Glossary of Variables

- A[WRADS] - a coefficient that is used to adjust the VN number.
- A[PDAM] - the lower limit of integration for the Gauss-Legendre quadrature.

- AA - the difference between weapon i and installation j  
x coordinates in feet.
- ACC - the ZXCGR convergence control parameter.
- ACC2 - the second stage ZXCGR convergence control parameter.
- B - the upper limit of integration for the Gauss-Legendre  
quadrature.
- BB - the difference between weapon i and installation j  
y coordinates in feet.
- BESB  
and BESC - polynomial approximations of the modified zeroth order  
Bessel function that are used to determine  $Pd_{i,j}$ .
- BETA(j) - the beta value for installation j.
- CC(j) - an intermediate value that is used to calculate the  
gradient of the CEDF.
- CEP(i) - the circular error probable of weapon i in feet.
- CEPA(i) - the adjusted circular error probable of weapon i in feet.
- CEPS(i) - intermediate storage of the circular error probable of  
weapon i in feet.
- DFPRED - an estimate of the expected increase in the CEDF.
- DGLN(i,3) - the degree-minute-second longitude coordinate for weapon i.
- DGLT(i,3) - the degree-minute-second latitude coordinate for weapon i.
- DLNC(i) - the east/west direction from the prime meridian for  
weapon i.
- DLTC(i) - the north/south direction from the equator for weapon i.
- DNCD(i) - the longitude coordinate in degrees for weapon i.
- DTCD(i) - the latitude coordinate in degrees for weapon i.
- E(i) - the P<sub>W</sub>MIN convergence control parameter.
- EC - the value of CEDF.
- EF - the value of -CEDF from P<sub>W</sub>MIN.
- ERF - a polynomial approximation of the error function that is  
used to determine a distance damage function value.

ESCALE - the maximum step size multiplier for a single step of each x.

EV(j) - the expected target value damage contribution to EC from installation j.

EX - an exponent that is used to calculate the VN reduction factor.

F - the value of -CEDF from FUNCT and GFUNCT.

F(5,2) - the ten Gauss-Legendre function evaluations.

FACTOR(j) - PS(j) \* value(j).

FN - the sum of the ten Gauss-Legendre function evaluations.

FV - the value of -CEDF from ZXOGR.

G(2) - a polynomial expression that is used to determine an SWR.

GR(i) - the 2m gradient elements of the CEP-Excluded CEDF model.

GRAD(i) - same as GR(i).

H - an intermediate value that is used to determine the appropriate Bessel Function approximation, BESB or BESC.

HOB(i) - the height of burst for weapon i in feet.

I - generally, the subscript of a weapon array.

IER - an error code from ZXOGR.

ILNC(j) - the east/west direction from the prime meridian for installation j.

ILTC(j) - the north/south direction from the equator for installation j.

INASG(j) - a logical decision variable that indicates whether an installation's coordinates have been assigned to a DGZ.

INC - the user-specified indicator variable that controls the assignment of initial DGZ locations.

INCD(j) - the longitude coordinate in degrees for installation j.

ISHOB(1,2) - the low and high scaled heights of burst for weapon i in feet.

ISLN(j,3) - the degree-minute-second longitude coordinate for installation j.

- ISLT(j,3) - the degree-minute-second latitude coordinate for installation j.
- ITCD(j) - the latitude coordinate in degrees for installation j.
- ITERS - the number of ZXCGR calls of function GFUNCT.
- J - generally, the subscript of an installation array.
- JJ - the argument of the modified zeroth order Bessel functions, BESB and BESC.
- K(j) - the K factors for installation j.
- KK - the incremental contribution to grad(i) or grad(i+m) from installation j.
- K0 thru K7 - the eight coefficients of the polynomial G(2).
- LNGMN - the length of one minute of longitude in feet.
- M - the number of weapons for the target complex.
- MAXFN - the maximum number of function evaluations ZXCGR is authorized.
- MAXIT - the maximum number of iterations PwMIN is authorized.
- MSQ - the dimension variable for a PwMIN work array  $[-2m * (2m + 3)]$ .
- MTM - the dimension variable for all  $2m$ -element weapon arrays.
- MTN - the dimension variable for all  $2n$ -element installation arrays.
- MXM - the dimension variable for all  $m$ -element weapon arrays.
- MKN - the dimension variable for all  $n$ -element installation arrays.
- M12 - the dimension variable for a ZXCGR work array  $[-12 * m]$ .
- N - the number of installations in the target complex.
- NOM - an intermediate value in calculating the gradient of the CEDF.
- NS - the standard deviation scaled distance between weapon i and installation j.
- NW - the dimension variable for a PwMIN work array.
- NWR - the standard deviation scaled weapon radius.

- N2 - the dimension of the xy weapon coordinate vector  $\underline{x}$ .
- ONCE - a logical decision variable that controls the algorithm so that ZXGGR runs a second time with a smaller ACC.
- ORLN - the longitude coordinate in degrees for the origin of the XY coordinate system.
- ORLT - the latitude coordinate in degrees for the origin of the XY coordinate system.
- Pa(i) - the probability of arrival for weapon i.
- PDAM - the probability of achieving a specified level of damage to installation j from weapon i.
- PDMG(i,j) -  $Pd_{i,j}$  - the probability of achieving a specified level of damage to installation j from weapon i.
- PDR - the distance damage function value.
- PP - the distance damage function value used to calculate  $Pd_{i,j}$  for the CEP-Included CEDF model.
- PS(j) - the probability of not achieving a specified level of damage to installation j.
- R[PDAM] - the standard deviation scaled distance between the impact point and the installation.
- R[PDR] - a distance, either S or R, from the subroutine PDAM.
- REM - a remainder that is used to translate the final DGZ coordinates from feet into degree-minute-second coordinates.
- RR - the flat earth distance between weapon i and installation j.
- R1 - an intermediate value that is used to calculate the VN reduction factor.
- R2 - the VN reduction factor.
- S - the known distance between weapon i and installation j.
- SHOB(i) - the scaled height of burst for weapon i in feet.
- SIG - the square root of the quantity,  $(1 - \sigma_d^2)$ .
- SIGMA(j) - the distance damage sigma for installation j.
- SWR - the scaled weapon radius.
- T(j) - the T-factor for installation j.



- TLAT - the sum of all installation latitude coordinates that is used to determine the number of feet per minute of longitude.
- U - the argument of the error function.
- UU - an intermediate exponent that is used to calculate the gradient of the CEDF.
- V[PDAM] - the dummy argument of BESB and BESC.
- V[PDR] - the dummy argument of ERF.
- V[WRADS] - the change in an installation's VN number when it is subjected to yields other than 20-kt.
- VAL - the current value of the highest valued installation.
- VALUE(j) - the value of installation j.
- VIND - the subscript of the current highest value/hardest installation.
- VN(j) - the integer VN number for installation j.
- VNA - the adjusted VN number.
- VNI - the current VN number of the hardest installation.
- W(5)[PDAM] - the Gauss-Legendre quadrature coefficients.
- W[WRADS] - the low and high SWR that are linearly interpolated between to determine the actual SWR.
- WR(i,j) - the weapon radius for the weapon i-installation j interaction.
- WW(MI2) - a ZXCGR work array.
- WWW(MSQ) - a PWIN work array.
- X(i) - the X coordinate of weapon i in feet.
- X(i + m) - the Y coordinate of weapon i in feet.
- XX(j) - the X coordinate of installation j in feet.
- XX(j + n) - the Y coordinate of installation j in feet.
- XXX - same as X(i) and X(i + m).
- X4 - the  $(X_1, Y_1)$  coordinates of the m weapons after ZXCGR maximization, but before PWIN maximization. Used with the mixed CEDF maximization algorithm.

- YIELD(i) - the yield of weapon i in kilotons.
- Z5 - the Gauss-Legendre quadrature base points.
- ZZ - a standard normal random variable.

Source Code

The next 27 pages list the FORTRAN V code of the CEDF maximization algorithm.

PROGRAM OPTMZ

C\*\*\*\*\*

C OPTMZ IS THE DRIVER MODULE FOR THE COMPLEX EXPECTED  
 C DAMAGE FUNCTION (CEDF) MAXIMIZATION ALGORITHM. THE  
 C ALGORITHM DETERMINES THE OPTIMAL DGT LOCATIONS FOR A  
 C FINITE NUMBER OF NUCLEAR WEAPONS AGAINST INSTALLATIONS  
 C IN A TARGET COMPLEX BY MAXIMIZING THE CEDF.

C\*\*\*\*\*

PARAMETER(MXM=10,MXN=10,MTM=20,MTN=20,MSQ=430,M12=120)  
 EXTERNAL GFUNCT  
 INTEGER M,N,VN(MXN),K(MXN),WR(MXM,MXN),N2,MAXFN,IER,MAXIT,NW  
 REAL VALUE(MXN),YIELD(MXM),CEP(MXM),HOB(MXM),PA(MXM),SIGMA(MXN)  
 REAL X(MTM),XX(MTN),GR(MTM),FV,BETA(MXN),WW(M12),ACC,DFPRED  
 REAL E(MTM),WWW(MSQ),XXX(MTM),X4(MTM),ESCALE,EF,CEPS(MXM),ACC2  
 LOGICAL ONCE  
 CHARACTER T(MXN)  
 COMMON/INSTLN/ N,VALUE,VN,K,XX  
 COMMON/PQIND/ T  
 COMMON/WPNS/ M,YIELD,CEP,HOB,PA  
 COMMON/PARAMS/ WR,SIGMA,BETA,ITERS  
 COMMON/CNTRL/ N2,ACC,ACC2,DFPRED,ESCALE,E

C  
 100 WRITE(6,101)  
 FORMAT(1X,5I(10))  
 WRITE(6,\*) ' CEDF MAXIMIZATION ALGORITHM'  
 WRITE(6,101)  
 ONCE=.TRUE.

C  
 CALL INITLZ(X)  
 CALL WRADS

C  
 DO 10 I=1,N2  
 XXX(I)=X(I)  
 10 CONTINUE

C  
 C CONJUGATE GRADIENT OPTIMIZATION OF THE CEP-EXCLUDED  
 C CEDF MODEL

C  
 WRITE(6,100)  
 WRITE(6,\*) ' ZXCGR MAXIMIZATION'  
 WRITE(6,100)  
 ITERS=1  
 MAXFN=100  
 DO 20 I=1,M  
 CEPS(I)=CEP(I)  
 CEP(I)=0.

20 CONTINUE  
 25 CONTINUE  
 WRITE(6,\*) ' ACC= ',ACC  
 CALL ZXCGR(GFUNCT,N2,ACC,MAXFN,DFPRED,X,GR,FV,WW,IER)  
 WRITE(6,\*) ' IER= ',IER  
 WRITE(6,\*) ' FUNCTION= ',-FV  
 WRITE(6,\*) ' FUNCTION EVALUATIONS: ',ITERS

```

DO 30 I=1,N2
  WRITE(6,*) * X(*,I,*)=*,X(I)
  WRITE(6,*) * GRAD(*,I,*)=*,GR(I)
30 CONTINUE
CALL OUTDGZ(X)

C
C CONJUGATE GRADIENT OPTIMIZATION OF THE CEP-EXCLUDED
C CEDF MODEL USING A REDUCED CONVERGENCE CRITERIA
C

IF(ONCE) THEN
  DO 35 I=1,N2
    X4(I)=X(I)
35 CONTINUE
  WRITE(6,100)
  WRITE(6,*) * ZXCGR WITH ACC REDUCED*
  WRITE(6,100)
  ONCE=.FALSE.
  ACC=ACC2
  ITERS=1
  GO TO 25
ENDIF

C
C POWELL'S CONJUGATE DIRECTIONS OPTIMIZATION OF THE
C CEP-INCLUDED CEDF MODEL
C

WRITE(6,100)
WRITE(6,*) * PWMIN MAXIMIZATION*
WRITE(6,100)
MAXIT=500
DO 40 I=1,M
  CEP(I)=CEPS(I)
40 CONTINUE
NW=N2*(N2+3)
CALL PWMIN(XXX,E,N2,EF,ESCALE,MAXIT,WWW,NW)
WRITE(6,*) * FUNCTION=*, -EF
DO 50 I=1,N2
  WRITE(6,*) * XXX(*,I,*)=*,XXX(I)
50 CONTINUE
CALL OUTDGZ(XXX)

C
C MIXED OPTIMIZATION OF THE CEDF MODEL. THE DGZ
C COORDINATES FROM THE FIRST CONJUGATE GRADIENT OPTIMI-
C ZATION BECOME THE INITIAL DGZ COORDINATES FOR POWELL'S
C CONJUGATE DIRECTIONS OPTIMIZATION.
C

WRITE(6,100)
WRITE(6,*) * MIXED TECHNIQUE MAXIMIZATION*
WRITE(6,100)
CALL PWMIN(X4,E,N2,EF,ESCALE,MAXIT,WWW,NW)
WRITE(6,*) * FUNCTION=*, -EF
DO 70 I=1,N2
  WRITE(6,*) * X4(*,I,*)=*,X4(I)
70 CONTINUE
CALL OUTDGZ(X4)
93 CONTINUE
END

```

C\*\*\*\*\*

SUBROUTINE GFUNCT(N2,X,F,GRAD)

C 1. CALCULATES THE CEDF(X), THE COMPLEX EXPECTED  
C DAMAGE FUNCTION, FOR M WEAPONS AND N INSTALLATIONS  
C USING THE CEP-EXCLUDED CEDF MODEL.  
C 2. CALCULATES THE 2M ELEMENTS OF THE GRADIENT OF  
C THE CEDF(X).

C\*\*\*\*\*

PARAMETER (MXM=10, MXN=10, MTM=20, MTN=20)  
INTEGER M,N,VM(MXN),K(MXN),WR(MXM,MXN),N2  
REAL VALUE(MXN),YIELD(HXM),CEP(MXM),HOB(MXM),PA(MXM)  
REAL X(MTM),XX(MTN),EC,EV(MXN),PS(MXN),PDAM,SIGMA(MXN)  
REAL PDMG(MXM,MXN),BETA(MXN),F  
REAL FACTOR(MXN),CC(MXN),GRAD(MTM),AA,BB,RR,UU,KK,NOM  
CHARACTER T(MXN)  
COMMON/INSTLN/ N,VALUE,VM,K,XX  
COMMON/POIND/ T  
COMMON/WPNS/ M,YIELD,CEP,HOB,PA  
COMMON/PARAMS/ WR,SIGMA,BETA,ITERS

C  
100 FORMAT(' WEAPON ',I2,' XY COORDINATES: (',F7.3,',',F7.3,',)')  
EC=0.0  
ITERS=ITERS+1

DO 60 L=1,M  
WRITE(6,100) L,X(L),X(L+M)  
60 CONTINUE

C  
C CALCULATES THE CEDF(X).  
C

DO 20 J=1,N  
PS(J)=1.0  
DO 10 I=1,M  
PDMG(I,J)=PDAM(I,J,X)  
PS(J)=PS(J)\*(1.-PA(I)+PDMG(I,J))

10 CONTINUE  
EV(J)=(1.-PS(J))\*VALUE(J)  
WRITE(6,\*) ' PS(',J,') = ',PS(J)  
EC=EC+EV(J)  
FACTOR(J)=S(J)+VALUE(J)  
CC(J)=2.5166282\*Beta(J)

20 CONTINUE  
WRITE(6,\*) ' EC = ',EC  
F=-EC

C  
C  
C

CALCULATES THE GRADIENT OF THE CEDF(X).

```
DO 40 I=1,M
  GRAD(I)=0.0
  GRAD(I+M)=0.0
  DO 30 J=1,N
    AA=XX(J)-X(I)
    BB=XX(J+N)-X(I+M)
    RR=SQRT(AA**2+BB**2)
    IF(RR.LT.0.001) RR=10.0
    UU=ABS(((1.0/BETA(J))*LOG(WR(I,J)/RR)-BETA(J))/1.4142135)
    NOM=FACTOR(J)*PA(I)*EXP(-UU**2)
    KK=NOM/((1.0-PA(I))*PDMG(I,J)+CC(J)*RR**2)
    GRAD(I)=GRAD(I)+KK*AA
    GRAD(I+M)=GRAD(I+M)+KK*BB
30  CONTINUE
40  CONTINUE
DO 50 L=1,N/2
  GRAD(L)=-GRAD(L)
50  CONTINUE
END
```

C\*\*\*\*\*

SUBROUTINE FUNCT(N2,X,F)

C           1. CALCULATES THE CEDF(X) FOR M WEAPONS AND N  
C           INSTALLATIONS USING THE CEP-INCLUDED MODEL.

C\*\*\*\*\*

PARAMETER(MXM=10,MXN=10,MTM=20,MTN=20)  
INTEGER M,N,VN(MXN),K(MXN),WR(MXM,MXN),N2  
REAL VALUE(MXN),YIELD(MXM),CEP(MXM),HOB(MXM),PA(MXM)  
REAL X(MTM),XX(MTN),EC,EV(MXN),PS(MXN),PDAM,F,BETA(MXN)  
REAL PDMG(MXM,MXN),SIGMA(MXN)  
CHARACTER T(MXN)  
COMMON/INSTLN/ N,VALUE,VN,K,XX  
COMMON/PQIND/ T  
COMMON/WPNS/ M,YIELD,CEP,HOB,PA  
COMMON/PARAMS/ WR,SIGMA,BETA,ITERS

C  
EC=0.0  
DO 20 J=1,N  
  PS(J)=1.0  
  DO 10 I=1,M  
    PDMG(I,J)=PDAM(I,J,X)  
    PS(J)=PS(J)+(1.0-PA(I))\*PDMG(I,J)  
1   CONTINUE  
  EV(J)=(1.0-PS(J))\*VALUE(J)  
  EC=EC+EV(J)  
2   CONTINUE  
C  
F=-EC  
RETURN  
END

C\*\*\*\*\*

SUBROUTINE INITLZ(X)

- C 1. READS USER-SPECIFIED WEAPON AND INSTALLATION
- C PARAMETERS FROM THE EXTERNAL FILE, INDATA.
- C 2. ASSIGNS INITIAL DGZ COORDINATES ACCORDING TO
- C THE USER OPTION VARIABLE, INC.
- C 3. TRANSFORMS ALL WEAPON AND INSTALLATION COORDINATES
- C INTO FEET RELATIVE TO A COMMON ORIGIN IN A XY
- C COORDINATE SYSTEM.
- C 4. INITIALIZES ACCURACY AND CONVERGENCE CRITERIA
- C FOR THE OPTIMIZATION SUBROUTINES, ZXCGR AND PWMIN.

C\*\*\*\*\*

```
PARAMETER(MXM=10,MXN=10,MTM=20,MTN=20)
INTEGER DGLN(MXM,3),DGLT(MXM,3),ISLN(MXN,3),ISLT(MXN,3)
INTEGER VN(MXN),K(MXN),M,N,INC,N2,VIND,VNI
REAL DNCD(MXM),DTCD(MXM),INCD(MXN),ITCD(MXN),ORLN,ORLT
REAL YIELD(MXM),CEP(MXM),HOB(MXM),PA(MXM),VALUE(MXN)
REAL X(MTM),XX(MTN),ACC,ACC2,DFPRED,ESCALE,E(MTM),VAL
REAL NDGLN,NDGLT,NISLN,NISLT,TLAT,LNGMN
LOGICAL INASG(MXN)
CHARACTER DLNC(MXM),DLTC(MXM),ILNC(MXN),ILTC(MXN),T(MXN)
CHARACTER PH*28
COMMON/INSTLN/ N,VALUE,VN,K,XX
COMMON/PQIND/ T
COMMON/WPNS/ M,YIELD,CEP,HOB,PA
COMMON/CNTRL/ N2,ACC,ACC2,DFPRED,ESCALE,E
COMMON/ORIGIN/ CRLN,ORLT,LNGMN
100 FORMAT(2X,I4,I2,I2,A1,4X,I3,I2,I2,A1,4X,
*F5.0,2X,F5.0,2X,F6.0,1X,F4.2)
105 FORMAT(3X,I2,5X,F5.0,2X,F5.0,2X,F6.0,1X,F4.2)
110 FORMAT(2X,I4,I2,I2,A1,4X,I3,I2,I2,A1,4X,I2,A1,I1,2X,F6.0)
120 FORMAT(/,'INITLZ',/)
130 FORMAT(' THIS PROBLEM USES ',I2,' WEAPONS',/)
140 FORMAT(' WEAPON YIELD CEP HOB PA')
150 FORMAT(/,' THIS COMPLEX CONTAINS ',I2,' INSTALLATIONS',/)
160 FORMAT(' LONGITUDE LATITUDE VNTK VALUE')
170 FORMAT(/,' THE XY COORDINATES OF THE INSTALLATIONS IN FEET',/)
180 FORMAT(/,' INITIAL DGZ LOCATIONS ARE ',A28,/)
C
WRITE(6,120)
OPEN(15,FILE='INDATA')
REWIND 15
C
CC READ THE USER INITIAL DGZ COORDINATE OPTION VARIABLE,INC.
C IF INC = 1, THEN USER-SPECIFIED COORDINATES
C IF INC = 2, THEN HIGHEST VALUE INSTALLATION COORDINATES
C IF INC = 3, THEN HARDEST INSTALLATION COORDINATES
C
READ(15,*) INC
```



```

C
C   READ USER-SPECIFIED WEAPON PARAMETERS.
C
  READ(15,*) M
  WRITE(6,130) M
  WRITE(6,140)
  DO 10 I=1,M
    READ(15,100) (DGLN(I,L),L=1,3),DLNC(I),(DGLT(I,L),L=1,3),
*DLTC(I),YIELD(I),CEP(I),HOB(I),PA(I)
  WRITE(6,105) I,YIELD(I),CEP(I),HOB(I),PA(I)
10  CONTINUE
C
C   READ USER-SPECIFIED INSTALLATION PARAMETERS.
C
  READ(15,*) N
  WRITE(6,150) N
  WRITE(6,160)
  DO 20 J=1,N
    READ(15,110) (ISLN(J,L),L=1,3),ILNC(J),(ISLT(J,L),L=1,3),
*ILTC(J),VN(J),T(J),K(J),VALUE(J)
    WRITE(6,110) (ISLN(J,L),L=1,3),ILNC(J),(ISLT(J,L),L=1,3),
*ILTC(J),VN(J),T(J),K(J),VALUE(J)
20  CONTINUE
C
  SMNCD=180.0
  SMTCD=180.0
  TLAT=0.0
C
C   TRANSLATES INSTALLATION J DEGREE-MINUTE-SECOND
C   COORDINATES INTO DEGREES.
C
  DO 30 J=1,N
    IF(ILNC(J).EQ.'E') THEN
      INCD(J)=REAL(ISLN(J,1))+(REAL(ISLN(J,2))/60.0)+
* (REAL(ISLN(J,3))/3600.0)
    ELSE
      NISLN=-REAL(ISLN(J,1))
      INCD(J)=NISLN-(REAL(ISLN(J,2))/60.0)-
* (REAL(ISLN(J,3))/3600.0)
    ENDIF
    IF(INCD(J).LT.SMNCD) SMNCD=INCD(J)
    IF(ILTC(J).EQ.'N') THEN
      ITCD(J)=REAL(ISLT(J,1))+(REAL(ISLT(J,2))/60.0)+
* (REAL(ISLT(J,3))/3600.0)
    ELSE
      NISLT=-REAL(ISLT(J,1))
      ITCD(J)=NISLT-(REAL(ISLT(J,2))/60.0)-
* (REAL(ISLT(J,3))/3600.0)
    ENDIF
    IF(ITCD(J).LT.SMTCD) SMTCD=ITCD(J)
    TLAT=TLAT+ITCD(J)
30  CONTINUE

```



```

C
C   TRANSFORM WEAPON I DEGREE COORDINATES INTO FEET
C   RELATIVE TO A COMMON ORIGIN.
C
      DO 60 I=1,M
        X(I)=(DNCD(I)-OPLN)*6300.*LNGMN
        X(I+M)=(DTCD(I)-ORLT)*364800.*1
50      CONTINUE
C
      ELSEIF(INC.EQ.2) THEN
C
C   IF INC = 2, THEN ASSIGN THE COORDINATES OF THE M
C   HIGHEST VALUED INSTALLATIONS AS THE INITIAL DGZ
C   COORDINATES OF THE M WEAPONS.
C
      PH='HIGHEST VALUED INSTALLATIONS'
      DO 70 I=1,M
        VAL=0.0
        VIND=0
        DO 75 J=1,N
          IF(INASG(J)) GO TO 75
          IF(VALUE(J).LT.VAL) GO TO 75
          VAL=VALUE(J)
          VIND=J
75      CONTINUE
        X(I)=XX(VIND)
        X(I+M)=XX(VIND+N)
        INASG(VIND)=.TRUE.
70      CONTINUE
C
      ELSE
C
C   IF INC = 3, THEN ASSIGN THE COORDINATES OF THE M
C   HARDEST INSTALLATIONS AS THE INITIAL DGZ COORDINATES
C   OF THE M WEAPONS.
C
      PH='HARDEST INSTALLATIONS'
      DO 80 I=1,M
        VNI=0
        VIND=0
        DO 85 J=1,N
          IF(INASG(J)) GO TO 85
          IF(VN(J).LT.VNI) GO TO 85
          VNI=VN(J)
          VIND=J
85      CONTINUE
        X(I)=XX(VIND)
        X(I+M)=XX(VIND+N)
        INASG(VIND)=.TRUE.
80      CONTINUE
      ENDIF
      WRITE(6,180) PH
      DO 95 I=1,M
        WRITE(6,*) ' X(*,I,*) = ',X(I),'      X(*,I+M,*) = ',X(I+M)
95      CONTINUE

```

```
C
C      INITIALIZE THE CONVERGENCE PARAMETERS
C      OF THE SUBROUTINES, ZXCGR AND PWMIN.
C
      ACC=0.01
      READ(15,*) ACC2
      READ(15,*) DFPRED
      N2=2*M
      ESCALE=5000.0
      DO 99 I=1,N2
         E(I)=0.1
99    CONTINUE
      CLOSE(15)
      END
```

C\*\*\*\*\*

SUBROUTINE OUTDGZ(X)

C 1. TRANSLATES THE FINAL DGZ COORDINATES FROM FEET  
C INTO DEGREE-MINUTE-SECOND LONGITUDE AND LATITUDE  
C COORDINATES.

C\*\*\*\*\*

```
PARAMETER(MXM=10,MTM=20)
REAL X(MTM),ORLN,ORLT,REM,LNGMN
REAL YIELD(MXM),CEP(MXM),HOB(MXM),PA(MXM)
INTEGER DGLN(MXM,3),DGLT(MXM,3)
CHARACTER DLNC(MXM),DLTC(MXM)
COMMON/MPNS/ M,YIELD,CEP,HOB,PA
COMMON/ORIGIN/ ORLN,ORLT,LNGMN
100 FORMAT(5X,I2,5X,I4,I2,I2,A1,4X,I3,I2,I2,A1)
110 FORMAT(/,' WEAPON LONGITUDE LATITUDE')
120 FORMAT(/)
```

100  
110  
120  
C

```
WRITE(6,110)
DO 10 I=1,M
  IF(ORLN.GE.0.) THEN
    DGLN(I,1)=INT(ORLN)
    DLNC(I)='E'
    DGLN(I,2)=INT(X(I)/LNGMN)
    REM=X(I)-LNGMN*DGLN(I,2)
  ELSE
    DGLN(I,1)=ABS(INT(ORLN+1.0))
    DLNC(I)='W'
    DGLN(I,2)=INT(60.0-X(I)/LNGMN)
    REM=60.0*LNGMN-X(I)-LNGMN*DGLN(I,2)
  ENDIF
  DGLN(I,3)=INT(REM*60.0/LNGMN)
  IF(ORLT.GE.0.) THEN
    DGLT(I,1)=INT(ORLT)
    DLTC(I)='N'
    DGLT(I,2)=INT(X(I+M)/6080.0)
    REM=X(I+M)-6080.0*DGLT(I,2)
  ELSE
    DGLT(I,1)=ABS(INT(ORLT+1.0))
    DLTC(I)='S'
    DGLT(I,2)=INT(60.0-X(I+M)/6080.0)
    REM=364800.0-X(I+M)-6080.0*DGLT(I,2)
  ENDIF
  DGLT(I,3)=INT(REM/101.333333)
  WRITE(6,100) I,(DGLN(I,L),L=1,3),DLNC(I),(DGLT(I,L),L=1,3),DLTC(I)
1 CONTINUE
WRITE(6,120)
RETURN
END
```

1

C\*\*\*\*\*

SUBROUTINE WRADS

C 1. CALCULATES THE WEAPON RADII, WR(I,J), FOR EACH  
C WEAPON I - INSTALLATION J INTERACTION.  
C 2. CALCULATES THE BETA(J) FOR EACH INSTALLATION.

C\*\*\*\*\*

PARAMETER (MXM=10, MXN=10, MTM=20, MTN=20)  
REAL KK, YIELD(MXM), HOB(MXM), E, EX, A, SIGMA(MXN), SIG, R1, R2  
REAL V, VNA, SHOB(MXM), G(2), W(2), SWR, K0, K1, K2, K3, K4, K5, K6, K7  
REAL VALUE(MXN), CEP(MXM), PA(MXM), BETA(MXN), XX(MTN)  
INTEGER VN(MXN), K(MXN), ISHOB(MXM,2), WR(MXM,MXN), I, J, L, M, N  
CHARACTER T(MXN), TT, 5  
COMMON/INSTLN/ N, VALUE, VN, K, XX  
COMMON/PQIND/ T  
COMMON/WPNS/ M, YIELD, CEP, HOB, PA  
COMMON/PARAMS/ WR, SIGMA, BETA, ITERS  
FORMAT(/, 'WRADS', /)

10  
C

WRITE(6,10)

C  
C  
C  
C

SPECIFIES THE DISTANCE DAMAGE SIGMA AND THE BETA FOR EACH INSTALLATION J.

20  
C

J=1  
J=J+1  
IF((T(J).EQ.'L').OR.(T(J).EQ.'R')) THEN  
SIGMA(J)=0.1  
ELSEIF((T(J).EQ.'P').OR.(T(J).EQ.'S')) THEN  
SIGMA(J)=0.2  
ELSEIF((T(J).EQ.'M').OR.(T(J).EQ.'Q')) THEN  
SIGMA(J)=0.3  
ELSEIF((T(J).EQ.'N').OR.(T(J).EQ.'T')) THEN  
SIGMA(J)=0.4  
ELSE  
SIGMA(J)=0.5  
ENDIF  
IF((T(J).EQ.'L').OR.(T(J).EQ.'P').OR.(T(J).EQ.'M').OR.  
(T(J).EQ.'N').OR.(T(J).EQ.'Q')) THEN  
TT='PTYPE'  
ELSE  
TT='QTYPE'  
ENDIF  
IF(TT.EQ.'PTYPE') THEN  
EX=0.5  
SIG=1.96  
A=5.485  
R1=2.0  
ELSE  
EX=(1.0/3.0)  
SIG=1.91  
A=2.742  
R1=3.0  
ENDIF  
BETA(J)=SQRT(-LOG(1.0-SIGMA(J)\*\*2))

```

I=)
30 I=I+1
   W(1)=0.0
   W(2)=0.0
   G(1)=0.0
   G(2)=0.0
C
C CALCULATES THE VN REDUCTION FACTOR, R2, AND THE
C ADJUSTED VN NUMBER, VNA.
C
KK=REAL(K(J))
100 R2=1.0-(KK/10.0)+(KK/10.0)*(20.0/YIELD(I)**(1.0/3.0))*R1**EX
IF(ABS(R2-R1).GE.0.001) THEN
   R1=R2
   GO TO 100
ENDIF
V=A*LOG(R2)
VNA=REAL(VN(J))+V
C
C CALCULATES THE SCALED HEIGHT OF BURST (SHOB).
C
SHOB(I)=HOB(I)/YIELD(I)**(1.0/3.0)
IF(SHOB(I).GT.900.0) THEN
   WRITE(6,*) 'HOB TOO BIG'
   SHOB(I)=900.0
ENDIF
ISHOB(I,1)=INT(SHOB(I)/100.0)*100
ISHOB(I,2)=ISHOB(I,1)+100
E=(SHOB(I)-REAL(ISHOB(I,1)))/100.0
C
L=0
110 L=L+1
C
C DETERMINES THE POLYNOMIAL COEFFICIENTS TO CALCULATE
C G(VNA,ISHOB).
C
IF(TT.EQ.'PTYPE') GO TO 200
GO TO 210
120 G(L)=K0+K1*VNA+K2*VNA**2+K3*VNA**3+K4*VNA**4
GO TO 140
130 G(L)=K0+K1*VNA+K2*VNA**2+K3*VNA**3+K4*VNA**4+
*K5*VNA**5+K6*VNA**6+K7*VNA**7
C
C CALCULATES THE SCALED WEAPON RADIUS (SWR).
C
140 W(L)=EXP(G(L))
IF(E.LT.0.0001) GO TO 150
IF(L.LT.2) GO TO 110
150 SWR=W(1)+E*(W(2)-W(1))
C
C INVERSE YIELD SCALES THE SWR TO DETERMINE THE WEAPON
C RADIUS, WR(I,J), FOR THE WEAPON I -INSTALLATION J
C INTERACTION.
C
WR(I,J)=INT((SWR*YIELD(I)**(1.0/3.0))*SIG/(1.0-SIGMA(J)**2))+0.5)
WRITE(6,*) ' WR(',I,',',J,') = ',WR(I,J)
GO TO 170

```

```

C
160 WRITE(6,*) * VN TOO LARGE FOR HOBO
    WP(I,J)=0
170 IF(I.LT.M) GO TO 30
    IF(J.LT.N) GO TO 20
    GO TO 220
200 IF(ISHOB(I,L).LT.100) THEN
C
C   COEFFICIENTS OF G(VNA,ISHOB) FOR OVERPRESSURE (P-TYPE)
C   TARGETS FOR ISHOB FROM 0 FEET TO 900 FEET.
C
    IF(VNA.LE.7.5) THEN
        K0=8.206936
        K1=-9.8662222E-02
        K2=-4.2705319E-03
        K3=44.67361800E-03
        K4=0.0
    ELSE
        K0=8.263243
        K1=-1.2109524E-01
        K2=12.74266E-04
        K3=-9.2065496E-06
        K4=0.0
    ENDIF
    GO TO 120
ELSEIF(ISHOB(I,L).LT.200) THEN
    IF(VNA.GT.51.0) GO TO 160
    IF(VNA.LE.7.5) THEN
        K0=8.29123
        K1=-1.132939E-01
        K2=31.19908E-03
        K3=0.0
        K4=0.0
    ELSE
        K0=8.29959
        K1=-1.1043338E-01
        K2=-4.6494085E-04
        K3=65.8301E-06
        K4=-9.1680378E-07
    ENDIF
    GO TO 120
ELSEIF(ISHOB(I,L).LT.300) THEN
    IF(VNA.GT.41.0) GO TO 160
        K0=8.395223
        K1=-1.4717856E-01
        K2=12.74489E-03
        K3=-2.0632771E-03
        K4=16.67591E-05
        K5=-6.89342E-06
        K6=14.23714E-08
        K7=-1.1675015E-09
    GO TO 130

```



```

ELSEIF(ISHOB(I,L).LT.400) THEN
  IF(VNA.GT.34.0) GO TO 160
  K0=8.419584
  K1=-9.9827816E-02
  K2=-4.1872797E-03
  K3=54.49084E-05
  K4=-3.758352E-05
  K5=14.70969E-07
  K6=-2.0170989E-08
  K7=0.0
  GO TO 130
ELSEIF(ISHOB(I,L).LT.500) THEN
  IF(VNA.GT.30.0) GO TO 160
  K0=8.499489
  K1=-1.0965211E-01
  K2=-3.4445747E-03
  K3=72.61706E-05
  K4=-7.20905E-05
  K5=33.19013E-07
  K6=-5.6685057E-08
  K7=0.0
  GO TO 130
ELSEIF(ISHOB(I,L).LT.600) THEN
  IF(VNA.GT.27.0) GO TO 160
  K0=8.525985
  K1=-6.3120552E-02
  K2=-2.5622191E-02
  K3=54.26447E-04
  K4=-5.926339E-04
  K5=34.85504E-06
  K6=-1.0228646E-06
  K7=11.4432E-09
  GO TO 130
ELSEIF(ISHOB(I,L).LT.700) THEN
  IF(VNA.GT.25.0) GO TO 160
  K0=8.586222
  K1=-1.002711E-01
  K2=-9.9171759E-03
  K3=26.0232E-04
  K4=-3.6028224E-04
  K5=28.02515E-06
  K6=-1.0826364E-06
  K7=15.41557E-09
  GO TO 130
ELSEIF(ISHOB(I,L).LT.800) THEN
  IF(VNA.GT.22.0) GO TO 160
  K0=3.655962
  K1=-1.3679886E-01
  K2=14.26281E-03
  K3=-4.0529993E-03
  K4=50.24125E-05
  K5=-2.5712239E-05
  K6=43.79003E-08
  K7=0.0
  GO TO 130

```

```

ELSEIF(ISHOB(I,L).LT.90 ) THEN
  IF(VNA.GT.21.0) GO TO 160
  IF(VNA.LE.7.5) THEN
    K0=8.681285
    K1=-1.1432864E-01
    K2=-1.7888646E-03
    K3=15.95909E-05
    K4=0.0
  ELSE
    K0=12.51342
    K1=-1.516344
    K2=17.69944E-02
    K3=-8.900635E-03
    K4=14.00736E-05
  ENDIF
  GO TO 120
ELSE
  IF(VNA.GT.20. ) GO TO 160
  IF(VNA.LE.7.5) THEN
    K0=8.719654
    K1=-1.2198526E-01
    K2=12.03604E-04
    K3=-1.3863251E-04
    K4=0.0
  ELSE
    K0=13.47289
    K1=-1.971983
    K2=25.47267E-02
    K3=-1.4325115E-02
    K4=26.40371E-05
  ENDIF
  GO TO 120
ENDIF

```

C  
C  
C  
C  
210

COEFFICIENTS OF G(VNA,ISHOB) FOR DYNAMIC PRESSURE  
(Q-TYPE) TARGETS FOR ISHOB FROM 0 FEET TO 900 FEET.

```

IF(ISHOB(I,L).LT.10. ) THEN
  IF(VNA.GT.35.0) GO TO 160
  K0=8.315159
  K1=-0.1060868
  K2=0.0005224
  K3=-0.000313
  K4=3.22649E-05
  K5=-1.23227E-06
  K6=1.96777E-08
  K7=-1.05880E-10
  GO TO 130

```

```

ELSEIF(ISHOB(I,L).LT.20) THEN
  IF(VNA.GT.35.0) GO TO 160
  K0=8.376082
  K1=-0.1042945
  K2=-0.0012014
  K3=-3.91136E-05
  K4=1.26757E-05
  K5=-4.97579E-07
  K6=5.77257E-09
  K7=0.0
  GO TO 130
ELSEIF(ISHOB(I,L).LT.30) THEN
  IF(VNA.GT.35.0) GO TO 160
  K0=8.42024
  K1=-1.09473E-01
  K2=14.62288E-04
  K3=-5.969792E-14
  K4=66.97002E-06
  K5=-3.3149459E-06
  K6=61.86220E-09
  K7=-4.866633E-10
  GO TO 130
ELSEIF(ISHOB(I,L).LT.40) THEN
  IF(VNA.GT.35.0) GO TO 160
  K0=8.485315
  K1=-0.1031393
  K2=-0.0034114
  K3=0.0003087
  K4=-1.07267E-05
  K5=3.15662E-07
  K6=-5.56646E-09
  K7=0.0
  GO TO 130
ELSEIF(ISHOB(I,L).LT.50) THEN
  IF(VNA.GT.31.0) GO TO 160
  K0=8.576003
  K1=-0.1039995
  K2=-0.0065788
  K3=0.0012362
  K4=-0.0001333
  K5=8.01387E-06
  K6=-2.34684E-07
  K7=2.51295E-09
  GO TO 130
ELSEIF(ISHOB(I,L).LT.60) THEN
  IF(VNA.GT.28.0) GO TO 160
  K0=8.643504
  K1=-0.1110564
  K2=-0.0041904
  K3=0.0006644
  K4=-7.76848E-05
  K5=8.90695E-06
  K6=-2.27079E-07
  K7=3.00626E-09
  GO TO 130

```

```

ELSEIF(ISHOB(I,L).LT.70) THEN
  IF(VNA.GT.26) GO TO 160
  K0=8.686697
  K1=-0.1164822
  K2=0.0003634
  K3=-0.0006169
  K4=8.57541E-05
  K5=-4.07263E-06
  K6=5.66402E-18
  K7=0.0
  GO TO 130
ELSEIF(ISHOB(I,L).LT.80) THEN
  IF(VNA.GT.25) GO TO 160
  K0=8.707449
  K1=-0.1175502
  K2=0.0023483
  K3=-0.0013054
  K4=0.0001909
  K5=-1.15200E-05
  K6=2.33079E-07
  K7=-2.44704E-09
  GO TO 130
ELSEIF(ISHOB(I,L).LT.90) THEN
  IF(VNA.GT.23) GO TO 160
  K0=8.736328
  K1=-0.1151605
  K2=0.0021175
  K3=-0.0015218
  K4=0.0002654
  K5=-1.96750E-05
  K6=6.18015E-07
  K7=-7.20862E-09
  GO TO 130
ELSE
  IF(VNA.GT.22) GO TO 160
  K0=8.793042
  K1=-0.1154885
  K2=0.0001871
  K3=-0.0011008
  K4=0.0002357
  K5=-2.01562E-05
  K6=6.97520E-07
  K7=-8.74866E-09
  GO TO 130
ENDIF
220 CONTINUE
230 FORMAT(//)
WRITE(6,230)
END

```



```

C
C CEP-EXCLUDED CEDF MODEL. THE PD(I,J) IS THE
C DISTANCE DAMAGE FUNCTION.
C
IF(CEPA.LT.0.001) THEN
  IF(S.GT.0.0) THEN
    PDM=PDR(REAL(WR(I,J)),S,BETA(J))
  ELSE
    PDM=1.0
  ENDIF
C
ELSE
C
C CEP-INCLUDED CEDF MODEL. DETERMINATION OF THE
C INTEGRATION LIMITS A AND B.
C
  NWR=1.1774*REAL(WR(I,J))/CEPA
  NS=1.1774*S/CEPA
  B=1.06*NWR*EXP(2.86*SIGMA(J))
  IF(B.GT.(NS+4.0)) B=NS+4.0
  A=NS-4.0
  IF(A.LT.0.0) A=0.0
  FN=0.0
C
C GAUSS-LEGENDRE TEN POINT QUADRATURE TO
C DETERMINE PD(I,J).
C
  DO 110 K2=1,5
    DO 100 L2=1,2
      R=0.5*((B-A)+Z(K2)*(-1)**L2+A+B)
      PP=PDR(NWR,R,BETA(J))
      H=NS+R
      IF(H.EQ.0.0) THEN
        F(K2,L2)=PP+R*EXP((-R**2)/2.0)
      ELSEIF(H.LE.3.75) THEN
        JJ=(H/3.75)**2
        F(K2,L2)=PP+R*EXP(-(NS**2+R**2)/2.0)*BESB(JJ)
      ELSE
        JJ=3.75/H
        F(K2,L2)=PP+R*EXP(-(NS-R)**2/2.0)*BESC(JJ)/SQRT(H)
      ENDIF
      FN=FN+W(K2)*F(K2,L2)
100 CONTINUE
110 CONTINUE
    PDM=0.5*(B-A)*FN
  ENDIF
120 PDAM=INT(100*J.0)*PDM+0.5/10.0.0
END

```

C\*\*\*\*\*

REAL FUNCTION PDR(WR,R,BETA)

C 1. CALCULATES THE DISTANCE DAMAGE FUNCTION-- THE  
C PROBABILITY OF ACHIEVING A SPECIFIED LEVEL OF  
C DAMAGE TO INSTALLATION J FROM WEAPON I WHEN THEY  
C ARE SEPARATED A KNOWN DISTANCE R.

C\*\*\*\*\*

PARAMETER(E1=0.0705230784,E2=0.0422820123,E3=1.0092705272,  
E4=0.000152143,E5=1.0002765672,E6=0.0000430633)

REAL ERF,ZZ,BETA,WR,R,U,SIGN,V

ERF(V)=1.0-1.0/(1.0+V\*(E1+V\*(E2+V\*(E3+V\*(E4+V\*(E5+V\*E6))))))\*\*16

C  
C CALCULATES ZZ, A STANDARD NORMAL PANDOM VARIABLE, AND  
C TESTS ZZ TO DETERMINE THE EXTREMES OF THE PROBABILITY  
C OF DAMAGE FUNCTION.  
C

ZZ=(1.0/BETA)\*LOG((WR\*EXP(-BETA\*\*2))/R)

IF(ZZ.GT.3.87) THEN

PDR=1.0

RETURN

ENDIF

IF(ABS(ZZ).LT.3E-06) THEN

PDR=0.5

RETURN

ENDIF

IF(ZZ.LT.-3.87) THEN

PDR=0.0

RETURN

ENDIF

U=ABS(ZZ)/SQRT(2.0)

SIGN=1.0

IF(ZZ.LT.0.0) SIGN=-1.0

C  
C CALCULATES THE DISTANCE DAMAGE FUNCTION USING A  
C POLYNOMIAL APPROXIMATION OF THE ERROR FUNCTION.  
C

PDR=0.5+SIGN\*0.5\*ERF(U)

RETURN

END

C+\*\*\*\*\*

SUBROUTINE PWMIN(X,E,N,EF,ESCALE,MAXIT,W,NW)

C 1. POWELL'S METHOD OF CONJUGATE DIRECTIONS  
C DETERMINES THE MINIMUM OF A FUNCTION USING  
C ONLY FUNCTION EVALUATIONS.

C\*\*\*\*\*

REAL X(N),E(N),W(NW)

DDMAG=.1\*ESCALE

SCER=.05/ESCALE

JJ=N\*(N+1)

JJJ=JJ+N

K=N+1

NFC=1

IND=1

INN=1

WRITE(6,\*) ' PWMIN'

DO 4 I=1,N

W(I)=ESCALE

DO 4 J=1,N

W(K)=0.0

IF(I.EQ.J) W(K)=ABS(E(I))

4 K=K+1

ITERC=1

ISGRAD=2

CALL FUNCT(N,X,F)

FKEEP=2.0\*ABS(F)

C

C

C

5

START THE NEXT ITERATION.

ITONE=1

DO 200 I=1,N

WRITE(6,\*) ' X(\*,I,\*)= ',X(I)

200

CONTINUE

WRITE(6,\*) ' EF= ',-F

FP=F

SUM=0.0

IXP=JJ

DO 6 I=1,N

IXP=IXP+1

6

W(IXP)=X(I)

IDIRN=N+1

ILINE=1

C

C

C

7

START THE NEXT ONE DIMENSIONAL SEARCH.

DMAX=W(ILINE)

DACC=DMAX+SCER

DMAG=AMIN1(DDMAG,.1\*DMAX)

DMAG=AMAX1(DMAG,20.0\*DACC)

DDMAX=.0\*DMAG

GO TO (70,71),ITONE



```

70 DL=0.0
   D=DMAG
   FPREV=F
   IS=5
   FA=FPREV
   DA=DL
8   DD=D-DL
   DL=0
C
C   SELECT THE NEXT SEARCH DIRECTION FOR ITERATION I.
C
50 K=IDIRN
   DO 9 I=1,N
     X(I)=X(I)+DD*W(K)
9   K=K+1
   CALL FUNCT(N,X,F)
   NFCC=NFCC+1
   GO TO (10,11,12,13,14,96), IS
14  IF(F.EQ.FA) THEN
     IF(ABS(D).LE.DMAX) THEN
       D=D+D
       GO TO 8
     ENDIF
     WRITE(6,*) ' MAX CHANGE DOES NOT ALTER FUNCTION '
     GO TO 20
   ELSEIF(F.LT.FA) THEN
     FB=F
     DB=D
   ELSE
     FB=FA
     DB=DA
     FA=F
     DA=D
   ENDIF
C
   GO TO (43,23), ISGRAD
23  D=DB+DB-DA

   IS=1
   GO TO 8
83  D=.5*(DA+DB-(FA-FB)/(DB-DA))
   IS=4
   IF((DA-D)+(D-DB).GE.0.0) GO TO 8
25  IS=1
   IF(ABS(D-DB).LE.DDMAX) GO TO 8
26  D=DB+SIGN(DDMAX,DB-DA)
   IS=1
   DDMAX=DDMAX+DDMAX
   DDMAG=DDMAG+DDMAG
   IF(DDMAG.GE.1.0E+6) DDMAG=1.0E+60
   IF(DDMAX.LE.DMAX) GO TO 8
   DDMAX=DMAX
   GO TO 9

```

```

13 IF(F.GE.FA) GO TO 23
28 FC=FB
   DC=DB
29 FB=F
   DB=D
   GO TO 30
12 IF(F.LE.FB) GO TO 23
   FA=F
   DA=D
   GO TO 30
11 IF(F.GE.FB) GO TO 10
   FA=FB
   DA=DB
   GO TO 29

C
71 DL=1.0
   DDMAX=5.0
   FA=FB
   DA=-1.0
   FB=FHOLD
   DB=1.0
   D=1.0
10 FC=F
   DC=D
30 A=(DB-DC)+(FA-FC)
   B=(DC-DA)+(FB-FC)
   IF((A+B)*(DA-DC).GT.0.0) GO TO 34
   FA=FB
   DA=DB
   FB=FC
   DB=DC
   GO TO 26
34 D=.5*(A+(DB+DC)+B*(DA+DC))/(A+B)
   DI=DB
   FI=FB
   IF(FB.LE.FC) GO TO 44
   DI=DC
   FI=FC
44 GO TO (86,86,35), ITONE
85 ITONE=2
   GO TO 45

C
C CHECK THE ONE DIMENSIONAL MINIMIZATION SEARCH
C FOR CONVERGENCE.
C
86 IF(ABS(D-DI).LE.DACC) GO TO 41
   IF(ABS(D-DI).LE.(0.3*ABS(D))) GO TO 41
45 IF((DA-DC)*(DC-D).GE.0.0) THEN
   FA=FB
   DA=DB
   FB=FC
   DB=DC
   GO TO 25

```

```

ELSE
  IS=2
  IF((DB-D)*(D-DC).GE.0.0) GO TO 8
  IS=3
  GO TO 8
ENDIF
41 F=F?
D=DI-DL
RE=(DC-DB)*(DC-DA)*(DA-DB)/(A+B)
IF(RE.LE.0.0) THEN
  WRITE(6,*) ' ACCURACY LIMITED BY THE FUNCTION'
  RETURN
ENDIF
DD=SQRT(RE)
C
C COMPLETES ONE OF THE N ONE DIMENSIONAL SEARCHES
C FOR ITERATION I. UPDATE X(I).
C
DO 49 I=1,N
  X(I)=X(I)+D*W(IDIRN)
  W(IDIRN)=DD*W(IDIRN)
49 IDIRN=IDIRN+1
  W(ILINE)=W(ILINE)/DD
  ILINE=ILINE+1
C
IF(ITONE.EQ.2) GO TO 39
IF((FPREV-F-SUM).LT.0.0) GO TO 94
  SUM=FPREV-F
  JIL=ILINE
94 IF(IDIRN.LE.JJ) GO TO 7
C
C ALL ONE DIMENSIONAL SEARCHES COMPLETED
C
GO TO (92,72), IND
92 FHOLD=F
  IS=6
  IXP=JJ
  DO 59 I=1,N
    IXP=IXP+1
59 W(IXP)=X(I)-W(IXP)
  DD=1.0
C
C CALCULATES THE EXPANDED POINT.
C
GO TO 58
96 GO TO (112,87), IND

```

```

C
C THE MODIFICATION TEST
C
112 IF(FP.LE.F) GO TO 37
D=2.0*(FP+F-2.0*FHOLD)/(FP-F)*v2
IF((D*(FP-FHOLD-SUM)**2-SUM).GE.0.0) GO TO 37
87 J=JIL*N+1
IF(J.GT.JJ) GO TO 61
DO 62 I=J,JJ
K=I-N
62 W(K)=W(I)
DO 97 I=JIL,N
97 W(I-1)=W(I)
C
C SEARCH IN DIRECTION OF THE EXPANDED POINT.
C
61 IDIRN=IDIRN-N
ITONE=3
K=IDIRN

IXP=JJ
AAA=0.0
DO 67 I=1,N
IXP=IXP+1
W(K)=W(IXP)
IF(AAA.LT.ABS(W(K)/E(I))) THEN
AAA=ABS(W(K)/E(I))
ENDIF
67 K=K+1
DDMAG=1.0
W(N)=ESCALE/AAA
ILINE=4
GO TO 7

```

```

C
C UPDATE X(I) AND USE THE PREVIOUS SEARCH DIRECTIONS.
C
37 IXP=JJ
AAA=0.0
F=FHOLD
DO 99 I=1,N
    IXP=IXP+1
    X(I)=X(I)-W(IXP)
    IF((AAA+ABS(E(I))).LT.ABS(W(IXP))) THEN
        AAA=ABS(W(IXP)/E(I))
    ENDIF
99 CONTINUE
GO TO 72
35 AAA=AAA*(1.0+DI)
GO TO (72,106), IND
72 GO TO (109,88), IND
109 IF(AAA.LE.0.1) GO TO 20
C
IF(F.LT.FP) GO TO 35
WRITE(6,*) ' ACCURACY LIMITED BY THE FUNCTION'
GO TO 20
88 IND=1
35 DD MAG=0.4*SQRT(ABS(FP-F))
IF(DDMAG.GE.1.0E+60) DD MAG=1.0E+60
ISGPAD=1
C
ITERC=ITERC+1
IF(ITERC.LE.MAXIT) GO TO 5
IF(F.LE.FKEEP) GO TO 20
F=FKEEP
DO 111 I=1,N
    JJJ=JJJ+1
111 X(I)=W(JJJ)
20 WRITE(6,*) ' ITERATIONS= ',ITERC
EF=F
RETURN
106 IF(AAA.LE.0.1) GO TO 20
INN=1
GO TO 35
C
END

```

## Appendix E: User Guidelines and a Sample Problem

This appendix provides basic instructions for inputting user-specified weapon and installation parameters to the CEDF maximization algorithm. These instructions are presented using an example.

Initially, the user must determine the values of the convergence control parameters, ACC, DFPRED, E, and ESCALE. These values depend on installation values and the number of weapons and installations. User guidelines in Chapter V discuss specific considerations. The source code initializes the PWMIN convergence parameters to  $E(i) = 0.1$  and ESCALE = 5000. Two minor code changes would be necessary to change either of these values. The user must input values for the ZXCGR convergence parameters, ACC and DFPRED.

Next, the user must decide on the type of initial DGZ coordinates to use. The user has three options. The user communicates the desired DGZ location option to the algorithm through the input variable -- INC. If INC = 1, then the algorithm uses the user-specified estimates of the initial DGZ locations. If INC = 2, then the algorithm assigns the coordinates of the m highest valued installations to be the initial coordinates of the m weapons in decreasing order of yield. Finally, if INC = 3, then the algorithm assigns the coordinates of the m hardest installations to be the initial coordinates of the m weapons in decreasing order of yield.

Then the user needs to compile the necessary input data in a FORTRAN external file, INDATA. Figure E-1 is the input data file, INDATA, for a two weapon-four installation example. The first line is the decision variable, INC. For this example, INC = 2 and the initial DGZ

```

2
2
  451115E      460325N      70.   250.   1000.   .99
  451040E      460310N      70.   250.   1000.   .99
4
  431000E      460330N      16P2   3500.
  451050E      460400N      22P2   2500.
  451100E      460350N      21P4   5000.
  451130E      460305N      19Q3   7000.
0.001
1000.0

```

Figure E-1. The CEDEF maximization algorithm input file, INDATA, for a two weapon-four installation complex.

coordinates were the coordinates of the two highest valued installations. The second line in the file INDATA is  $m$ , the number of weapons for the complex; for this example,  $m = 2$ . The next  $m$  lines contain the user-specified weapon parameters. The FORTRAN input format for these parameters is statement 100 in subroutine INITLZ of the source code. The order and units of the weapon parameters are: the longitude and latitude coordinates (these must be initialized to some value even if  $INC = 2$  or  $3$ ), the yield in kilotons, the CEP in feet, the HOB in feet, and the Pa.

The line after the last weapon's parameters is  $n$ , the number of installations in the complex; for this example,  $n = 4$ . The next  $n$  lines contain the user-specified installation parameters. The FORTRAN input format statement for these parameters is statement 110 in subroutine INITLZ of the source code. The order of the installation parameters is: the longitude and latitude coordinates, a VNIK code, and a value (a real number less than 10000.0).

Finally, the ZXGGR convergence control parameters complete the

external file, INDATA. The line after the last installation's parameters contains the value of ACC for the second stage of ZXCGR maximization. The last line of the file contains the value of DFPRED. For this example, ACC = 0.001 and DFPRED = 1000.

The CEDF maximization algorithm outputs the results of a problem to another external file, TAPE6. The results of four maximizations are: (1) a ZXCGR maximization for ACC = 0.01; (2) a ZXCGR maximization for a user-specified value of ACC; (3) a PWMIN maximization; and (4) a mixed maximization.

The next six pages list the results of the two weapon-four installation problem.



\*\*\*\*\*  
 CDF MAXIMIZATION ALGORITHM  
 \*\*\*\*\*

INITLZ

THIS PROBLEM USES 2 WEAPONS

WEAPON	YIELD	CEP	HOB	PA
1	70.	250.	1000.	.99
2	70.	250.	1000.	.99

THIS COMPLEX CONTAINS 4 INSTALLATIONS

LONGITUDE	LATITUDE	VNTK	VALUE
4510 DE	46 33 N	16P2	3500.
451030E	46 4 5N	22P2	2500.
4511 DE	46 35 N	21P4	5000.
451130E	46 3 5N	1903	7000.

THE XY COORDINATES OF THE INSTALLATIONS IN FEET

XX(1) = 42199.35367441	XX(5) = 21280.00000002
XX(2) = 44298.82135815	XX(6) = 24319.99999998
XX(3) = 46408.23904184	XX(7) = 23306.66666666
XX(4) = 48517.75672559	XX(8) = 18746.66666664

INITIAL DGZ LOCATIONS ARE HIGHEST VALUED INSTALLATIONS

X(1) = 48517.75672559	X(3) = 18746.66666664
X(2) = 46409.28904184	X(4) = 23306.66666666

WRADS

WR(1,1) = 3272
WR(2,1) = 3272
WR(1,2) = 1947
WR(2,2) = 1947
WR(1,3) = 2200
WR(2,3) = 2200
WR(1,4) = 2863
WR(2,4) = 2863

\*\*\*\*\*  
 ZXCGR MAXIMIZATION  
 \*\*\*\*\*

ACC= .J1  
 WEAPON 1 XY COORDINATES: ( 48518., 18747.)  
 WEAPON 2 XY COORDINATES: ( 46408., 23307.)  
 PS(1)= .97624  
 PS(2)= .86833  
 PS(3)= .0J99999999999998  
 PS(4)= .0098415999999998  
 EC= 12293.4438  
 WEAPON 1 XY COORDINATES: ( 48518., 18747.)  
 WEAPON 2 XY COORDINATES: ( 46333., 23331.)  
 PS(1)= .97228  
 PS(2)= .82873  
 PS(3)= .0099999999999998  
 PS(4)= .0098514999999998  
 EC= 12406.2345  
 WEAPON 1 XY COORDINATES: ( 48517., 18747.)  
 WEAPON 2 XY COORDINATES: ( 45657., 23554.)  
 PS(1)= .91585  
 PS(2)= .17315  
 PS(3)= .0099999999999998  
 PS(4)= .0099405999999998  
 EC= 14192.0658  
 WEAPON 1 XY COORDINATES: ( 48517., 18747.)  
 WEAPON 2 XY COORDINATES: ( 44188., 24137.)  
 PS(1)= .65845  
 PS(2)= .0099999999999998  
 PS(3)= .69578  
 PS(4)= .0099900999999998  
 EC= 12125.9943  
 WEAPON 1 XY COORDINATES: ( 48517., 18747.)  
 WEAPON 2 XY COORDINATES: ( 45281., 23678.)  
 PS(1)= .86239  
 PS(2)= .02589  
 PS(3)= .01198  
 PS(4)= .0099603999999998  
 EC= 14799.7872  
 WEAPON 1 XY COORDINATES: ( 48517., 18747.)  
 WEAPON 2 XY COORDINATES: ( 45124., 23729.)  
 PS(1)= .83566  
 PS(2)= .01099  
 PS(3)= .0238600000001  
 PS(4)= .0099702999999998  
 EC= 14858.6229  
 WEAPON 1 XY COORDINATES: ( 48516., 18747.)  
 WEAPON 2 XY COORDINATES: ( 44110., 23312.)  
 PS(1)= .17632  
 PS(2)= .05257  
 PS(3)= .63023  
 PS(4)= .0099772999999998  
 EC= 13790.5129

PS(2)= .02683  
 PS(3)= .13226  
 PS(4)= .009960399999998  
 EC= 15253.7322  
 WEAPON 1 XY COORDINATES: ( 48517., 18747.)  
 WEAPON 2 XY COORDINATES: ( 44829., 23019.)  
 PS(1)= .51787  
 PS(2)= .08821  
 PS(3)= .09613  
 PS(4)= .009940599999998  
 EC= 15416.6958  
 WEAPON 1 XY COORDINATES: ( 48517., 18747.)  
 WEAPON 2 XY COORDINATES: ( 44812., 23034.)  
 PS(1)= .51391  
 PS(2)= .07831  
 PS(3)= .10306  
 PS(4)= .009940599999998  
 EC= 15420.6558  
 WEAPON 1 XY COORDINATES: ( 48516., 18747.)  
 WEAPON 2 XY COORDINATES: ( 44835., 23069.)  
 PS(1)= .53767  
 PS(2)= .06742000000001  
 PS(3)= .03019000000001  
 PS(4)= .009940599999998  
 EC= 15429.0708  
 WEAPON 1 XY COORDINATES: ( 48516., 18747.)  
 WEAPON 2 XY COORDINATES: ( 45040., 23386.)  
 PS(1)= .72775  
 PS(2)= .02287  
 PS(3)= .02584  
 PS(4)= .009950499999999  
 EC= 15196.8465  
 WEAPON 1 XY COORDINATES: ( 48516., 18747.)  
 WEAPON 2 XY COORDINATES: ( 44851., 23094.)  
 PS(1)= .55351  
 PS(2)= .06148  
 PS(3)= .08129000000001  
 PS(4)= .009940599999998  
 EC= 15433.0308  
 IER= 0  
 FUNCTION= 15433.0308  
 FUNCTION EVALUATIONS: 18  
 X(1)= 48516.46037407  
 GRAD(1)= .0003386697914471  
 X(2)= 44850.73876378  
 GRAD(2)= .0194870170614  
 X(3)= 18747.18690065  
 GRAD(3)= -.0001474502035606  
 X(4)= 23093.65196727  
 GRAD(4)= .0193911576447  
  
 WEAPON      LONGITUDE      LATITUDE  
           1           451129E       46 3 5N  
           2           451037E       46 347N

\*\*\*\*\*  
 ZXCGR WITH ACC REDUCED  
 \*\*\*\*\*

ACC= .J01  
 WEAPON 1 XY COORDINATES: ( 48516., 18747.)  
 WEAPON 2 XY COORDINATES: ( 44851., 23094.)  
 PS(1)= .55351  
 PS(2)= .06148  
 PS(3)= .08128000000001  
 PS(4)= .009940599999998  
 EC= 15433.0308

IER= 0  
 FUNCTION= 15433.0308  
 FUNCTION EVALUATIONS: 2  
 X(1)= 48516.46037407  
 GRAD(1)= .0003386697914471  
 X(2)= 44850.73876378  
 GRAD(2)= .0194870170614  
 X(3)= 18747.19690065  
 GRAD(3)= -.0001474502035606  
 X(4)= 23093.65196727  
 GRAD(4)= .0193911576447

WEAPON	LONGITUDE	LATITUDE
1	451129E	46 3 5N
2	451037E	46 347N

\*\*\*\*\*  
PWMIN MAXIMIZATION  
\*\*\*\*\*

PWMIN

X(1)= 48517.75672559  
X(2)= 46438.28904184  
X(3)= 18746.66666664  
X(4)= 23306.66666666  
EF= 12358.3581

X(1)= 48517.75672559  
X(2)= 44888.94497861  
X(3)= 18746.66666664  
X(4)= 23169.22996394  
EF= 15137.8158

X(1)= 48517.75672559  
X(2)= 44888.83071814  
X(3)= 18746.66666664  
X(4)= 23165.79903085  
EF= 15141.9708

ACCURACY LIMITED BY THE FUNCTION  
ITERATIONS= 3  
FUNCTION= 15141.9708

XXX(1)= 48517.75672559  
XXX(2)= 44881.97031154  
XXX(3)= 18746.66666664  
XXX(4)= 23159.52991093

WEAPON	LONGITUDE	LATITUDE
1	451130E	46 3 5N
2	451038E	46 348N

\*\*\*\*\*  
 MIXED TECHNIQUE MAXIMIZATION  
 \*\*\*\*\*

PWMIN

X(1)= 48516.46037407  
 X(2)= 44850.73876378  
 X(3)= 18747.19690065  
 X(4)= 23093.65196727  
 EF= 15133.0608

X(1)= 48516.46037407  
 X(2)= 44851.32790653  
 X(3)= 18747.19690065  
 X(4)= 23127.72924026  
 EF= 15136.0308

X(1)= 48516.46037407  
 X(2)= 44851.74210346  
 X(3)= 18747.19690065  
 X(4)= 23123.46811256  
 EF= 15138.0108

X(1)= 48516.46037407  
 X(2)= 44853.60958023  
 X(3)= 18747.19690065  
 X(4)= 23123.46811256  
 EF= 15139.4958

ACCURACY LIMITED BY THE FUNCTION  
 ITERATIONS= 4

FUNCTION= 15132.0700  
 X\*(1)= 48516.46037407  
 X\*(2)= 44855.35435102  
 X\*(3)= 18747.19690065  
 X\*(4)= 23105.5184597

WEAPON	LONGITUDE	LATITUDE
1	451129E	46 3 5N
2	451037E	46 348N

Appendix F: Verification of the Gradient  
of the CEP-Excluded CEDF Model

The results of two example problems verified that the subroutine GFUNCT correctly calculates the gradient of the CEP-Excluded model. The pencil and paper results for each example were compared with the results from GFUNCT.

The first example included one weapon and two installations. The weapon and installation parameters are presented below. This verification example used a graph of CEDF(x) versus x. For 40 equally spaced DGZ locations, values of CEDF(x) were calculated. The x direction was along the line connecting the two installations. Table F-1 lists the 40 values of x and the corresponding function and gradient values. Figure 9 in Chapter IV is a plot of this data. A DGZ between the two installations was selected (x = 63500), and the gradient was calculated using two methods. In this example, the gradient had only one element because the y variable was constant; only the x variable was allowed to vary. The gradient values for the two calculation methods were compared with the gradient value from GFUNCT.

The first method used a difference equation,  $\frac{\Delta \text{CEDF}}{\Delta x}$ , to approximate the gradient. The slope of the line segment connecting the CEDF values for the two DGZs on either side of the selected DGZ was an approximate gradient value. From Table F-1,

$$\text{CEDF}(x = 63000) = 6257$$

$$\text{CEDF}(x = 64000) = 10196$$

TABLE F-1

The CEDF(x) and the Gradient of the CEDF(x) for  
a One Weapon-Two Installation Complex

\*\*\*\*\*  
GRADIENT VERIFICATION  
\*\*\*\*\*

X(1)	X(2)	EC	GRAD(1)	GRAD(2)
54000.	20000.	2386.	1.6274	0.0000
54500.	20000.	3218.	1.6494	0.0000
55000.	20000.	3985.	1.3530	0.0000
55500.	20000.	4534.	.8339	0.0000
56000.	20000.	4826.	.3564	0.0000
56500.	20000.	4930.	.0895	0.0000
57000.	20000.	4950.	.0106	0.0000
57500.	20000.	4950.	.0004	0.0000
58000.	20000.	4950.	.0000	0.0000
58500.	20000.	4950.	.0002	.0000
59000.	20000.	4950.	.0003	0.0000
59500.	20000.	4950.	.0017	0.0000
60000.	20000.	4950.	.0053	0.0000
60500.	20000.	4962.	.0168	0.0000
61000.	20000.	4974.	.0513	0.0000
61500.	20000.	5021.	.1493	0.0000
62000.	20000.	5152.	.4064	0.0000
62500.	20000.	5485.	1.0098	0.0000
63000.	20000.	6257.	2.2036	0.0000
63500.	20000.	7793.	3.9791	0.0000
64000.	20000.	10196.	5.4652	0.0000
64500.	20000.	12910.	4.9543	0.0000
65000.	20000.	14724.	1.9935	0.0000
65500.	20000.	14931.	-.8246	0.0000
66000.	20000.	14266.	-1.5783	0.0000
66500.	20000.	13514.	-1.3643	0.0000
67000.	20000.	12920.	-1.0078	0.0000
67500.	20000.	12499.	-.6735	0.0000
68000.	20000.	12231.	-.4157	0.0000
68500.	20000.	12068.	-.2407	0.0000
69000.	20000.	11979.	-.1325	0.0000
69500.	20000.	11930.	-.0701	0.0000
70000.	20000.	11905.	-.0648	0.0000
70500.	20000.	11724.	-.8426	0.0000
71000.	20000.	10744.	-3.3551	0.0000
71500.	20000.	9380.	-5.7974	0.0000
72000.	20000.	5370.	-5.8235	0.0000
72500.	20000.	2863.	-4.0695	0.0000
73000.	20000.	1307.	-2.2145	0.0000
73500.	20000.	530.	-1.1004	0.0000



The difference equation approximation of the gradient at  $x = 63500$  was

$$\frac{\Delta \text{CEDF}}{\Delta x} = \frac{10196 - 6257}{1000} = 3.939$$

The second method was pencil and paper calculations of all the steps necessary to determine the gradient. Chapter II presented these steps. Only a summary of the calculations are presented here.

Given:	Weapon	Yield	CEP	HOB	Pa	(x,y) in feet
	1	100-kt	0 feet	1000 feet	0.99	(63500,20000)
	Target	VNIK	Value(v)	WR		(xx,yy) in feet
	1	11P2	5000	6194		(60000,20000)
	2	15P2	12000	4066		(68000,20000)

Note: In this example,  $y = x(2) = \text{constant}$ . Hence,  $\frac{\partial \text{CEDF}}{\partial y} = 0$  and  $\text{CEDF}(x) = \text{CEDF}(x)$ .

From Eq (1),

$$\text{CEDF}(x) = v_1 * Pa_1 * Pd(1,1) + v_2 * Pa_1 * Pd(1,2)$$

However,  $v_j$  and  $Pa_1$  are constants, so

$$\text{CEDF}(x) = 4950 * Pd(1,1) + 11880 * Pd(1,2)$$

and 
$$\frac{d \text{CEDF}(x)}{dx} = 4950 * \frac{d Pd(1,1)}{dx} + 11880 * \frac{d Pd(1,2)}{dx}$$

where 
$$\frac{d Pd(1,j)}{dx} = \frac{e^{-u^2}}{\sqrt{2\pi} \beta r^2} (xx_j - x)$$

and 
$$u = \frac{1}{\sqrt{2}} * \text{abs} \left[ -\beta + \frac{1}{\beta} \ln \left( \frac{WR(1,j)}{r} \right) \right]$$

For overpressure (P-type) targets,  $\sigma_d = 0.2$  and

$$\beta = \sqrt{-\ln(1 - \sigma_d^2)} \quad (F-1)$$
$$= 0.202045$$

Let  $AA = xx_j - x_j \quad (F-2)$

$$BB = xx_{j+n} - x_{i+m} \quad (F-3)$$

$$r = AA^2 + BB^2 \quad (F-4)$$

For this verification example,  $BB = 0$  for both targets and  $r = |AA|$ , the absolute difference between the x coordinates of the weapon and installation j.

For target 1:  $AA = 60000 - 63500 = -3500$

$$r = 3500$$

$$u = 1.8548527$$

$$\frac{d Pd(1,1)}{dx} = -1.8080608 * 10^{-5}$$

For target 2:  $AA = 68000 - 63500 = 4500$

$$r = 4500$$

$$u = 0.49780381$$

$$\frac{d Pd(1,2)}{dx} = 3.4247393 * 10^{-4}$$

Therefore,

$$\frac{d CEDF(x)}{dx} = 4950.0 * (-1.8080608 * 10^{-5}) + 11880.0 * (3.4247393 * 10^{-4})$$
$$= 3.97909$$

The value of the gradient of the CEDF(x) from GFUNCT for the DGZ selected (x = 63500) was 3.9791. The gradient results from the difference equation approximation and the pencil and paper calculations were compared with the value from GFUNCT. These two comparisons indicated the subprogram GFUNCT was properly calculating the gradient of the CEDF(x).

The second gradient verification example included two weapons and three installations. The gradient of the CEDF(x) had 2m or four elements. However, only one element was completely checked by pencil and paper calculations.

Given:	Weapon	Yield	CEP	HOB	Pa	(x,y) in feet
	1	100 kt	0 feet	1000 feet	0.99	(61000,21500)
	2	100 kt	0 feet	1000 feet	0.99	(62000,17500)

Target	VNIK	Value(v)	WR	(x,y) in feet
1	12P2	5000	5550	(60000,19500)
2	14P2	8000	4495	(68000,20500)
3	12P2	4000	5550	(63000,23500)

From Eq (1)

$$\begin{aligned} \frac{\partial \text{CEDF}(x)}{\partial x_2} &= v_1 * Pa_2 * (1 - Pa_2 * Pd(1,1)) * \frac{\partial Pd(2,1)}{\partial x_2} \\ &+ v_2 * Pa_2 * (1 - Pa_2 * Pd(1,2)) * \frac{\partial Pd(2,2)}{\partial x_2} \\ &+ v_3 * Pa_2 * (1 - Pa_2 * Pd(1,3)) * \frac{\partial Pd(2,3)}{\partial x_2} \end{aligned} \quad (\text{F-5})$$

From the subprogram FUNCT,

$$Pd(1,1) = 1.000$$

$$Pd(1,2) = 0.007$$

$$Pd(1,3) = 0.999$$

Hence,

$$V_1 * Pa_2 = 4950$$

$$V_2 * Pa_2 = 7920$$

$$V_3 * Pa_2 = 3960$$

and

$$Pa_2 * Pd(1,1) = 0.99000$$

$$Pa_2 * Pd(1,2) = 0.00693$$

$$Pa_2 * Pd(1,3) = 0.98901$$

Eq (F-5) becomes

$$\begin{aligned} \frac{\partial CEDF(x)}{\partial x_2} = & 49.50 * \frac{\partial Pd(2,1)}{\partial x_2} + 7865.1144 * \frac{\partial Pd(2,2)}{\partial x_2} \\ & + 43.5204 * \frac{\partial Pd(2,3)}{\partial x_2} \end{aligned}$$

where

$$\frac{\partial Pd(2,j)}{\partial x_2} = \frac{e^{-u^2}}{\sqrt{2\pi} \beta r^2} (xx_j - x_2)$$

and

$$u = \frac{1}{\sqrt{2}} * \text{abs} \left[ -\beta + \frac{1}{\beta} \ln \left( \frac{WR(2,j)}{r} \right) \right]$$

$\beta$ , AA, BB, and r are calculated from Eqs (F-1) through (F-4).

For target 1: AA = 60000 - 62000 = -2000  
 BB = 19500 - 17500 = 2000  
 r = 2828.427

$$\frac{\partial Pd(x,1)}{\partial x_2} = -3.633135 \times 10^{-6}$$

For target 2: AA = 68000 - 62000 = 6000  
 BB = 20500 - 17500 = 3000  
 r = 6708.204

$$\frac{\partial Pd(2,2)}{\partial x_2} = 2.426656 \times 10^{-5}$$

For target 3: AA = 63000 - 62000 = 1000  
 BB = 23500 - 17500 = 6000  
 r = 6082.763

$$\frac{\partial Pd(2,3)}{\partial x_2} = 4.304235 \times 10^{-5}$$

Therefore,

$$\begin{aligned} \frac{\partial CEDF(x)}{\partial x_2} &= 49.50 \times (-3.633135 \times 10^{-6}) \\ &\quad + 7865.1144 \times (2.426656 \times 10^{-5}) \\ &\quad + 43.5204 \times (4.304235 \times 10^{-5}) \\ &= 0.19254823 \end{aligned}$$

The value of the gradient element of the CEDF(x) for x<sub>2</sub> from GFUNCT was 0.19255136. This comparison also indicated that the routine GFUNCT was correctly forming the gradient of the CEDF(x).

## Bibliography

1. Abramowitz, Milton and Irene A. Stegun, editors. Handbook of Mathematical Functions with Formulas, Graphs, and Mathematical Tables. Washington: Government Printing Office, March 1965.
2. Aoki, Masano. Introduction to Optimization Techniques Fundamentals and Applications of Nonlinear Programming. New York: The Macmillan Company, 1971.
3. Avriel, Mordecai. Nonlinear Programming Analysis and Methods. Englewood Cliffs: Prentice-Hall Inc., 1976.
4. Bertapelle, Maj. Telephone Interview. SIOP Simulation and Analysis Branch, JSTPS. Offutt AFB NE, 3 May 1983.
5. Beveridge, Gordon S. G. and Robert S. Schechter. Optimization: Theory and Practice. New York: McGraw-Hill Book Company, 1970.
6. Defense Intelligence Agency, Mathematical Background and Programming Aids for the Physical Vulnerability System for Nuclear Weapons. DI-550-27-74. Washington DC (AD B010375L), 1 November 1974.
7. Department of the Air Force. An Introduction to Air Force Targeting. AFP 200-17. Washington: HQ USAF, 11 October 1978.
8. Department of the Air Force. Functions and Basic Doctrine of the United States Air Force. AFM I-1. Washington: HQ USAF, 14 February 1979.
9. Fletcher, R. and C. M. Reeves. "Function Minimization by Conjugate Gradients," Computer Journal, 7:149-153 (1964).
10. Gill, Phillip E., Walter Murray, and Margaret H. Wright. Practical Optimization. New York: Academic Press, 1981.
11. Glasstone, Samuel and Philip J. Dolan. The Effects of Nuclear Weapons. Washington: Government Printing Office, 1977.
12. Greenwood, Dr J. A. "Optimum Placement of DGZ's on a Target Complex - Successive Approximation Method". Report by AF Intelligence Center for the Assistant Chief of Staff Intelligence, HQ USAF. Washington DC, 16 May 1960.
13. Hamm, Maj. Wesley. Telephone Interview. Military Studies and Analysis, Command and Control Technical Center, Pentagon. Washington DC, 5 May 1983.
14. Hastings, Cecil. Approximation for Digital Computers. NJ: Princeton University Press, 1955.

15. Hildebrand, Francis B. Introduction to Numerical Analysis. New York: McGraw-Hill Book Company, 1974.
16. International Mathematical and Statistical Libraries, Inc. Library Reference Manual Edition 9, Volume 4, June 1982.
17. Kuester, James L. and Joe H. Mize. Optimization Techniques with FORTRAN. New York: McGraw-Hill Book Company, 1973.
18. Lee, Maj. Thomas E. Targeting, The Key to Effective Air Power. Armed Forces Staff College. Norfolk VA, 19 December 1975.
19. Mason, Ralph B. Description of Mathematics for the Single Integrated Damage Analysis Capability (SIDAC). Technical Memorandum 15-80. Command and Control Technical Center, Pentagon, 13 June 1980.
20. Monaco, Capt. S. J. and Dana Billings. Optimal Targeting of Ballistic Missiles in a Tiered Aimpoint System. Seiler Research Laboratory TR 78-0005 (AD A062928), August 1978.
21. Nessler, L. J. MOST Final Report, Volume I. Science Applications, Inc. La Jolla CA (AD A079944), August 1978.
22. Orlicky, Capt. Mark. Candidate Topic for AFIT Research. undated letter. Strategic Bomber Branch, Studies and Analysis, HQ USAF, April 1983.
23. Powell, M. J. D. "An Efficient Method for Finding the Minimum of Several Variables Without Calculating Derivatives," Computer Journal, 7: 155-162 (1964).
24. ----- "Restart Procedures for the Conjugate Gradient Method," Mathematical Programming, 12, 241-254 (1977).
25. Renna, V. and A. Hylton. NUCWAVE Model Methodology Analysis. Technical Memorandum 210-79. Command and Control Technical Center, Pentagon (AD B039419L), 1 July 1979.
26. Shannon, Robert E. Systems Simulation -- the Art and Science. Englewood Cliffs: Prentice-Hall Inc., 1975.
27. Siegel. Theory and Problems of Numerical Analysis. New York: McGraw-Hill Book Company, 1968.
28. Sperry, Maj. Steve. Telephone Interview. JSTPS, Offutt AFB NE, 12 October 1983.
29. Strom, Carol. Personal Correspondence. Computer Sciences Corporation, Arlington VA, 3 January 1984.

## Vita

Captain Edmund Glen Boy was born on 25 February 1949 in Tokyo, Japan, the son of Edmund G. and Jeannette C. Boy. He graduated from Nurnberg American High School in Nurnberg, Germany in 1967. After two years of college, Glen enlisted in the United States Air Force. In 1971, the Air Force selected him for the Airman's Education and Commissioning Program. In 1973, he graduated from Colorado State University with a Bachelor of Science degree in Electrical Engineering, and on 4 September 1973 he received his Air Force commission. Next, he served for two years as an Electronic Warfare Test Engineer with the 3246th Test Wing at Eglin AFB, FL. Then he entered Undergraduate Pilot Training at Vance AFB, OK. On 1 February 1977, he pinned on his pilot's wings. After completing B-52G Combat Crew Training at Castle AFB, CA, Glen was assigned to the 320th Bomb Wing at Mather AFB, CA. He served as a squadron copilot, a Stan/Eval copilot, and an aircraft commander. In August 1982, he entered the School of Engineering at the Air Force Institute of Technology.

He is married to the former Mary Beth Russell of North Platte, NE. They have three children, Gregory, Rebecca, and Leanne.

Permanent Address: 2552 Bethel Drive  
Anaheim, CA 92806